CRANFIELD UNIVERSITY

School of Water, Energy and Environment
PhD in Agrifood and the Environment

Doctor of Philosophy

Academic Year 2016 - 2021

Christopher S. McCloskey

Measuring and modelling plant-driven soil carbon dynamics

Supervisor: Professor Guy Kirk
Associate Supervisors: Professor Wilfred Otten and Dr Eric Paterson
January 2021

ABSTRACT

Plant root activity and deposition of root carbon (C) into the rhizosphere are known to influence the turnover of existing soil organic matter (SOM) in so-called rhizosphere priming effects (RPE). Thereby soil microbes may access nutrients in SOM which are otherwise unavailable to them. However the magnitudes, drivers and mechanisms of these effects are poorly understood. In this thesis I develop a field system to measure such effects on diurnal, seasonal and longer timescales, and use it to explore RPEs and their drivers in contrasting soils under grass.

The field system measures CO_2 fluxes and their ^{13}C isotope composition ($\delta^{13}C$) near continuously in large (0.8 m diameter, 1 m deep) lysimeters containing two naturally-structured C_3 soils planted with a C_4 grass. The difference in $\delta^{13}C$ between C_3 SOM and C_4 plants is used to partition fluxes between plant and soil sources. The system's accuracy and precision were sufficient to resolve diurnal and seasonal patterns in both plant and soil fluxes. Diurnal changes in plant $\delta^{13}C$ can cause large partitioning errors. I show how, with long-term datasets with sufficient temporal resolution, part of the dataset can be used to allow for transient shifts in plant and soil $\delta^{13}C$.

I explored the magnitude and mechanisms of RPEs in the two contrasting soils over two years, and the effect of differences in nitrogen supply. I used solar radiation as a proxy for photosynthesis, root activity and rhizodeposition. I found that seasonal and particularly diurnal patterns in SOM turnover were tightly coupled to solar radiation, and more so than in previously published studies. Model estimates of SOM turnover were improved by the inclusion of solar radiation as an explanatory variable alongside soil moisture and temperature, consistent with RPEs. There was no evidence for differences in RPEs with nitrogen supply in either soil.

Keywords: Plant and soil carbon fluxes, soil organic matter. C_3 and C_4 photosynthesis, rhizosphere priming effects

ACKNOWLEDGEMENTS

Firstly, I am immensely grateful to my supervisors, Professor Guy Kirk, Professor Wilfred Otten and Dr Eric Paterson. Your guidance, experience, wisdom and encouragement has been a tremendous help through my PhD, and a strong source of support. I have learned a great deal working with you, and greatly enjoyed it.

Secondly, I thank the technical teams at Cranfield and the James Hutton Institute. Particular thanks to Alan Nelson, Ceri Dawson, Cristinel Putinica, Nuanatt Simmons and Richard Andrews at Cranfield, and Allan Sim and Barry Thornton at the JHI. Your support and help throughout my experimental work has been invaluable.

The STARS CDT not only funded this research, but also provided a wealth of training, experience, and added richness to the past four years. Particular thanks to Phil Haygarth, Davey Jones, Olivia Lawrenson and all other members of the consortium for creating these opportunities. Equally, I thank my friends in STARS, and at Cranfield, for companionship and keeping me smiling throughout any hurdles or frustrations I came across.

Finally, I must thank my family. Thank you to my parents for fostering my love of the natural world from a young age, and providing support and encouragement throughout my PhD. I thank my wife Gwen for her endless support and kindness – you have been a great help over the past years, and held down the fort while I have been writing up. Last, but by no means least, I thank my son Theo, born during my PhD. Your smiles have been an unending source of joy while writing this thesis, as has your own energetic enthusiasm to explore the soil-plant interface.

TABLE OF CONTENTS

LIST OF FIGURES

LIST OF TABLES

LIST OF EQUATIONS

LIST OF ABBREVIATIONS

AIC	Akaike information criterion
C	Carbon
C	CO_2 concentration
CRDS	Cavity ring-down spectroscopy
ER	Ecosystem respiration
FACE	Free air carbon enrichment
f_{plant}	Plant flux as a proportion of net ecosystem flux
f_{soil}	Soil flux as a proportion of net ecosystem flux
F_{plant}	Plant respiration flux
F_{soil}	Soil respiration flux
GPP	Gross primary productivity
IRMS	Isotope ratio mass spectrometry
LME model	Linear mixed-effects model
N	Nitrogen
NEE	Net ecosystem exchange
NPP	Net primary productivity
PLFAs	Phospholipid-derived fatty acids
RPE	Rhizosphere priming effect
SOM	Soil organic matter
WFL	Wolfson Field Laboratory

1 Introduction

1.1 Soil carbon stocks

Soils are a major carbon (C) store, with an estimated 2.5×10^{15} g of organic C in the upper 2 m of soils worldwide (Batjes, 2014). This is more than is stored in the atmosphere and terrestrial vegetation combined, and C fluxes between the soil and atmosphere are an order of magnitude greater than annual CO_2 emissions from the use of fossil fuels (Ciais *et al*., 2013). While globally the land surface is at present a net sink for atmospheric CO_2, accounting for about 25% of emissions from fossil fuels as vegetation grows faster with rising atmospheric CO_2 concentrations (Ciais *et al*., 2013), models predict that at some point in the coming decades this 'CO_2-fertilization' effect will run its course as water, nutrients and other factors become limiting for plant growth (Cox *et al.*, 2000). Meanwhile the rate of turnover of soil carbon will increase with soil warming, and it is predicted that at a tipping point the land surface will switch from being a sink to source of atmospheric CO_2 (Cox *et al*., 2000; Friedlingstein *et al*., 2006).

Therefore preserving and, if possible, increasing soil carbon stocks is seen as crucial for tackling climate change (National Academies of Sciences, Engineering, and Medicine, 2018; Royal Society, 2018). There is substantial interest in how changes in land management could increase soil C sequestration. Possibilities include forest restoration or changes in forestry management (Nave, 2018; Veloso, 2018; Ontl *et al*., 2020); peatland restoration (Leifeld & Menichetti, 2018); and changing agricultural practices, such as no or reduced tillage (Brown *et al*., 2020), and the use of cover crops and retention of crop residues (Bolinder *et al*., 2020). Other possibilities include the application of biochar as a potential method for increasing soil C storage (Smith, 2016), and application of finely-divided silicate rocks to sequester CO_2 as inorganic carbonates in soil (Royal Society, 2018). The 4 per mille initiative, launched in 2015 at COP 21, seeks to increase global carbon stocks in the top 2 m of soils by 4 ‰ to offset anthropogenic greenhouse gas emissions (Minasny *et al.*, 2017). This has been shown over a decadal timescale to be possible in some

soils and agricultural systems (Lord & Sakrabani, 2019), although unlikely in others (Schiefer *et al*., 2010; Wiesmeier *et al*., 2020).

Nonetheless, soils in many parts of the world are currently losing carbon. Local studies and regional-scale inventories showing losses of soil carbon include those on arable and grassland in France (Saby *et al*., 2008), arable land following land-use change in Brazil (Medeiros *et al.*, 2020), pasture in New Zealand for several soil types (Schipper *et al*., 2017), pasture in the permafrost region of the Tibetan Plateau (Yuan *et al*., 2020), and forests and grassland in China (Zhou *et al*., 2019). Examples showing gains in carbon include abandoned former arable land in Russia (Kurganova *at al*., 2012), arable soils in Java (Minasny *et al*., 2010), Mediterranean semiarid forest (Qubaja *et al*., 2020) and forest land in France (Jonard *et al*., 2017). Bellamy *et al*. (2005) found widespread losses of C from soils across England and Wales during the 1980s and 90s. This was mostly due to historic and continuing changes in land management, but potentially also due to warming during that period (Kirk & Bellamy, 2010). Warming is expected to have a particularly large effect on carbon stocks in Arctic soils (Xue *et al*., 2016; Plaza *et al.*, 2019).

Responses of soil respiration to changing climatic conditions are unclear, with potential drivers acting in contradictory directions. Increasing temperatures are expected to promote greater SOM turnover, driving the loss of soil C (Crowther *et al*., 2016). Rising temperatures and atmospheric CO_2 concentrations, meanwhile, are likely to enhance plant growth, increasing plant C inputs to the soil through both elevated rhizodeposition and litterfall (Lewis *et al*., 2009; Pausch & Kuzyakov, 2018). Whether this leads to an increase or decrease in soil C will depend on how soil microbial communities respond. The future of soil carbon stocks is dependent on how processes driving SOM turnover, and those promoting C sequestration, respond to environmental change. Forecasts of SOM turnover are thus reliant on our understanding of these mechanisms.

1.2 Processes controlling soil carbon stocks

The maintenance of soil C stocks depends on the balance between inputs of plant C and losses through the turnover of soil organic matter (SOM). The

capacity of a particular soil to accumulate SOM is finite and depends on complex interactions between physical, chemical and biological processes. Pathways for SOM accumulation differ between the compounds in plant inputs, with non-structural compounds being most-rapidly incorporated into microbial biomass, followed by stabilisation through mineral association. Over time, decomposition products may become physically incorporated into soil aggregates, and proposed mechanisms of stabilisation include both recalcitrance of such compounds and isolation from microbes within aggregates (Dungait *et al*., 2012; Cotrufo *et al*., 2015; Lehmann & Kleber, 2015). Chemical recalcitrance in the form of large, stable 'humic' compounds has traditionally been viewed as the key factor in protecting SOM from microbial decomposition. But more recently physical protection within aggregates has become accepted as the more important process (Schmidt *et al*., 2011; Dungait *et al*., 2012; Lehmann & Kleber, 2015).

Plant-derived C inputs to the soil include root turnover, root exudation and mycorrhizal turnover. Each of these has different seasonal and spatial dynamics in the soil, and different dependencies on plant and soil conditions. Variation in litter inputs and rhizodeposition are seasonal in many ecosystems, and rhizodeposition also varies diurnally, closely linked to changes in solar radiation and the transport and exudation of photosynthetic assimilates (Mencuccini & Hölttä, 2009; Mitra *et al*., 2019). Of these plant C inputs, the dominant source is via plant roots, mediated by processes in the rhizosphere that are not well understood (Hassan *et al*., 2019; Huang *et al*., 2019).

Inputs of fresh plant-derived C and other root-induced changes in the soil may stimulate the turnover of existing SOM and nutrients by soil microbes in so-called 'rhizosphere priming effects' (RPEs), potentially coupling SOM turnover to photosynthesis. There is increasing evidence from field experiments that such effects are important, and that rhizodeposition may be one of the major drivers of SOM turnover (Kuzyakov & Gavrichkova, 2010). However, our understanding of how the magnitudes of RPEs are affected by different plant species and soil types and conditions, such as nitrogen content and

temperature, remains poor (Hopkins *et al*., 2013). Furthermore, patterns of rhizodeposition and RPEs are still unclear, including with regards to variation on diel and seasonal timescales, and the effects of plant phenology (Hopkins *et al*., 2013; Hartmann *et al*., 2020).

One reason for our lack of understanding is that it is challenging to measure below-ground plant and soil dynamics compared with above-ground plant processes. Direct measurement of the processes driving SOM turnover, or of C fluxes through plant and soil pools, is difficult (Bailey *et al*., 2018). Likewise, direct measurement of changes in SOM stocks is not straightforward as such changes are slow and short-term changes are therefore small relative to the much larger total soil C pool (Harden *et al*., 2017), and they may be obscured by soil spatial heterogeneity. While soil-atmosphere C fluxes are easily measured, these necessarily conflate the flux from the plant and recent plant inputs with that from existing SOM. It is nonetheless essential to separate these to disentangle the true responses of SOM turnover to driving variables.

Most existing models with which to analyse plant-driven SOM dynamics determine decomposition based on litter and SOM pool sizes, without considering microbial limitations and dynamics (Schmidt *et al*., 2011). As such, only substrate availability is considered to drive or limit soil respiration and C turnover, and microbial limitations and dynamics are in most cases assumed to be unimportant on seasonal or annual time scales. Given the importance of rhizodeposition as a driver of SOM turnover, an improved understanding of RPEs and their drivers over seasonal to diurnal timescales, and their representation in models, are vital for our understanding of the mechanisms controlling soil C balances.

1.3 Rhizosphere priming effects

Rhizosphere priming effects may be defined as the alteration of rates of existing SOM turnover due to plant root activity and inputs of C through rhizodeposition (Trumbore, 2006; Kuzyakov & Gavrichkova, 2010). While this was first detected in the early 20th century (Löhnis, 1926) interest in it sharply increased following a review by Kuzyakov *et al*. (2000) of possible mechanisms behind it, and the

past two decades have seen a large corpus of work testing priming effects and exploring possible mechanisms behind them.

RPEs ranging from an increase in the rate of SOM turnover of up to 382 % to a decrease of up to 50 % have been measured (Cheng *et al*, 2014). Such results are for bulk soil; within the rhizosphere itself the increase in SOM turnover can be substantially greater (Cheng *et al*, 2014). Given the potential magnitude of RPEs it is vitally important that we understand how they may respond to a changing climate. It has been suggested that RPEs will increase as global temperatures rise (Kuzyakov, 2010); there is some evidence of this, although findings are mixed (Zhu & Cheng, 2011; Yin *et al*., 2019). Increased atmospheric CO_2 concentration may also drive an increase in priming effects due to enhanced plant growth. Under higher CO_2 levels plant rooting depth and C allocation to roots are expected to increase (Nie *et al.*, 2013; Mueller *et al*., 2018), extending the rhizosphere and exposing deeper SOM to increased microbial decomposition. Increased rhizodeposition is also expected, linked with increases in root biomass (Johanson *et al*., 2009 Pritchard, 2011; Jílková *et* al., 2020), and increased SOM decomposition under experimental CO_2 enrichment (Carrillo *et al*., 2014; Nie & Pendall, 2016) may be indicative of increased RPEs. This is particularly significant as greater soil C turnover due to heightened RPEs might work to mitigate any enhancement of C sequestration from increased plant inputs into the soil. This could potentially result in a positive feedback loop, causing further increases in atmospheric CO_2 concentrations. We therefore need to understand controls on rhizosphere priming, both within and between soils, and in terms of broader environmental effects.

The inherent complexity of the soil system and the soil-root interface makes it very difficult to unpick the role of individual factors on the RPE in the field. Past studies have therefore mostly used simplified systems, such as investigations of carbon fluxes in planted pots in controlled or glasshouse conditions (e.g. Shazad *et al*., 2012; Paterson *et al*., 2016; Henneron *et al.*, 2019) or by applying priming compounds to soil samples in the laboratory (e.g. Derrien *et al*., 2014, Lloyd *et al*., 2016, and Zang *et al*., 2016). While not fully representative of

natural environmental variability, such studies have been instrumental in investigating the potential magnitude and behaviour RPEs, including interactions between labile C additions and nitrogen (N) availability on SOM turnover (discussed below).

Until relatively recently most studies of priming effects had been short-term, with few extending beyond a few months (Kuzyakov, 2010). This led to questions surrounding whether priming effects persist over long periods, or are simply short-lived phenomena. More recent research, however, has demonstrated that priming effects may be long-lasting on the scale of months to decades (Huo *et al*., 2017), and priming is maintained under long-term addition of a priming substrate, indicating that it is likely to have a substantial impact on SOM turnover in the field (Zhou *et al*., 2021).

While much of the clearest evidence comes from laboratory studies RPEs have also been investigated in the field. It has been suggested that priming effects are an artefact arising from disturbance in laboratory studies, exposing previously protected soil C to microbial decomposition. (Tian *et al*., 2015; Moinet *et al*., 2018). While measurement in the field is substantially more difficult than in controlled laboratory conditions, strong evidence for RPEs has been found under field conditions (Kumar *et al*., 2016), alongside evidence for diurnal trends in soil respiration in response to plant inputs (Bahn *et al*., 2009; Kuzyakov & Gavrichkova 2010; Hopkins *et al*., 2013; Mitra *et al*., 2019). This temporal linkage between photosynthesis and priming effects over a diurnal scale suggests a close coupling between rates of photosynthesis and RPEs. We do, however, lack studies which combine long-term measurements with high-resolution sampling under field conditions, necessary to investigate how such effects vary over seasonal timescales.

1.3.1 Mechanisms behind rhizosphere priming

The presence and extent of rhizosphere priming effects depend on a broad range of interacting variables. These include those which are plant-driven (including primary production, resource allocation, and root traits), climate-driven (including precipitation, soil temperature, and solar radiation) and soil-

driven (including soil texture, structure, chemistry, and microbial activity) (Cheng *et al*., 2014). While it is not fully clear why both positive and negative priming effects have been found, or the causes for the wide range of magnitudes observed, this may in part be due to variation in soils and plants. Observed RPEs appear to be greater in finer-texture soils and from woody plants rather than grasses (Huo *et al*., 2017). A particularly significant factor controlling RPEs appears to be soil nitrogen availability, which may point to mechanisms driving priming effects.

Nitrogen (N) mining and preferential substrate utilisation are two proposed processes controlling the priming of soil C. The theory behind N mining is based on the principle that microbes physiologically require a stoichiometric balance between C and N. As such, the addition of substrates rich in easily utilised C but relatively poor in N via rhizodeposition provides an excess of C, which is only of use if additional N is obtained. This drives soil microbes to attack previously stable SOM, mobilising N but also mineralising soil C which would otherwise have remained in the soil (Bengtson *et al*., 2012). It has been suggested that this evolved as a mutualism between plants and soil microbes, with the release of labile root exudates mobilising N, some of which may be taken up by the plant (Murphy *et al*., 2017).

Reduction in SOM mineralisation in response to N addition has been found across a broad range of soils in both planted and unplanted systems (Ramirez *et al*., 2012, Zang *et al*., 2016). However, the effects of N addition may vary between soils, and in C-limited systems may cause additional SOM mineralisation (Dijkstra *et al*., 2013). Investigation into the organic compounds decomposed following the addition of a priming sugar in high and low N conditions have indicated that N mining may not, at least in some soils, be a driver of rhizosphere priming (Wild *et al*., 2019). Evidence for N mining is therefore mixed, and variation in response to N addition between soils appears high.

Preferential substrate utilisation has been suggested as a mechanism behind negative priming effects, again linked to N availability. This proposition is that in

soils with high nutrient availability, microbes may preferentially use labile C compounds introduced via rhizodeposition without any need to acquire N from older SOM. As such, rhizodeposition would lead to a decrease in soil respiration (Dijkstra *et al*., 2013). These contrasting priming responses have been suggested as a reason why SOM turnover may vary in its response to N application differ between soils (Dijkstra *et al*., 2013).

1.3.2 Rhizosphere priming in models of soil carbon turnover

At present few models of soil C turnover account for rhizosphere priming effects. Figure 1-1 shows a generic atmosphere-plant-soil C model of the sort that is the basis of the widely-used RothC (Jenkinson, 1990) and CENTURY (Parton *et al*., 1993) models. The model has five below-ground C pools, and the overall rate of change in C is calculated from the sum of the rates of change in each pool, given for the *i*th pool by

$$\mathrm{d}C_\mathrm{i}/\mathrm{d}t = \sum_{j=0,\,j\neq i}^{5} F_\mathrm{ji} - \sum_{i=0,i\neq j}^{5} F_\mathrm{ij}$$

Equation 1-1

where F_{ji} is the flux of C from pool *j* to pool *i* and F_ij is the flux in the opposite direction. The fluxes are defined with first order kinetics:

$$F_\mathrm{ij} = p_\mathrm{ij} q_\mathrm{i} k_\mathrm{i} C_\mathrm{i}$$

Equation 1-2

where k_i is the first order decomposition rate constant of pool *i*, p_ij is the proportion of pool *i* converted to pool *j*, and q_i is a modifier for the effects of temperature, moisture and other variables. All the pool transformations produce CO_2: the above-ground CO_2 flux from plant respiration is $F_\mathrm{sa} - F_\mathrm{as}$; the below-ground CO_2 flux from roots and recent root inputs is $F_\mathrm{0b} + F_\mathrm{1b} + F_\mathrm{2b}$, and that from SOM turnover is $F_\mathrm{3b} + F_\mathrm{4b} + F_\mathrm{5b}$.

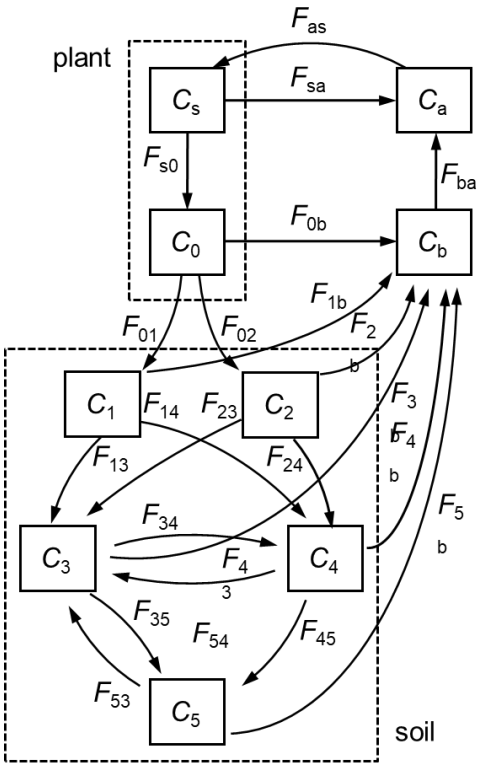

Figure 1-1 Generic plant-soil-atmosphere C model. C_i = pool C contents, F_{iF} = fluxes, *a* = atmos., *b* = soil air, *s* = shoot, 0 = root, 1–2 = plant inputs, 3–5 = SOM of decreasing decomposability

Such models work reasonably well for predicting long-term SOM dynamics in environments for which they have been calibrated (Smith *et al*., 1997). However, they are not so useful for investigating the mechanisms of SOM stabilization and turnover on seasonal and annual time-scales, where microbial limitations and dynamics are important, in addition to the substrate limitations allowed for in the standard models. Where microbial limitations are allowed for, they produce qualitatively different short- and long-term behaviour (Wutzler & Reichstein, 2008; Blagodatsky *et al*., 2010).

Wutzler & Reichstein (2008) and Blagodatsky *et al*. (2010) discuss how priming effects can be allowed for in SOM models. A simple scenario is that priming is the result of fresh C fuelling biological activity such that there is an immediate enhanced decomposition of less reactive SOM pools. This can be modelled using dual-substrate kinetics (Blagodatsky *et al*., 2010). A further level of complexity is that priming is a function of the size or activity of the microbial

biomass, which in turn depends on the supply of fresh C. This implies a time lag between a change of fresh C supply and the priming response, with corresponding differences in kinetics (Wutzler & Reichstein, 2008). Alternatively, priming may occur through disruption of physical protection by specific root exudates (Keiluweit et al., 2015), again with distinct kinetics. Depth-resolved versions of such models can be constructed, with the soil profile divided into horizontal layers each with a version of the scheme in Figure 1-1, and allowing for the vertical distributions of driving variables such as rooting, temperature and moisture (Jenkinson & Coleman, 2008; Phillips *et al*., 2011; Roland *et al*., 2015; Faimon & Langa, 2018).

The need to account for RPEs in models of SOM turnover is clear. Cheng *et al*. (2014) found that accounting for RPEs in the PhotoCent model by increasing decay rates for soil C pools under elevated CO_2 levels was necessary to predict the lack of change in soil C stocks experimentally measured under free-air carbon enrichment (FACE). Such a modification, however, does not properly represent mechanisms behind priming, such as interactions between the microbial C pool and SOM pools, and will not reflect plant-driven seasonal or diurnal variation. Sulman *et al*. (2017) describe the results of a recently developed model which went beyond first-order kinetics, treating microbial biomass as a driver of decomposition alongside soil temperature and moisture. Furthermore, RPEs were simulated by enhancing microbial growth and N mineralisation based on estimated labile C root inputs. The study's results suggested that ecosystem C balances may be dependent on the balance between increased SOM turnover and enhanced plant growth due to increased N availability. The data used to test and validate this model did not include measurements of soil and plant C fluxes on the diel timescales over which rhizodeposition may drive RPEs; however, this is important to consider. The development of such models, and their validation requires datasets of plant and soil C fluxes and their drivers under field conditions with sufficient temporal resolution to gauge diurnal and seasonal patterns.

1.4 Approaches for studying ecosystem and soil C dynamics

Over seasonal, yearly, or longer timescales soil carbon dynamics can be investigated through measurement of soil C content. This can reveal changes in soil C stocks, both as a whole or fractionated to estimate changes in specific SOM pools (e.g. Plaza *et al*., 2016; Awale *et al*., 2017; Craig *et al.*, 2019). While this method is ideally suited to monitoring long-term changes in soil C it is not, however, able to provide resolution within a growing season or a single day. Over shorter timescales direct measurement and partitioning of C fluxes, however, can provide a near-continuous measurement of ecosystem respiration and SOM turnover.

1.4.1 Measurement of plant and soil C fluxes

Two widely used methods for measuring plant and soil fluxes and net ecosystem exchange are the eddy covariance technique and flux chamber methods. The eddy covariance technique is a micrometeorological method using towers equipped with anemometers across three axes and instrumentation for the measurement of C concentration, the data from which are used to measure fluxes based on covariance of fluctuations in vertical wind velocity and CO_2 concentration (Goulden *et* al., 1996; Liang *et al*., 2012). Although usually CO_2 concentration alone is recorded, such systems can also be coupled with an instrument for measuring its $\delta^{13}C$ (Sturm *et al*., 2012). The eddy covariance technique allows measurement of C fluxes from a whole ecosystem, and can be scaled to allow ecosystem respiration measurements in forests (e.g. Barr *et al*., 2013; Rebane *et al*., 2019).

Eddy covariance measures net ecosystem exchange, and is well-suited for gathering data needed to calculate C balances over a whole ecosystem. It is not, however, a useful means of measuring soil C fluxes as partitioning of soil and plant respiration is not possible during daylight. Furthermore, the spatial resolution of eddy covariance systems is in the region of 100 to 2000 m (Liang *et al*., 2012), which may not be too large for investigations of soil C fluxes using smaller plots or mesocosms. Eddy covariance measurements can, however, be

coupled with measurements of soil respiration, for example to explore links between photosynthesis and soil respiration (Vargas *et al*., 2011).

Flux chambers provide a method better suited for measuring respiration fluxes and partitioning them into plant and soil components. This method involves placing a soil flux chamber atop a soil collar or lysimeter and, during chamber closure, connecting the chamber via a pumped sampling loop to instrumentation for measuring CO_2 concentration and $\delta^{13}C$. Opaque chambers can ensure photosynthesis is not occurring when respiration measurements are taken; if opacity is due to removable covers net ecosystem exchange measurements can also be made. Until recently the majority of studies using this method relied upon laborious, manually-operated systems; however, increasing use of automation in flux chambers can allow high-resolution sampling (Görres *et al*., 2016).

The presence of a flux chamber, however, inevitably alters soil C fluxes to a degree. Lateral gas movement within the soil is impeded by the presence of a chamber collar, while during chamber closure build-up of CO_2 in the chamber headspace progressively impedes diffusion of CO_2 from the soil (Görres *et al*., 2016). The latter factor limits the duration of chamber measurements due to increasing nonlinearity of CO_2 concentration increase with increasing closure time. Investigation of different chamber methodologies have shown all to exhibit bias due to disturbance of the steady-state diffusion profile (Nickerson & Risk, 2009). The methodologies examined, however, all used a chamber placed atop a soil collar, and the major cause of bias was diffusion of CO_2 in the soil around the collar. This might be mitigated through an alternative system, such as flux chambers mounted upon deeper collars or fully-enclosed soil monoliths. While these potential sources of error need to be considered, this method is the most suitable technique for allowing partitioning of soil C fluxes from a planted system.

1.4.2 Partitioning of fluxes using stable isotope methods

Studies which seek to explore soil C dynamics in planted systems by measuring carbon fluxes must necessarily separate these fluxes. This can be performed

based on isotopic differences between CO_2 from soil and plant sources. While oxygen isotopes can be used, by far the most common approach is to rely on differences in C isotope ratios. Either labelling or natural abundance methods can be used. Labelling methods use a C isotope as a tracer – this may either be the radionucleotide ^{14}C or the stable isotope ^{13}C. In planted systems this will be in the form of labelled CO_2 (Wang *et al.*, 2020), while in incubation studies a labelled priming sugar can be used (Murphy *et al*., 2015). This creates a difference in the ratio between ^{14}C and ^{12}C, or ^{13}C and ^{12}C (recorded as $\delta^{13}C$), between new photosynthetic assimilates or C additions and the older SOM. Pulse-labelling methods create a signal which can be followed through an ecosystem, and allow the flow of C to be traced from plant into SOM pools, microbial biomass, or back to the atmosphere through plant or soil respiration (Werth and Kuzyakov, 2008; Paterson *et al*., 2009). This method is relatively simple, and well suited to studies into the temporal flow of C through a system (Paterson *et al*., 2009). Pulse signals may fade quickly, however, and need to be regularly repeated over a long experiment (Zhu *et al*., 2019). Furthermore, pulsed ^{13}C or ^{14}C does not distribute uniformly throughout the plant, and concentrate in actively-growing tissues; this may elide respiration from older plant sources (Paterson *et al*., 2009). This method does not create a steady difference between plant and soil isotopic end-members and is not suited to long-term partitioning of plant and soil C fluxes.

An alternative approach is steady ^{13}C labelling. This can be performed by exposing plants air containing an atmospheric level CO_2, but enriched or depleted in ^{13}C, in a controlled environment. This can create large and stable differences between plant and soil end-members, and can allow reliable long-term flux partitioning. Due to the need to airtight conditions, however, this method cannot be used in the field. Open-air continuous ^{13}C labelling requires venting ^{13}C-enriched CO_2, exposing plants to elevated CO_2 levels. This method has been used extensively in free-air carbon enrichment (FACE) experiments (e.g. Andersen *et al*., 2014; Miller *et al*., 2016) to test plant and soil responses to elevated CO_2 scenarios. While this creates a ^{13}C signal which can be traced through the ecosystem, however, this is not a method suitable for separating

plant and soil C fluxes where we wish to investigate soil C flux dynamics under current conditions due to factors such as enhanced rates of photosynthesis and plant growth (Bader *et al*., 2010; Bourgault *et al*., 2017;).

Exploiting differences in the natural abundance of ^{13}C and ^{12}C is more appropriate for systems aiming to represent realistic field conditions and where a constant difference between plant and soil end-member is desired. $\delta^{13}C$ differences exist between the respiration of a given plant, and the CO_2 flux from turnover of SOM residues from that same plant. Such differences are, however, small, in the region of 1-2 ‰ (Bowling *et al*., 2018). Greatly increased distance between plant and SOM end-members can, however, be created by exploiting the difference in $\delta^{13}C$ between the C_3 and C_4 photosynthetic pathways. Growing a C_4 plant in a soil with a history of C_3 vegetation only, or vice versa, can give a difference of approximately 10–20 ‰ (Balesdent *et al*., 1987; Farquhar *et al*., 1989). Both C_3 to C_4 vegetation shifts (Rochette & Flanagan, 1997; Werth & Kuzyakov, 2008; Sun *et al.*, 2020) and the reverse (Wang *et al*., 2016, Xu *et al.*, 2018) have been successfully employed to allow the partitioning of plant and soil respiration, including in studies which have detected rhizosphere priming effects.

This is not, however, to say that there are no difficulties or potential sources of error associated with this method. Firstly, there is a risk that growing a C_4 plant under conditions it is not suited to may not result in interactions between the plant and the soil microbial community representative of a natural system. Secondly, the isotopic distance between C_3 and C_4 plants is less than that which can be achieved by constant ^{13}C labelling (Paterson *et al*., 2009). Furthermore, Kuzyakov (2010) notes that high uncertainties exist due to variation in end-member $\delta^{13}C$ values. Such transient variation may be caused by a range of environmental, spatial, and temporal factors. As stable isotope methods rely on the accuracy of plant and soil end-members, these factors require consideration.

1.5 Factors affecting plant C isotope signatures

Three subtypes of the C_4 pathway exist within grasses, which differ in the enzyme used to decarboxylate the pathway's eponymous C_4 acids: the NAD-ME, NADP-ME, and PEPCK (or PCK) subtypes (Cernusak *et al*. 2013). Differences in mean leaf $\delta^{13}C$ exist between these subtypes; Hattersley *et al*. (1982) found NAD-ME leaves to average -12.70 ‰, NADP-ME -11.95 ‰, and PEPCK -12.70 ‰. Ghannoum *et al*. 2002 found a similar difference between NAD-ME and NAPD-ME leaf $\delta^{13}C$ in a study of 18 C_4 grass species grown in both well-watered and water-stressed treatments. These differences are, however, unlikely to create uncertainty in a system where a single C_4 species or stable community is used, where differences in $\delta^{13}C$ arising from variation in ^{13}C enrichment in plant structures or resulting from environmental influences may predominate.

1.5.1 Differences between plant pools and fluxes

Within a plant, different post-photosynthesis ^{13}C fractionation steps take place in the synthesis of different compounds and structures. Meta-analysis by Werth and Kuzyakov (2010) found the mean enrichment of C_3 plant roots to be 1.2 ‰ compared to shoots; below-ground ^{13}C enrichment was also present in C_4 plants although to a lesser degree, at 0.3 ‰. Further differences have been found between root tissue $\delta^{13}C$ and root respiration $\delta^{13}C$, with mean root respiration 2.1 ± 2.2 ‰ depleted compared to root tissues in C_3 plants, and 1.3 ± 2.0 ‰ in C_4 plants (Werth & Kuzyakov, 2010). This is, however, based on relatively few studies, and the differences found are highly variable. For this reason we focus on testing root:shoot ^{13}C differences in the context of our planted system.

Plant root-shoot ratios change both during growth from a seedling to maturity and in response to environmental conditions such as nutrient availability (Mašková & Herben, 2018) and over seasonal timescales (Haolin et al. 2008 and Parsons & Robson, 1981). As such, any difference in ^{13}C fractionation between root and shoot respiration will result in seasonal differences in net $\delta^{13}C_{plant}$; however, such changes cannot be measured in an intact planted

system without destructive sampling and may present an unavoidable source of partitioning error.

1.5.2 Water stress

Stomatal closure in response to water stress reduces conductance into the leaf and lowers the internal ^{12}C:^{13}C ratio. This results in a lessening of the usual photosynthetic discrimination against ^{13}C (Peters *et al*., 2018). In C_3 plants the change in plant $\delta^{13}C$ due to water availability creates a signal which persists in plant biomass: mean annual precipitation correlates with $\delta^{13}C$ of both C_3 taxa and community assemblages, with ^{13}C depletion increasing with increased precipitation (Diefendorf *et al.*, 2010; Kohn, 2010; Wittimer *et al*., 2008). This relationship is sufficiently strong that Auerswald *et al*. (2009) proposed that precipitation data, when used alongside data on altitude, could be used to predict C_3 $\delta^{13}C$ in their studied area.

C_4 photosynthesis is an adaptation to drier environments, and is inherently more water-efficient than the C_3 pathway. Although water stress can increase or decrease the $\delta^{13}C$ of C_4 respiration the effect is relatively small, most often a decrease of under 1 ‰ (Cernusak *et al.* 2013). A study of 18 C_4 grasses by Ghannoum *et al*. (2002) found a decrease in plant $\delta^{13}C$ of just 0.5 ‰ (smaller than the difference between NAD-ME and NADP-ME species), with the direction of the shift consistent over 18 tested species. In a study of plant $\delta^{13}C$ changes from the wet season to the dry season in an arid region of northwest China, Wang *et al*. (2005) found that the leaf $\delta^{13}C$ of C_3 species decreased by 1.7 ‰, while that of C_4 species showed change in the opposite direction, an enrichment of 1.1 ‰. When C_3 and C_4 plants are subjected to comparable water stress the difference in their responses is clear, such as in a study by Zhong *et al*. (2017) which found that, following a 7-day drought treatment, the $\delta^{13}C$ of the leaf respiration flux of two C_4 grasses increased by 0.6 ‰; in comparison, the leaf respiration $\delta^{13}C$ of a C_3 grass under the same conditions increased by 3.2 ‰. While end-member variation due to water stress may still present a small source of inaccuracy in a C_4 planted system, the lower sensitivity of C_4

photosynthesis is an advantage to employing a C_3 to C_4 shift, rather than the reverse.

1.5.3 Light exposure

Exposure to light and variation in light intensity may affect the $\delta^{13}C$ of plant biomass as plant tissues produced under lower light levels exhibit greater ^{13}C depletion (Cernusak *et al*., 2013). The effect of decreased irradiance on C_4 plant tissue $\delta^{13}C$ can be relatively large, with decreases from 2 ‰ to 8 ‰ observed; this is the greatest source of variation in C_4 plant and isotopic composition (Cernusak *et al*., 2013). This may introduce inaccuracy into flux partitioning reliant on a C_4 plant end-member both spatially and temporally: plants grown in shaded conditions will fix C with a lower $\delta^{13}C$, as may plants during seasonal periods with lower light levels.

Separate from the effect of light levels on carbon fixation, recent illumination or darkness can alter the $\delta^{13}C$ of respiration fluxes. Leaf respiration (by necessity measured in the dark) immediately after a period of illumination is ^{13}C-enriched; its $\delta^{13}C$ progressively decreases throughout a period of darkness. Studying C_3 grasses over a period of 6 h of darkness, Barbour *et al*. (2011) observed a decrease of approximately 5 ‰, with the change almost entirely taking place within the first 2 h. Tcherkez *et al*. (2003) found a longer decrease of approximately 10 ‰ over the course of 5 days in darkness in a C_3 forb; $\delta^{13}C_{plant}$ returned to close to its original value after 6 h in light conditions. Although most studies of this effect have looked at C_3 species, it also exists in C_4 plants. A night-time shift in respiration $\delta^{13}C$ has been observed in two C_4 grasses by Zhong *et al*. (2017), with changes of ranging from -1 ‰ to over -4 ‰ measured over 6 h of darkness. Sun *et al*. (2010) found a similar decrease over 6h of night, ranging from -2 ‰ to over -4 ‰. This effect may cause substantial inaccuracies when partitioning fluxes from a planted system over diurnal timescales.

1.5.4 Nutrient availability

Nutrient availability can alter plant $\delta^{13}C$ by affecting photosynthetic capacity, and is best-studied for N (Cernusak *et al*., 2013). Werth and Kuzyakov (2006) found the shoots, roots, and root respired CO_2 of maize grown under high nutrient conditions to be significantly more ^{13}C-depleted than those from maize grown under lower, or absent, nutrient supply. This effect was relatively small, with a mean decrease in $\delta^{13}C$ of root respiration under high nutrient conditions of -1.6 ‰ when compared to plants grown without nutrient addition. A study comparing levels of N addition by Yang *et al*. (2017) did not find significant effects on C_4 $\delta^{13}C$, although a correlation between higher leaf N content and lower $\delta^{13}C$ was found.

1.6 Factors affecting soil C isotope signatures

Just as $\delta^{13}C$ varies within a single plant, plant inputs to the soil are heterogenous in terms of $\delta^{13}C$, both at the level of whole tissue and molecular level (Bowling *et al*., 2008). SOM, whether developing under C_3 or C_4 vegetation, therefore contains substances with a range of $\delta^{13}C$ values. Here we assess how this can lead to variation in SOM end-member fluxes.

1.6.1 Preferential substrate use

Werth and Kuzyakov (2010) discuss preferential substrate utilization: the selective use of more easily decomposed substances (e.g. glucose) by microbes before more recalcitrant compounds (e.g. lignins). They found that, due to fractionation in the production of new microbial biomass and preferential use of more ^{13}C enriched compounds, microbial biomass was on average 1.2 ‰ enriched compared to SOM in both C_3 and C_4 soils. Microbial respiration presents a further fractionation step, although one which is highly variable, ranging from an enrichment of 4.3 ‰ to a depletion of 3.2 ‰ compared to microbial biomass. Overall, microbial respiration appears to be ^{13}C enriched compared to SOM due to preferential use of compounds higher in ^{13}C, such as sugars (Werth & Kuzyakov, 2010). Soil end-member values obtained by directly measuring the isotopic composition of a soil will therefore introduce

inaccuracies (most likely excessively ^{13}C-depleted) compared to isotopic analysis of respired CO_2.

Inputs of plant residues are not constant through the year, with above- and below-ground residue inputs following seasonal patterns, alongside root exudates. Differences in the rates of decomposition of these inputs will add to temporal variation in the $\delta^{13}C$ of cycling soil C pools (Werth & Kuzyakov, 2010). Due to this the $\delta^{13}C$ of SOM-derived respiration will differ from the isotopic composition of the bulk SOM itself, and may also vary across seasonal timescales. When imposing a C_3–C_4 vegetation change the addition of C_3 material to the soil will cease, and C_4 residues will rapidly start becoming incorporated into the soil. While the incorporation of C_4 litter poses a long-term problem when exploiting isotopic differences in plant and soil respiration to partition net respiration fluxes, and so limits the useful lifespan of a C_3–C_4 system for this, it may work in a study's favour in the short-term as a lack of C_3 inputs will reduce variability in the C_3 SOM end-member.

A further complication is added by differences in $\delta^{13}C$ between bacteria and fungi. Fungal PLFAs have been found to be relatively ^{13}C depleted (ranging from -40.1 ‰ to -30.6 ‰) compared to bacterial PLFAs (-31.1 ‰ to -24.6 ‰), and changes in the net microbial $\delta^{13}C$ with depth can result from changes in the relative dominance of bacteria and fungi (Kohl *et al*., 2015). This may cause inaccuracy in estimations of the soil end-member based on sampling depth, and temporal inaccuracies as seasonal shifts in microbial community structure have been observed (Koranda *et al*., 2013; Shigyo *et al*., 2019). A progressive change in microbial community composition following a C_3–C_4 vegetation switch would introduce a further potential source of inaccuracies; Mellado-Vázquez *et al*. (2019), however, show that this does not necessarily occur.

1.6.2 Changes in $\delta^{13}C$ with depth

The ^{13}C enrichment of SOM typically increases with depth down a soil profile (e.g. Boström *et al*., 2007; Bowling *et al*., 2002; Bowling *et al*., 2003; Flanagan *et al*. 1996; Pausch and Kuzyakov, 2012). This is likely not due to preferential substrate utilisation, which would tend to decrease $\delta^{13}C$ with depth (Boström *et*

al., 2007). Instead, the dilution of atmospheric ^{13}C through the burning of fossil fuels, depleted in ^{13}C relative to the atmosphere, causes $\delta^{13}C_{soil}$ values to change over time (the Suess effect). Between preindustrial measurements from ice cores and 2014, the mean atmospheric $\delta^{13}C$ has decreased from -6.4 ‰ to -8.4 ‰ (Keeling *et al.*, 2017). More recently incorporated plant residues (produced by similar plants under equivalent environmental circumstances) are thus progressively more ^{13}C depleted.

Differences in SOM $\delta^{13}C$ with depth down the soil profile can be substantial, and there is clear evidence of enrichment in ^{13}C between the litter layer and underlying soil. Bowling *et al*. (2002) report a relatively large increase (2.0 ‰) in $\delta^{13}C$ descending down the soil profile from fresh litter to old litter (mean of three sites), and a further increase of 1.2 ‰ from old litter to the upper 0–5 cm of soil (mean of 4 sites). Similar increases with depth are present between the upper, organic horizon and the underlying mineral soil horizon, such as a mean increase of 0.8 ‰ between the organic-rich upper soil layer and mineral soil at 10 cm depth found by Fessenden & Ehleringer (2003) and a mean increase of 1.2 ‰ between the O horizon and 0–10 cm depth A horizon found by Trudell *et al*., (2004) at two sites. SOM $\delta^{13}C$ continues to increase further down the mineral soil profile, although in some soils this effect has been observed to decline with depth (Bowling *et al*., 2002, Fessenden & Ehleringer, 2003). The increase in $\delta^{13}C$ with depth does not only apply to bulk SOM, but also SOM derived respiration, which Boström *et al*. (2007) found to increase from -28.6 ± 1.5 ‰ in the litter layer to -24.9 ± 2.0 ‰ at 20-50 cm depth.

The impact of this on studies using a C_3 to C_4 vegetation shift primarily relates to sampling soil to measure the soil end-member. Measurements of bulk soil $\delta^{13}C$ which neglect to sample a representative soil profile risk skewing the soil end-member. Sampling to depth down a soil profile, however, also risks introducing inaccuracies. Soil respiration declines with depth in undisturbed soil (Kellman *et al*., 2015); $\delta^{13}C$ measurements made by direct isotopic analysis of sampled soil may overestimate the contribution of deeper SOM to soil respiration fluxes. $\delta^{13}C$ measurements based on respiration fluxes from

sampled soil, however, also risk inaccuracies as disturbance is likely to increase the accessibility of previously protected SOM to microbes, and may increase the rate of respiration in soil from deeper in the profile. If roots can be excluded, sampling the soil end-member *in situ* may minimise inaccuracies.

1.6.3 Incorporation of C_4 material into C_3 SOM and microbial C pools

As time since a C_3–C_4 vegetation switch progresses the ^{13}C abundance of both SOM pools and microbial biomass will increase as C_4 plant residues are incorporated. An estimation of the rate of C_4 C incorporation can be found in McCloskey *et al*. (2020). This may provide a useful estimation of the usable lifespan of such a system for flux partitioning. Kramer and Gleixner (2006) report increases in SOM $\delta^{13}C$ of 4.6 ‰ and 2.4 ‰ following 23 and 39 years of maize cultivation respectively at two separate sites. The changes in PLFA isotopic composition at the same sites were larger (7 ‰ and 3.4 ‰ respectively) and indicate that the microbial pool was composed of approximately 50% and 20% respectively of newer, C_4, carbon. Over time, partitioning based on the original C_3 soil end-member will therefore no longer be representative of SOM fluxes, limiting the lifespan of such systems.

1.7 Aims and objectives

While previous studies have partitioned plant and soil C fluxes in the field and examined evidence for rhizosphere priming effects, there exists no long-term, high-resolution dataset of plant and soil C fluxes alongside potential drivers from undisturbed soils in field conditions with which to investigate the magnitude and mechanisms of rhizosphere priming effects. Such data are required both to assess mechanisms driving rhizosphere priming on diurnal scales and how these may vary seasonally, and to allow us to test and improve dynamic models of SOM turnover. Through this study I therefore first sought to establish such a system and validate the methodology for measuring and analysing plant and soil C fluxes, before using the system to explore the extent to which rhizosphere priming could be detected in the system and possible mechanisms behind it, including diurnal and seasonal effects. Towards these ends I had the following three objectives.

Objective 1: To establish an experimental system for measuring plant and soil C fluxes near-continuously under field conditions using stable isotope techniques

To assess rhizosphere priming and its drivers under realistic field conditions, a field laboratory system is required capable of high-resolution and long-term flux measurements. The system needs to be automated to allow high-resolution measurements over long periods. Under Objective I used the Wolfson Field Laboratory (WFL) at Cranfield University, which was established in 2011 to provide such a system. To my knowledge, the WFL is unique in being able to measure (a) both plant and soil carbon fluxes; (b) potential drivers of these, such as soil moisture and temperature; (c) with sufficient frequency to resolve diurnal patterns; and (d) over seasonal and annual timescales. Previous work in the WFL had not involved sufficient isotopic distance between plant and soil end-members to allow reliable flux partitioning. The first objective of this study was to refurbish this system and set it up in such a way that fluxes could be partitioned, and then to assess its capability for partitioning net respiration fluxes between plant and SOM sources.

Objective 2: To develop methods for analysing C fluxes measured with this system

The field system developed under Objective 1 generates large, complex datasets of C fluxes, isotope signatures and environmental drivers of fluxes. Under Objective 2 I developed methods for analysing such datasets. A particular issue is how to characterise the plant and soil end-member isotope signatures and their variation over time. A range of environmental factors affect both the plant and soil end-members. I needed to assess potential sources of error in flux partitioning and develop a methodology to mitigate these. This was a critical step between developing the capacity to measure fluxes and being able to confidently use the dataset gathered to test hypotheses relating to rhizosphere priming.

Objective 3: To use the system to investigate the extent and mechanisms of rhizosphere priming effects in two contrasting C_3 soils under a C_4 grass

Under this Objective I collected datasets of plant and soil C fluxes and their drivers over two growing seasons in two contrasting, naturally structured C_3 soils planted with a C_4 grass. I used these datasets to investigate factors affecting the plant and soil C fluxes and rhizosphere priming over diurnal and seasonal timescales. I explored whether N mining was a driver of priming under these conditions.

1.8 Thesis structure

Chapter 1. Introduction

Chapter 2. A field system for measuring plant and soil carbon fluxes using stable isotope methods. This chapter addresses Objective 1.

Chapter 3. On allowing for transient variation in end-member δ13C values in isotopic partitioning of ecosystem respiration. This chapter addresses Objective 2.

Chapter 4. Evidence for tight coupling between photosynthesis and soil carbon turnover from diurnal and seasonal patterns in a C4 grass grown in two C3 soils under field conditions. This chapter addresses Objective 3.

Chapter 5. Discussion, conclusions and future work. Here I synthesise the results from Chapters 2–3, and assess the overall findings from this study.

1.9 Published and submitted work

McCloskey, C.S., Otten, W., Paterson, E., Ingram, B. & Kirk, G.J.D. 2020. A field system for measuring plant and soil carbon fluxes using stable isotope methods. *European Journal of Soil Science*, DOI: 10.1111/ejss.13016.

McCloskey, C.S., Otten, W., Paterson, E. & Kirk, G.J.D. 2021. On allowing for transient variation in end member δ^{13}C values in isotopic partitioning of ecosystem respiration. *European Journal of Soil Science*, in review.

McCloskey, C.S., Otten, W., Paterson, E. & Kirk, G.J.D. 2021. Evidence for tight coupling between photosynthesis and soil carbon turnover from diurnal and

seasonal patterns in a C4 grass grown in two C3 soils under field conditions. Target journal: *New Phytologist*, in preparation.

1.10 References

Auerswald, K., Wittmer, M.H.O.M., Männel, T.T., Bai, Y.F., Schäufele, R. & Schnyder, H. 2009. Large regional-scale variation in C_3/C_4 distribution pattern of Inner Mongolia steppe is revealed by grazer wool carbon isotope composition. *Biogeosciences, 6*, 795–805.

Andresen, L.C., Dungait, J.A.J., Bol, R, Selsted, M.B., Ambus, P. Selsted, M.B., Ambus, P. & Michelsen, A. 2014. Bacteria and Fungi Respond Differently to Multifactorial Climate Change in a Temperate Heathland, Traced with ^{13}C-Glycine and FACE CO_2. *PLOS ONE, 9*, e85070. https://doi.org/10.1371/journal.pone.0085070.

Awale, R., Emeson, M.A. & Machado, S. 2017. Soil Organic Carbon Pools as Early Indicators for Soil Organic Matter Stock Changes under Different Tillage Practices in Inland Pacific Northwest. *Frontiers in Ecology and Evolution*, *5*, https://doi.org/10.3389/fevo.2017.00096.

Bader, M.KF., Siegwolf, R. & Körner, C. 2010. Sustained enhancement of photosynthesis in mature deciduous forest trees after 8 years of free air CO_2 enrichment. *Planta*, *232*, 1115–1125.

Bahn M, Schmitt M, Siegwolf R, Richter A Brüggemann N. 2009. Does photosynthesis affect grassland soil-respired CO_2 and its carbon isotope composition on a diurnal timescale? *New Phytologist*, *182*, 451–460.

Bailey, VL, Bond-Lamberty, B, DeAngelis, K, Grandy, A.S., Hawkes, C.V., Heckman, K., Lajtha, K., Phillips, R.P., Sulman, B.N., Todd-Brown, K.E.O. & Wallenstein, M.D. 2018. Soil carbon cycling proxies: Understanding their critical role in predicting climate change feedbacks. *Global Change Biology*, *24*, 895–905.

Balesdent J, Mariotti A, Guillet B. 1987. Natural ^{13}C abundance as a tracer for studies of soil organic matter dynamics. *Soil Biology and Biogeochemistry, 19*, 25–30.

Barbour, M.M., Hunt, J.E., Kodama, N., Laubach, J., McSeveny, T.M., Rogers, G.N., Tcherkez, G. & Wingate, L. 2011. Rapid changes in $\delta^{13}C$ of ecosystem-respired CO_2 after sunset are consistent with transient ^{13}C enrichment of leaf respired CO_2. *New Phytologist, 190*, 990–1002.

Barr, J.G., Engel, V., Fuentes, J.D., Fuller, D.O. & Kwon, H. 2013. Modelling light use efficiency in a subtropical mangrove forest equipped with CO2 eddy covariance. *Biogeosciences*, *10*, 2145–2158.

Batjes, N.H. 2014. Total carbon and nitrogen in the soils of the world. *European Journal of Soil Science, 65*, 10–21.

Baumert, V.L., Vasilyeva, N.A., Vladimirov, A.A., Meier, I.C., Kögel-Knabner, I. & Mueller, C.W. 2018. Root Exudates Induce Soil Macroaggregation Facilitated by Fungi in Subsoil. *Frontiers in Environmental Science*, *6*, 140.

Blagodatsky, S., Blagodatskaya, E., Yuyukinaa, T., Kuzyakov, Y. 2010. Model of apparent and real priming effects: Linking microbial activity with soil organic matter decomposition. *Soil Biology and Biochemistry, 42*, 1275–1283.

Bellamy, P.H., Loveland, P.J., Bradley, R.I., Lark, R.M. & Kirk, G.J.D. 2005. Carbon losses from all soils across England and Wales 1978–2003. *Nature, 437*, 245–248.

Bengtson, P., Barker, J. & Grayston, S. J. 2012. Evidence of a strong coupling between root exudation, C and N availability, and stimulated SOM decomposition caused by rhizosphere priming effects. *Ecology and Evolution, 2*, 1843–1852.

Bolinder, M.A., Crotty, F., Elsen, A., Frac, M., Kismányoky, T., Lipiec, J., Tits, M., Tóth, Z. & Kätterer, T. 2020. The effect of crop residues, cover crops, manures and nitrogen fertilization on soil organic carbon changes in

agroecosystems: a synthesis of reviews. *Mitigation and Adaptation Strategies for Global Change*, *25*, 929–952.

Boström, B., Comstedt, D. & Ekblad, A. 2007. Isotope fractionation and 13C enrichment in soil profiles during the decomposition of soil organic matter. *Oecologia, 153*, 89–98.

Bourgault, M., Brand, J., Tausz-Posch, S., Armstrong, R.D., O'Leary, G.L., Fitzgerald, G.J. & Tausz, M. 2017. Yield, growth and grain nitrogen response to elevated CO_2 in six lentil (*Lens culinaris*) cultivars grown under Free Air CO_2 Enrichment (FACE) in a semi-arid environment. *European Journal of Agronomy*, *87*. 50–58.

Bowling, D.R., McDowell, N.G., Bond, B.J., Law, B.E. & Ehleringer, J.R. 2002. ^{13}C content of ecosystem respiration is linked to precipitation and vapor pressure deficit. *Oecologia*, *131*, 113–124.

Bowling, D.R, Pataki, D.E. & Ehleringer, J.R. 2003. Critical evaluation of micrometeorological methods for measuring ecosystem–atmosphere isotopic exchange of CO_2. *Agricultural and Forest Meteorology*, *116*, 159–179.

Bowling, D.R., Pataki, D.E. & Randerson, J.T. 2008. Carbon isotopes in terrestrial ecosystem pools and CO_2 fluxes. *New Phytologist*, *178*, 24–40.

Brown, J., Stobart, R., Hallett, P., Morris, N.L., George, T.S., Newton, A.C., Valentine, T.A. & McKenzie, B.M. 2020. Variable impacts of reduced and zero tillage on soil carbon storage across 4–10 years of UK field experiments. *Journal of Soils and Sediments*, https://doi.org/10.1007/s11368-020-02799-6

Carrillo, Y., Dijkstra, F.A., LeCain, D., Morgan, J.A., Blumenthal, D., Waldron, S. & Pendall., E. 2014. Disentangling root responses to climate change in a semiarid grassland. *Oecologia*, *175*, 699–711.

Cernusak, L.A., Ubierna, N., Winter, K., Holtum, J.A.M., Marshall, J.D. and Farquhar, G.D. 2013. Environmental and physiological determinants of carbon isotope discrimination in terrestrial plants. *New Phytologist*, *200*, 950–965.

Cheng, W., Parton, W. J., Gonzalez-Meler, M. A., Phillips, R., Asao, S., Mcnickle, G. G., Brzostek, E. & Jastrow, J. D. 2014. Synthesis and modelling perspectives of rhizosphere priming, *New Phytologist*, *201*, 31–44.

Ciais, P. *et al.* 2013. Carbon and other biogeochemical cycles. In T.F. Stocker, D. Qin, G.K. Plattner, M. Tignor, S.K. Allen, J. Boschung, A. Nauels, Y. Xia, V. Bex, P.M. Midgley *(eds) Climate Change 2013: The Physical Science Basis. Contribution of Working Group I to the Fifth Assessment Report of the Intergovernmental Panel on Climate Change*. Cambridge University Press, Cambridge.

Cotrufo M.F., Soong, J., Horton, A. *et al*. 2015. Formation of soil organic matter via biochemical and physical pathways of litter mass loss. *Nature Geoscience 8*, 776–779.

Cox, P.M., Betts, R.A., Jones, C.D., Spall, S.A. & Totterdell, I.J. 2000. Acceleration of global warming due to carbon-cycle feedbacks in a coupled climate model. *Nature, 408*, 184-187.

Craig, M.E., Lovko, N., Flory, S.L., Wright, J.P. & Phillips, R.P. 2019. Impacts of an invasive grass on soil organic matter pools vary across a tree-mycorrhizal gradient. *Biogeochemistry*, *144*, 149–164.

Crowther, T., Todd-Brown, K., Rowe, C. *et al*. 2016. Quantifying global soil carbon losses in response to warming. *Nature, 540*, 104–108.

De Souza Medeiros, A., Maia, S.M.F., dos Santos, T.C. & de Araújo Gomes, T.C. 2020. Soil carbon losses in conventional farming systems due to land-use change in the Brazilian semi-arid region. *Agriculture, Ecosystems & Environment*, *287*, https://doi.org/10.1016/j.agee.2019.106690.

Derrien, D., Plain, C., Courty, P.-C., Gelhaye, L., Moerdijk- Poortvliet, T.C.W., Thomas, F., Versini, A., Zeller, B., Koutika, L.-S., Boschker, H.T.S., & Epron, D. 2014. Does the addition of labile substrate destabilise old soil organic matter? *Soil Biology & Biogeochemistry*, *76*, 149–160.

Diefendorf, A.F., Mueller, K.E., Wing, S.L., Koch, P.L., Freeman, K.H. 2010. Global patterns in leaf ^{13}C discrimination and implications for studies of past and future climate. *Proceedings of the National Academy of Sciences*, *107*, 5738–5743.

Dijkstra, F.A., Carrillo, Y., Pendall, E. & Morgan, J.A. 2013. Rhizosphere priming: a nutrient perspective. *Frontiers in Microbiology*, *4*, 183–190.

Dungait, A.J., Hopkins, D.W., Gregory, A.S. & Whitmore, A.P. 2012. Soil organic matter turnover is governed by accessibility not recalcitrance. *Global Change Biology, 18*, 1781–1796.

Faimon, J. & Langa, M. 2018. What actually controls the minute to hour changes in soil carbon dioxide concentrations? *Geoderma*, *323*, 52–64.

Farquhar, G.D., Ehleringer, J.R. & Hubick, K.T. 1989. Carbon isotope discrimination and photosynthesis. *Annual Review of Plant Physiology and Plant Molecular Biology, 40,* 503–537.

Fessenden, J.E. and Ehleringer, J.R. 2003. Temporal variation in $\delta^{13}C$ of ecosystem respiration in the Pacific Northwest: links to moisture stress. *Oecologia*, 136, 129–136.

Friedlingstein. P., Cox, P. Betts, R. *et al*., 2006. Climate–carbon cycle feedback analysis: Results from the C^4MIP model intercomparison. *Journal of Climate, 19*, 3337–3353.

Ghannoum, O., von Caemmerer, S. & Conroy, J.P. 2002. The effect of drought on plant water use efficiency of nine NAD–ME and nine NADP–ME Australian C_4 grasses. *Functional Plant Biology*, *29*, 1337–1348.

Görres, C.-M., Kammann, C. & Ceulemans, R. 2016. Automation of soil flux chamber measurements: potentials and pitfalls. *Biogeosciences*, *13*, 1949–1966.

Hallama, M., Pekrun, C., Lambers, H. & Kandeler, E. 2019. Hidden miners – the roles of cover crops and soil microorganisms in phosphorus cycling through agroecosystems. *Plant and Soil*, *434*, 7–45.

Haolin, G., Yuhui, W., Fengyu, W. & Bingrui, J. 2008. Dynamics of root-shoot ratio and environmental effective factors of recovering *Leymus chinensis* steppe vegetation in Inner Mongolia, China. *Acta Ecologica Sinica*, *28*, 4629–4634.

Harden, J.W., Hugelius, G., Ahlström, A., et al. 2018. Networking our science to characterize the state, vulnerabilities, and management opportunities of soil organic matter. *Global Change Biology*, *24*, e705– e718.

Hartmann, H., Bahn, M., Carbone, M. & Richardson, A.D. 2020. Plant carbon allocation in a changing world – challenges and progress: introduction to a Virtual Issue on carbon allocation. *New Phytologist, 227*, 981–988.

Hassan, M.K., McInroy, J.A. & Kloepper, J.W. 2019. The Interactions of Rhizodeposits with Plant Growth-Promoting Rhizobacteria in the Rhizosphere: A Review. *Agriculture*, *9*, 10.3390/agriculture9070142.

Henneron, L., Cros, C., Picon-Cochard, C., Rahimian, V., & Fontaine, S. 2019. Plant economic strategies of grassland species control soil carbon dynamics through rhizodeposition. *Journal of Ecology*, *108*, 528– 545.

Henneron, L., Kardol, P., Wardle, D.A., Cros, C. & Fontaine, S. 2020. Rhizosphere control of soil nitrogen cycling: a key component of plant economic strategies. *New Phytologist*, *228*, 1269-1282.

Hopkins, F., Gonzalez-Meler, M.A., Flower, C.E., Lynch, D.L., Czimczik, C., Tang, J. & Subke, J.-A. 2013. Ecosystem-level controls on root-rhizosphere respiration. *New Phytologist, 199*, 339–351.

Huang, J., Liu, W., Deng, M., Wang, X., Wang, Z., Yang, L. & Liu, L. 2019. Allocation and turnover of rhizodeposited carbon in different soil microbial groups, *Soil Biology and Biochemistry*, *150*, https://doi.org/10.1016/j.soilbio.2020.107973.

Huo, C., Luo, Y. & Cheng, W. 2017. Rhizosphere priming effect: A meta-analysis. *Soil Biology and Biochemistry*, *111*, 78-84.

Jenkinson, D.S. 1990. The turnover of organic carbon and nitrogen in soil. *Philosophical Transactions of the Royal Society London* B, *329*, 361–388.

Jenkinson, D.S. & Coleman, K. 2008. The turnover of organic carbon in subsoils. Part 2. Modelling carbon turnover. *European Journal of Soil Science*, 59, 400–441.

Jílková, V., Sim, A., Thornton, B., Jandová, K., Cajthaml, T. & Paterson, E. 2020. Impact of plant species and atmospheric CO_2 concentration on rhizodeposition and soil microbial activity and community composition. *Journal of Plant Nutrition and Soil Science*, *183*, 327-337.

Johansson, E.M., Fransson, P.M.A., Finlay, R.D.& van Hees, P.A.W. 2009. Quantitative analysis of soluble exudates produced by ectomycorrhizal roots as a response to ambient and elevated CO_2. *Soil Biology and Biochemistry*, *41*, 1111-1116.

Jonard, M., Nicolas, M., Coomes, D.A., Caignet, I., Saenger, A. & Ponette, Q. 2017. Forest soils in France are sequestering substantial amounts of carbon. *Science of The Total Environment*, *574*, 616-628.

Keeling, R.F., Graven, H.D., Welp, L.R., Resplandy, L., Bi, J., Piper, S.C., Sun, Y., Bollenbacher, A. & Meijer, H.A.J. 2017. Trend in 13C discrimination of land photosynthesis. *Proceedings of the National Academy of Sciences*, *114*, 10361–10366.

Keiluweit, M., Bougoure, J.J., Nico PS, Pett-Ridge, J., Weber, P.K., Kleber, M. 2015. Mineral protection of soil carbon counteracted by root exudates. *Nature Climate Change,* DOI:10.1038/NCLIMATE2580.

Kellman, L., Myette, A. & Beltrami, H. 2015. Depth-dependent mineral soil CO_2 production processes: sensitivity to harvesting-induced changes in soil climate. *PLOS ONE*, 10: e0134171

Kirk, G.J.D., Bellamy, P.B. & Lark, R.M. 2010. Changes in soil pH across England and Wales in response to decreased acid deposition. *Global Change Biol*ogy, *16*, 3111–3119.

Kohl, L., Laganière, J., Edwards, K.A., Billings, S.A., Morrill, P.L., Van Biesen, G. & Zeigler, S.E. 2015. Distinct fungal and bacterial $\delta^{13}C$ signatures as potential drivers of increasing $\delta^{13}C$ of soil organic matter with depth. *Biogeochemistry*, *124*, 13–26.

Kohn, M.J. 2010. Carbon isotope compositions of terrestrial C_3 plants as indicators of (paleo)ecology and (paleo)climate. *Proceedings of the National Academy of Sciences*, *107*, 19691–19695.

Koranda, M., Kaiser, C., Fuchslueger, L., Kitzler, B., Sessitsch, A., Zechmeister-Boltenstern, S. & Richter, A. 2013. Seasonal variation in functional properties of microbial communities in beech forest soil. *Soil Biology and Biochemistry*, *60*, 95–105.

Kramer, C. and Gleixner, G. 2006. 'Variable use of plant- and soil-derived carbon by microorganisms in agricultural soils' *Soil Biology and Biochemistry*, 28, 3267–3278.

Kumar, A., Kuzyakov, Y. & Pausch, J. 2016. Maize rhizosphere priming: field estimates using ^{13}C natural abundance. *Plant and Soil*, *409*, 87–97.

Kurganova, I., Lopes de Gerenyu, V., Six, J. & Kuzyakov, Y. 2014. Carbon cost of collective farming collapse in Russia. *Global Change Biology*, *20*, 938-947.

Kuzyakov, Y., Friedel, J.K., Stahr, K. 2000. Review of mechanisms and quantification of priming effect. *Soil Biology and Biochemistry*, *32*, 1485-1498.

Kuzyakov, Y. 2006. Sources of CO_2 efflux from soil and review of partitioning methods. *Soil Biology & Biochemistry*, *38*, 425–448.

Kuzyakov, Y. 2010. Priming effects: Interactions between living and dead organic matter. *Soil Biology and Biochemistry*, *42*, 1363–1371.

Kuzyakov, Y. & Gavrichkova, O. 2010. Time lag between photosynthesis and carbon dioxide efflux from soil: A review of mechanisms and controls. *Global Change Biology*, *16*, 3386–3406.

Lehmann, J. & Kleber, M. 2015. The contentious nature of soil organic matter. *Nature*, *528*, 60–68.

Leifeld, J. & Menichetti, L. 2018. The underappreciated potential of peatlands in global climate change mitigation strategies. *Nature Communication*s, *9,* 1071.

Lewis, S., Lopez-Gonzalez, G., Sonké, B. et al. 2009. Increasing carbon storage in intact African tropical forests. *Nature*, *457*, 1003–1006.

Lloyd D., Ritz K., Paterson E. & Kirk G.J.D. 2016. Effects of soil type and composition of rhizodeposits on rhizosphere priming phenomena. *Soil Biology and Biochemistry*, *103*, 512–521.

Löhnis, F. 1926. Nitrogen availability of green manures. *Soil Science*, *22*, 253–290.

Lord, R. & Sakrabani, R. 2019. Ten-year legacy of organic carbon in non-agricultural (brownfield) soils restored using green waste compost exceeds 4 per mille per annum: Benefits and trade-offs of a circular economy approach. *Science of The Total Environment*, *686*, 1057–1068.

Mašková, T, Herben, T. 2018. Root:shoot ratio in developing seedlings: How seedlings change their allocation in response to seed mass and ambient nutrient supply *Ecology and Evolution*, *8*, 7143– 7150.

McCloskey, C.S., Otten, W., Paterson, E., Ingram, B. & Kirk, G.J.D. 2020. A field system for measuring plant and soil carbon fluxes using stable isotope methods. *European Journal of Soil Science*, DOI: 10.1111/ejss.13016.

Mellado-Vázquez, P.G., Lange, M. & Gleixner, G. 2019. Soil microbial communities and their carbon assimilation are affected by soil properties and season but not by plants differing in their photosynthetic pathways (C_3 vs. C_4). *Biogeochemistry*, *142*, 175–187.

Mencuccini, M. & Hölttä, T. 2010. The significance of phloem transport for the speed with which canopy photosynthesis and belowground respiration are linked. *New Phytologist*, *185*, 189–203.

Miller, A.D., Dietze, M.C., DeLucia, E.H. & Anderson-Teixeira, K.J. 2016. Alteration of forest succession and carbon cycling under elevated CO_2. *Global Change Biology*, *22*, 351-363.

Minasny, B., Sulaeman, Y. and McBratney, A.B.2011. Is soil carbon disappearing? The dynamics of soil organic carbon in Java. *Global Change Biology*, *17*, 1917-1924.

Minasny, B., Malone, B.P., McBratney, A.B., Angers, D.A., Arrouays, D., Chambers, A., Chaplot, V., Chen, Z.-S., Cheng, K., Das, B.S., Field, D.J., Gimona, A., Hedley, C.B., Hong S.Y., Mandal, B., Marchant, B.P., Martin, M., McConkey, B.G., Mulder, V.L., O'Rourke, S., Richer-de-Forges, A.C., Odeh, I., Padarian, J., Paustian, K., Pan, G., Poggio, L., Savin, I., Stolbovoy, V., Stockmann, U., Sulaeman, Y., Tsui, C.-C., Vågen, T.-C., van Wesemael, B. & Winowiecki, L. 2017. Soil carbon 4 per mille. *Geoderma*, *292*, 59-86.

Mitra B., Miao, G., Minick, K., McNulty, S.G., Sun, G., Gavazzi, M., King, J.S. & Noormets, A. 2019. Disentangling the effects of temperature, moisture, and substrate availability on soil CO_2 efflux. *Journal of Geophysical Research: Biogeosciences*, *124*, 2060–2075.

Moinet, G.Y.K., Midwood, A.J., Hunt, J.E., Whitehead, D., Hannam, K.D., Jenkins, M., Brewer, M.J., Adams, M.A. & Millard, P. 2018. Estimates of rhizosphere priming effects are affected by soil disturbance. *Geoderma*, *313*, 1–6.

Mueller, K.E., LeCain, D.R., McCormack, M.L., Pendall, E., Carlson, M. & Blumenthal, D.M. 2018. Root responses to elevated CO_2, warming and irrigation in a semi-arid grassland: Integrating biomass, length and life span in a 5-year field experiment. *Journal of Ecology*, *106*, 2176– 2189.

Murphy, C.J., Baggs, E.M., Morley, N., Wall, D.P. & Paterson, E. 2015. Rhizosphere priming can promote mobilisation of N-rich compounds from soil organic matter. *Soil Biology and Biochemistry*, *81*, 236-243.

Murphy, C.J., Baggs, E.M., Morley, N., Wall, D.P. & Paterson, E. 2017. Nitrogen availability alters rhizosphere processes mediating soil organic matter mineralisation. *Plant and Soil*, *417*, 499–510.

National Academies of Sciences, Engineering, and Medicine. 2018. *Negative Emissions Technologies and Reliable Sequestration: A Research Agenda*. The National Academies Press, Washington, DC. doi: https://doi.org/10.17226/25259.

Nave, L.E., Domke, G.M., Hofmeister, K.L., Mishra, U., Perry, C.H., Walters, B.F., Swanston, C.W. 2018. Reforestation can sequester two petagrams of carbon in US topsoils in a century. *Proceedings of the National Academy of Sciences*, *115*, 2776-2781.

Nie, M., Lu, M., Bell, J., Raut, S. & Pendall, E. 2013. Root traits at elevated CO_2. *Global Ecology and Biogeography*, *22*, 1095-1105.

Nie, M. & Pendall, E. 2016. Do rhizosphere priming effects enhance plant nitrogen uptake under elevated CO_2? *Agriculture, Ecosystems & Environment*, *224*, 50-55.

Ontl, T.A., Janowiak, M.K., Swanston, C.W., Daley, J., Handler, S., Cornett, M., Hagenbuch, S., Handrick, C., Mccarthy, L. & Patch, N. 2020. Forest Management for Carbon Sequestration and Climate Adaptation. *Journal of Forestry*, *118*, 86–101.

Parsons, A.J. & Robson M.J. 1981. Seasonal Changes in the Physiology of S24 Perennial Ryegrass (*Lolium perenne* L.): 3. Partition of Assimilates between Root and Shoot during the Transition from Vegetative to Reproductive Growth. *Annals of Botany*, *48*, 733–744.

Parton W.J., Scurlock J.M.O., Ojima D.S., Gilmanov T.G., Scholes R.J., Schimel D.S., Kirchner T., Menaut J.-C., Seastedt T., Garcia Moya E.,

Kamnalrut A. & Kinyama J.I. 1993. Observations and modelling of biomass and soil organic matter dynamics for the grassland biome worldwide. *Global Biogeochemical Cycles, 7*, 785–809.

Paterson E, Midwood AJ & Millard P. 2009. Through the eye of the needle: a review of isotope approaches to quantify microbial processes mediating soil carbon balance. *New Phytologist*, *184*, 19–33.

Pausch, J. & Kuzyakov, Y. 2018. Carbon input by roots into the soil: Quantification of rhizodeposition from root to ecosystem scale. *Global Change Biology*, *24*, 1– 12.

Peters, W., van der Velde, I.R., van Schaik, E., Miller, J.B., Ciais, P., Duarte, H.F., van der Laan-Luijkx, I.T., van der Molen, M.K., Scholze, M., Schaefer, K., Vidale, P.L., Verhoef, A., Wårlind, D., Zhu, D., Tans, P.P., Vaughn, B. & White, J. 2018. Increased water-use efficiency and reduced CO_2 uptake by plants during droughts at a continental-scale. *Nature Geoscience*, *11*, 744–748.

Plaza, C., Giannetta, B., Fernández, J.M., López-de-Sá, E.G., Polo, A., Gascó, G., Méndez, A. & Zaccone, C. 2016. Response of different soil organic matter pools to biochar and organic fertilizers. *Agriculture, Ecosystems & Environment*, *225*, 150-159.

Plaza, C., Pegoraro, E., Bracho, R., Celis, G., Crummer, K.G., Hutchings, J.A., Hicks Pries, C.E., Mauritz, M., Natali, S.M., Salmon, V.G., Schädel, C., Webb E.E. & Schuur, E.A.G. 2019. Direct observation of permafrost degradation and rapid soil carbon loss in tundra. *Nature Geoscience*, *12*, 627–631.

Qubaja, R, Grünzweig, JM, Rotenberg, E, Yakir, D. 2020. Evidence for large carbon sink and long residence time in semiarid forests based on 15 year flux and inventory records. *Global Change Biology*, *26*, 1626– 1637.

Ramirez, K.S., Craine, J.M. & Fierer, N. 2012. Consistent effects of nitrogen amendments on soil microbial communities and processes across biomes. *Global Change Biology*, 18, 1918–1927.

Rebane, S., Jõgiste, K., Põldveer, E., Stanturf, J.A. & Metslaid, M. 2019. Direct measurements of carbon exchange at forest disturbance sites: a review of results with the eddy covariance method. *Scandinavian Journal of Forest Research*, *34*, 585-597.

Paterson, E., Sim., A., Davidson, J. & Daniell., T.J. 2016. Arbuscular mycorrhizal hyphae promote priming of native soil organic matter mineralisation. *Plant and Soil*, *408*, 243–254.

Phillips, C.L., Nickerson, N., Risk, D. & Bond, B.J. 2011. Interpreting diel hysteresis between soil respiration and temperature. *Global Change Biology, 17*, 515–527.

Pritchard, S.G. 2011. Soil organisms and global climate change. *Plant Pathology*, *60*, 82-99.

Rochette, P. & Flanagan, L.B. 1997. Quantifying rhizosphere respiration in a corn crop under field conditions. *Soil Science Society of America Journal*, *61*, 466–474.

Roland, M., Vicca, S., Bahn, M., Ladreiter-Knauss, T., Schmitt, M. & Janssens, I.A. 2015. Importance of nondiffusive transport for soil CO_2 efflux in a temperate mountain grassland. *Journal of Geophysical Research: Biogeosciences*, *120*, 502–512

Royal Society. 2018. *Greenhouse Gas Removal*. https://royalsociety.org/greenhouse-gas-removal.

Saby, N.P.A., Arrouays, D., Antoni, V., Lemercier, B., Follain, S., Walter, C. & Schvartz, C. 2008. Changes in soil organic carbon in a mountainous French region, 1990–2004. *Soil Use and Management*, *4*, 254-262.

Schiefer, J., Lair, G.J., Lüthgens, C., Wild, E.M., Steier, P. & Blum, W.E.H. 2019. The increase of soil organic carbon as proposed by the “4/1000 initiative” is strongly limited by the status of soil development - A case study along a substrate age gradient in Central Europe. *Science of The Total Environment*, *628*–629, 840-847.

Schimel, J.P & Schaeffer, S.M. 2012. Microbial control over carbon cycling in soil. *Frontiers in Microbiology*, *3*, doi:10.3389/fmicb.2012.00348.

Schmidt MWI, Torn M, Abiyen S, Dittmar T, Guggenberger G, Janssens IA, Kleber M, Kögel-Knabner I, Lehmann J, Manning DAC, Nannipieri P, Rasse D, Weiner S & Trumbore S. 2011. Persistence of soil organic matter as an ecosystem property. *Nature, 478*, 49–56.

Shigyo, N., Umeki, K. & Hirao, T. 2019. Seasonal Dynamics of Soil Fungal and Bacterial Communities in Cool-Temperate Montane Forests. *Frontiers in Microbiology*, *10*, 1944.

Schipper, L.A., Mudge, P.L, Kirschbaum, M.U.F., Hedley, C.B., Golubiewski, N.E., Smaill, S.J. & Kelliher, F.M. 2017. A review of soil carbon change in New Zealand's grazed grasslands. *New Zealand Journal of Agricultural Research*, *60*, 93-118.

Shazad, T., Chenu, C., Repinçay, C., Mougin, C., Ollier, J.-L. & Fontaine, S. 2012. Plant clipping decelerates the mineralization of recalcitrant soil organic matter under multiple grassland species. *Soil Biology & Biogeochemistry*, *51*, 73–80.

Smith, P., Smith, J.U., Powlson, D.S., McGill, W.B., Arah, J.R.M, Chertov, O.G. *et al*. 1997 A comparison of the performance of nine soil organic matter models using datasets from seven long-term experiments. *Geoderma*, *81*, 153–255.

Smith, P. (2016), Soil carbon sequestration and biochar as negative emission technologies. *Global Change Biology*, *22*, 1315-1324.

Sulman, B.N., Brzostek, E.R., Medici, C., Shevliakova, E., Menge, D.N.L. & Phillips, R.P. 2017. Feedbacks between plant N demand and rhizosphere priming depend on type of mycorrhizal association. *Ecology Letters*, *20*, 1043-1053

Sun, W., Resco, V. & Williams, D.G. 2010. Nocturnal and seasonal patterns of carbon isotope composition of leaf dark-respired carbon dioxide differ among dominant species in a semiarid savanna. *Oecologia*, *164*, 297–310.

Sun, Y., Zang, H., Splettstößer, T, Kumar, A., Xu, X., Kuzyakov, Y. & Pausch, J. 2020. Plant intraspecific competition and growth stage alter carbon and nitrogen mineralization in the rhizosphere. *Plant, Cell & Environment*, https://doi.org/10.1111/pce.13945

Sturm, P., Eugster, W. & Knohl, A. 2012. Eddy covariance measurements of CO2 isotopologues with a quantum cascade laser absorption spectrometer. *Agricultural and Forest Meteorology*, *152*, 73-82.

Tcherkez, G., Nogues, S., Bleton, J., Cornic, G., Badeck, F. & Ghashghaie J. 2003. Metabolic origin of carbon isotope composition of leaf dark-respired CO_2 in French bean. *Plant Physiology*, *131*, 237–244.

Trudell, S.A., Rygiewicz, P.T. & Edmonds, R.L. 2004. Patterns of nitrogen and carbon stable isotope ratios in macrofungi, plants and soils in two old-growth conifer forests. *New Phytologist*, *164*, 317–335.

Trumbore, S.E. 2006. Carbon respired by terrestrial ecosystems – Recent progress and challenges. *Global Change Biology, 12*, 141–153.

Veloso, M.G., Dieckow, J., Zanatta, J.A., Bayer, C., Higa, R.V.C., Brevilieri, R.C., Comerford, N.B. & Stoppe, A.M. 2018. Reforestation with loblolly pine can restore the initial soil carbon stock relative to a subtropical natural forest after 30 years. European *Journal of Forest Research*, *137*, 593–604.

et al. Reforestation with loblolly pine can restore the initial soil carbon stock relative to a subtropical natural forest after 30 years. *European Journal of Forest Research*, *137*, 593–604 (2018).

Wang, G., Han, J., Zhou, L., Xiong, X. & Wu, Z. 2005. Carbon isotope ratios of plants and occurrences of C4 species under different soil moisture regimes in arid region of Northwest China. *Physiologia Plantarum*, *125*, 74–81.

Wang, R., Bicharanloo, B., Shirvan, M.B., Cavagnaro, T.R., Jiang, Y., Keitel, C. and Dijkstra, F.A. 2020. A novel ^{13}C pulse-labelling method to quantify the contribution of rhizodeposits to soil respiration in a grassland exposed to

drought and nitrogen addition. *New Phytologist*, https://doi.org/10.1111/nph.17118.

Wang, X., Tang, C., Severi, J., Butterly, C.R. & Baldock, J.A. 2016, Rhizosphere priming effect on soil organic carbon decomposition under plant species differing in soil acidification and root exudation. *New Phytologist*, *211*, 864-873.

Werth M. and Kuzyakov, Y. 2006. Assimilate partitioning affects ^{13}C fractionation of recently assimilated carbon in maize, *Plant and Soil*, *284*, 319–333.

Werth M. and Kuzyakov, Y. 2008. Root-derived carbon in soil respiration and microbial biomass determined by ^{14}C and ^{13}C. *Soil Biology and Biochemistry*, *40*, 625–637.

Werth M. and Kuzyakov, Y. 2010. ^{13}C fractionation at the root–microorganisms–soil interface: A review and outlook for partitioning studies, *Soil Biology and Biochemistry*, *42*, 1372–1384.

Wiesmeier, M., Mayer, S., Burmeister, J., Hübner, R. & Kögel-Knabner, I. Feasibility of the 4 per 1000 initiative in Bavaria: A reality check of agricultural soil management and carbon sequestration scenarios. *Geoderma*, *369*, https://doi.org/10.1016/j.geoderma.2020.114333.

Wild, B., Li, J., Pihlblad, J., Bengtson, P. & Rütting, T. 2019. Decoupling of priming and microbial N mining during a short-term soil incubation. *Soil Biology and Biochemistry*, *129*, 71–79.

Williams, A. and de Vries, F.T. 2020. Plant root exudation under drought: implications for ecosystem functioning. *New Phytologist*, *225*, 1899-1905.

Wittmer, M.H.O.M., Auerswald, K., Tungalag, R., Bai, Y.F., Schäufele, R. & Schnyder, H. 2008. Carbon isotope discrimination of C3 vegetation in Central Asian grassland as related to long-term and short-term precipitation patterns. *Biogeosciences*, *5*, 913–924.

Wutzler T. & Reichstein, M. 2008. Colimitation of decomposition by substrate and decomposers – a comparison of model formulations. *Biogeosciences*, 5, 749–759.

Xu, Q., Wang, X. & Tang, C. 2018. The effects of elevated CO2 and nitrogen availability on rhizosphere priming of soil organic matter under wheat and white lupin. *Plant and Soil*, *425*, 375–387.

Xue, K., M. Yuan, M., J. Shi, Z., Qin, Y., Deng, Y., Cheng, L., Wu, L., He, Z., Van Nostrand, J.D., Bracho, R., Natali, S. Schuur, E.A.G., Luo, C., Konstantinidis, K.T., Wang, Q., Cole, J.R., Tiedje, J.M., Luo, Y. & Zhou, J. 2016. Tundra soil carbon is vulnerable to rapid microbial decomposition under climate warming. *Nature Climate Change*, *6*, 595–600.

Yang, H., Yu, Q., Sheng, W-P., Ki, S-G. & Tian, J. 2017. Determination of leaf carbon isotope discrimination in C4 plants under variable N and water supply, *Scientific Reports*, *7*, 351.

Yin, L., Corneo, P.E., Richter, A., Wang, P., Cheng, W. & Dijkstra, F.A. 2019. Variation in rhizosphere priming and microbial growth and carbon use efficiency caused by wheat genotypes and temperatures. *Soil Biology and Biochemistry*, *134*, 54-61,

Yuan, Z.Q., Wu, Q.B., Song, X., Jiang, X.-J., Gao, S.-R., Wang, Q.-F. & Li, G.U. 2020. Pasture degradation impact on soil carbon and nitrogen fractions of alpine meadow in a Tibetan permafrost region. *Journal of Soils and Sediments*, *20*, 2330–2342.

Zang, H., Wang, J. & Kuzyakov, Y. 2016. N fertilization decreases soil organic matter decomposition in the rhizosphere. *Applied Soil Ecology, 108*, 47–53.

Zhong, S., Chai, H., Xu, Y., Li, Y., Ma, J.-Y. & Sun, W. 2017. Drought sensitivity of the carbon isotope composition of leaf dark-respired CO_2 in C_3 (*Leymus chinensis*) and C_4 (*Chloris virgata* and *Hemarthria altissima*) grasses in northeast China, *Frontiers in Plant Science*, *8*, 1996.

Zhou, Y., Hartemink, A.E., Shi, Z., Liang, Z. & Lu, Y. 2019. Land use and climate change effects on soil organic carbon in North and Northeast China. *Science of The Total Environment*, *647*, 1230-1238.

Zhou, J., Wen, Y., Shi, L., Marshall, M.R., Kuzyakov, Y., Blagodatskaya, E. & Zang, H. 2021. Strong priming of soil organic matter induced by frequent input of labile carbon. *Soil Biology and Biochemistry*, *152*, 108069.

Zhu, B. & Cheng, W. 2011. Rhizosphere priming effect increases the temperature sensitivity of soil organic matter decomposition. *Global Change Biology*, *17*, 2172-2183.

2 A field system for measuring plant and soil carbon fluxes using stable isotope methods

Christopher S. McCloskey[1,2] | Wilfred Otten[1] | Eric Paterson[2] | Ben Ingram[1] | Guy J. D. Kirk[1]

[1]School of Water, Energy & Environment, Cranfield University, Cranfield, Bedford MK43 0AL, UK

[2]The James Hutton Institute, Craigiebuckler, Aberdeen, AB15 8QH, Scotland, UK

Correspondence

Chris McCloskey, School of Water, Energy & Environment, Cranfield University, Cranfield, Bedford MK43 0AL, UK. E-mail: c.mccloskey@cranfield.ac.uk

Abstract

There is a lack of field methods for measuring plant and soil processes controlling soil organic matter (SOM) turnover over diurnal, seasonal, and longer time-scales with which to develop datasets for modelling. We describe an automated field system for measuring plant and soil carbon fluxes over such time-scales using stable isotope methods, and we assess its performance. The system comprises 24 large (1-m deep, 0.8-m diameter) cylindrical lysimeters connected to gas-flux chambers and instruments. The lysimeters contain intact, naturally-structured C_3 soil planted with a C_4 grass. Fluxes of CO_2 and their ^{13}C isotope composition are measured 3-times daily in each lysimeter, and the isotope composition is used to partition the fluxes between plant and soil sources. We investigate the following potential sources of error in the measurement system and show they do not significantly affect the measured CO_2 fluxes or isotope signatures: gas leaks; the rate of gas flow through sampling loops; instrument precision and drift; the concentration-dependence of isotope measurements; and the linearity of CO_2 accumulation in the chambers and associated isotope fractionation resulting from different rates of $^{13}CO_2$ and $^{12}CO_2$ diffusion from the soil. For the loamy grassland soil and US prairie grass

(*Bouteloua dactyloides*) tested, the precision of CO_2 flux measurements was ± 0.04 % and that of the flux partitioning ± 0.40 %. We give examples of diurnal and seasonal patterns of plant and soil C fluxes and soil temperature and moisture. We discuss the limitations of the isotope methodology for partitioning fluxes as applied in our system. We conclude the system is suitable for measuring net ecosystem respiration fluxes and their plant and soil components with sufficient precision to resolve diurnal and seasonal patterns.

Highlights

- We describe an automated system for measuring plant and soil carbon fluxes under field conditions.
- We exploit the large difference in isotope signatures between C_3 and C_4 soils and plants to partition the net flux.
- Possible sources of error are quantified and shown to be small.
- The system is capable of resolving diurnal and seasonal patterns.

Keywords

C_4 photosynthesis, lysimeter, soil organic matter

2.1 Introduction

Measurements of soil-atmosphere carbon (C) fluxes necessarily conflate fluxes from plants and recent plant inputs with those from the decomposition of existing soil organic matter (SOM). It is essential to disentangle the two to measure the true response of SOM turnover to driving variables. How to do this under field conditions is a key problem in studies of ecosystem C balances. In this paper we describe an automated field system for measuring plant and soil C fluxes separately using stable isotope methods, and we assess the limitations of the isotope methodology for partitioning fluxes as applied in our system.

Bowling *et al*. (2008), Paterson *et al*. (2009) and Zhu *et al*. (2019) review stable isotope approaches to quantify plant and soil C fluxes. The natural isotope composition of CO_2 (as gauged by $\delta^{13}C$) derived from SOM turnover differs from that from plant C turnover by small but detectable amounts. In principle, this provides a means of separating the plant and SOM derived fluxes. However, this approach requires a high degree of analytical precision, and isotopic partitioning may be confounded by minor variations in isotopic discrimination, such as during plant water stress. A much larger difference in $\delta^{13}C$ between plant and soil sources can be created by growing the plants in an atmosphere with CO_2 depleted or enriched in ^{13}C so as to continuously label the plant C inputs to the soil. Such continuous labelling has the advantages over 'pulse' labelling that plant-derived C is homogenously labelled, allowing quantitative partitioning of the CO_2 efflux. Continuous ^{13}C-labelling has been used in laboratory experiments to partition plant and soil sources, and to follow incorporation of plant-derived C into soil pools (Schnyder *et al*., 2003; Garcia-Pausas & Paterson, 2011). The potential for this under field conditions has been demonstrated in free-air CO_2 enrichment (FACE) experiments where long-term fumigation with fossil-derived CO_2 has inadvertently provided a ^{13}C-label for plant inputs relative to soil (Taneva *et al*., 2006; Carney *et al*., 2007; Iversen *et al*., 2012). However, this requires costly apparatus and large quantities of CO_2.

An alternative, more practicable approach is to exploit differences in the isotope signatures of plants with C_3 versus C_4 photosynthetic pathways (Farquhar *et al*.,

1989). Plants with C_4 photosynthesis typically respire CO_2 with $\delta^{13}C$ of approx. -12 ‰ (range -9 to -19 ‰) whereas those with C_3 photosynthesis typically have approx. -27 ‰ (range -23 to -40 ‰) (Balesdent *et al*., 1987). This provides a difference in $\delta^{13}C$ an order of magnitude larger than that between C_3 plants and C_3 SOM. Most studies exploiting these differences have been lab-based, and therefore not representative of undisturbed field soils, nor of in-field seasonal and annual climatic variations. Further, such studies are usually short-term, lasting only a few weeks or months. In longer-term studies (e.g. Bader & Cheng, 2007; Dijkstra & Cheng, 2007; Lu *et al*. 2019), measurements are generally infrequent. To date only a few studies have exploited plant and soil $\delta^{13}C$ differences to measure SOM turnover under field conditions (Millard *et al*., 2008; Snell *et al*., 2014; Moinet *et al*., 2018). These have relied on manual sample collection and processing, limiting the practicality of collecting long-term continuous datasets. Methods have been developed using portable chambers deployed in the field (e.g. Snell *et al*., 2014), but so far only for periods of a few weeks.

We have developed a field system allowing near-continuous, long-term measurements of soil and plant C fluxes and their drivers over multiple growing seasons, with C_4 plants in C_3 soils. We describe the system here and assess potential sources of error and the overall precision of the system. We assess how well plant and soil fluxes are separated, and how well diurnal and seasonal patterns in plant and soil fluxes can be quantified.

2.2 Materials and methods

2.2.1 System overview

The system comprises 24 cylindrical hydrologically-isolated, 1-m deep, 0.8-m diameter lysimeters containing intact soil monoliths and connected to gas-flux chambers with pneumatically operated lids (Figure 2-1). Gases accumulating when the lids are closed are circulated through a closed loop to gas analysis instruments in an instrument building. The closing of the chamber lids and the directing of gas flow to and from the chambers are controlled by bespoke software.

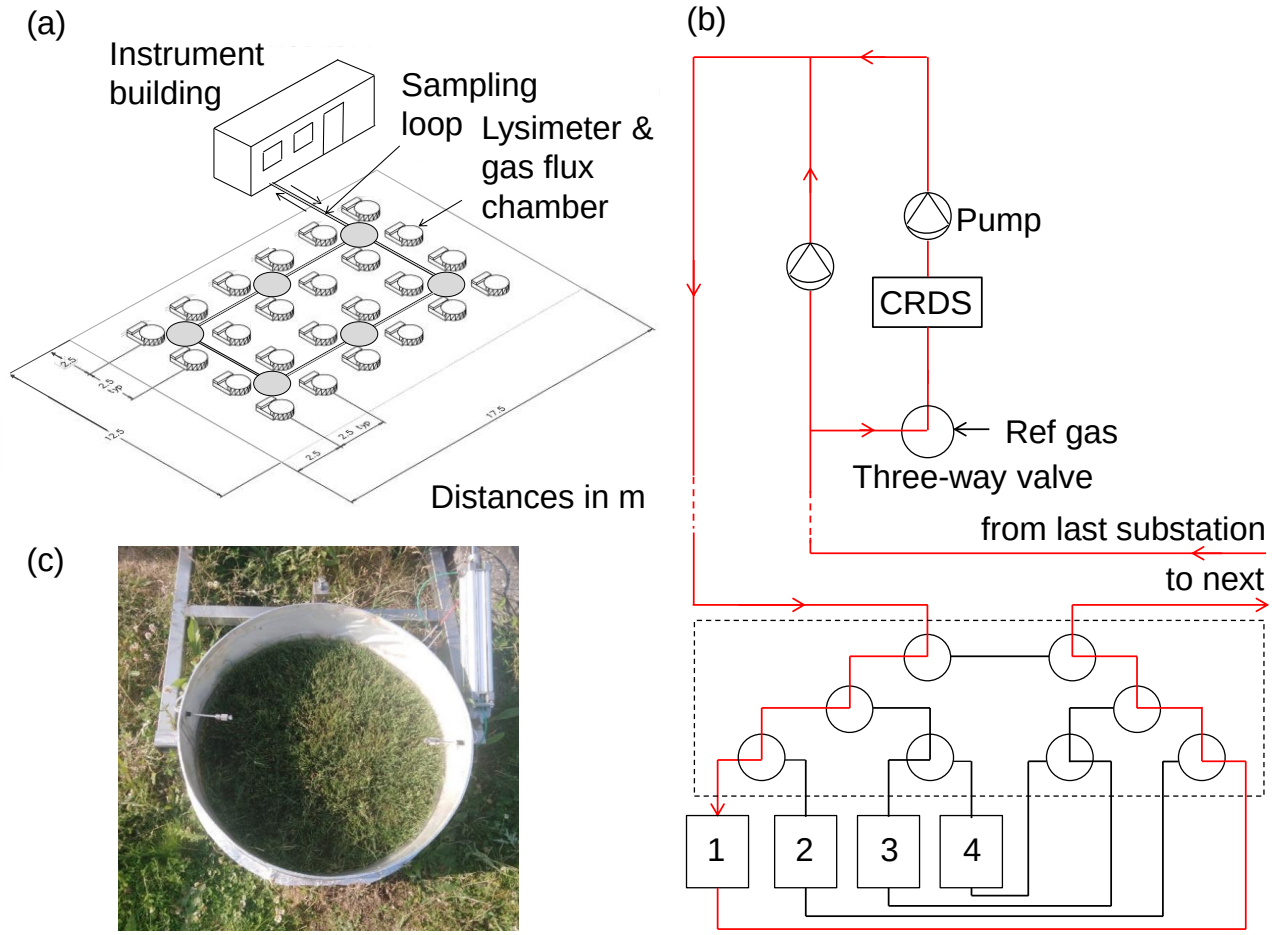

Figure 2-1 The field laboratory. (a) Layout of the 24 lysimeters around 6 manifold substations. (b) Schematic of a manifold substation (inside dashed line) connecting 4 lysimeters (numbered boxes) to the main sampling loop and a sub-sampling loop containing a cavity ring-down spectroscopy (CRDS) isotope analyser and reference gas unit. The valves are set for flow through chamber 1 (red lines). (c) Vertical view of a lysimeter and its gas flux chamber with C_4 buffalo grass growing in a C_3 soil monolith.

The soil monoliths were obtained intact (i.e. without changing inherent soil structure) from field sites and brought to Cranfield in south east England. They are contained in glass fibre sleeves with 5-mm thick walls and galvanised iron trays at the base to collect leachate. They were collected by driving the glass

fibre sleeves into the ground whilst digging the surrounding soil away and making a trench to one side, and then cutting the monolith at the base by driving across a steel plate with a car jack. There are two soil types: (1) a well-drained coarse loamy soil formerly under bracken/grass at Shuttleworth College, Bedfordshire, with initial properties (0–15 cm) pH 5.0 and organic C 62 g kg^{-1}; and (2) a poorly-drained, seasonally waterlogged loamy soil over clay formerly under old pasture at Temple Balsall, Warwickshire, with properties pH 5.4 and organic C 43 g kg^{-1}. Only results for the Temple Balsall soil are given here. The soil monoliths are buried so that the soil surface is flush with the surroundings. Temperature and moisture at depths of 6 and 12 cm are measured with Delta-T SM150T sensors (5 min resolution). Water and dissolved solutes passing out of the bottom are collected. The site has a weather station (Vaisala WXT520), which measures wind speed and direction, precipitation, barometric pressure, temperature and relative humidity.

In January 2018 the lysimeters were sown with a single C_4 pasture-grass species, *Bouteloua dactyloides* (buffalo grass), native to the North American prairies (USDA, 2019). This was shown to be suited to the two soils in a preliminary pot trial in which we grew it with three other C_4 species from similar habitats (*Bouteloua curtipendula*, sideoats grama; *Bouteloua gracilis*, blue grama; and *Schizachyrium scoparium*, little bluestem), and found *B. dactyloides* established most successfully and had the greatest growth rate. It has been maintained in the lysimeters at a mean canopy height of 10 cm by periodic clipping, reaching 20 cm height between clippings. The soils contain C_3 organic matter, having only ever previously been exposed to C_3 vegetation. The C isotope signature of CO_2 emitted from the soil can therefore be used to partition the CO_2 flux between plant and soil sources (Section 2.2.3).

2.2.2 Gas sampling and analysis

2.2.2.1 Lysimeter chambers and main sampling loop

The lysimeters are arranged in six groups of four around six manholes to which they are connected at different depths (Figure 2-1a). The manholes contain manifolds to deliver gases to analytical instruments, collectors for the lysimeter

drainage, and connections for the chamber pneumatics and soil temperature and moisture sensors.

Each chamber has a pneumatically-operated 80-cm diameter lid which closes to give a gas-tight seal. The lid contains a 5-cm diameter vent valve which closes a few seconds after the lid to dampen pressure changes. The chamber wall and lid are made of 10 mm thick clear acrylic plastic. The wall and lid are covered in reflective foil-backed glass fibre cloth, and the lid cover is removable to allow flux measurements to be made in both dark and light conditions. The height of the lid above the soil surface is 26 cm, so the internal chamber volume is 131 L. When closed, the air inside the chamber is mixed by a 2.1 W electric fan (air flow 0.7 m^3 min^{-1}).

The main sampling loop links the chambers to analytical instruments via manifold substations. Secondary loops connect the manifold substations to the chambers, and a further sampling loop connects a Picarro G2201-*i* cavity ring-down spectroscopy (CRDS) instrument (Picarro, Santa Clara, USA) to the main loop. Air is pumped through the main loop at approx. 10 L min^{-1} by a diaphragm pump (Charles Austen B100 SE), and through the CRDS sampling loop at approx. 0.025 L min^{-1} by a smaller diaphragm pump (Picarro A0702) located downstream from the analyser. The main loop is made of ⅜ inch 316 stainless steel tube (7.5 mm ID), polished to 0.8 µm RA and cleaned. This was chosen over cheaper plastic tubing both to minimise gas losses over its long length (46 m) and for longevity. The manifold substations are connected to the individual chambers with ¼ inch 316 stainless steel tube (3.2 mm ID). The length from substation to each chamber is 3 m. The total volume of air within the sampling loop (main loop plus one secondary loop to a chamber) is 1.9 L (i.e. 1.5 % of the chamber head space). With a flow rate of 10 L min^{-1}, the pressure drop across the sampling loop and associated valves is < 1 kPa. The CRDS subsample loop is 1/8 inch ID Bev-A-line flexible plastic tubing (Cole-Parmer, UK) and flexible steel tubing with a total length of 200 cm.

Figure 2-1b shows the layout of a manifold substation. Each substation serves four lysimeter chambers, linking them to the main sampling loop in a pre-

programmed automated sequence. Each substation contains eight three-port ¼ inch ID solenoid valves (SMC Pneumatics VT307-5DZ-02-Q, Mead Engineering Services Ltd, UK), powered by a 24 V DC supply, and connected by 6-mm OD, 4-mm ID nylon tubing. The control units for the valves were custom built by Sercon Ltd (Crewe, UK) and are housed in the instrument building. The valves are arranged in three rows (as shown in Figure 2-1b) and are activated in pairs. The top row determines which of the six substations is connected to the main loop; the other two determine which of the lysimeters in the selected substation is connected.

2.2.2.2 Sampling process and protocol for isotope measurements

The opening and closing of the chamber lids and the switching of valves in the sample loops are controlled by software written in Python. The sequence of samplings is randomised across the 24 chambers in each measurement cycle, with three measurement cycles per 24 h. There are four stages to the process of a chamber measurement, as follows.

1. The lid of the previous chamber is opened and simultaneously the valves connecting it to the sampling loop are deactivated and those connecting the new chamber are activated. Air is pumped continuously through the loop, hence the gas lines are flushed with air from the external atmosphere (approx. 2.5 min).
2. The lid of the new chamber closes (approx. 0.5 min).
3. Time is allowed for the air in the closed chamber and gas lines to equilibrate, and for the accumulation of CO_2 in the chamber to become linear (approx. 3.5 min).
4. Measurements of the CO_2 concentration and its $\delta^{13}C$ every 0.5 s are continued for a further 13 min.

There is hence a period of 6.5 min from the previous chamber closing to the start of the flux measurements in the new chamber, which last 13 min. Therefore, each sampling event takes 19.5 min and so it is possible to sample each of the 24 lysimeters three times over 24 h.

A three-point slope and offset calibration is performed every two months, and applied to baseline data collected within one month of the calibration date following the manufacturer's guidelines for the Picarro G2201-*i* analyser. We used three reference standards with differing CO_2 concentrations in air and three with differing $\delta^{13}C$ values spanning the expected range of measured values: (1) 358 µmol mol^{-1}, -9.35 ‰ (Air Products, UK); (2) 712 µmol mol^{-1}, used only for CO_2 concentration calibration (BOC, UK); (3) 1010 µmol mol^{-1}, -34.44 ‰ (BOC, UK); and (4) 800-1000 µmol mol^{-1}, -21.7 ‰ (prepared by mixing 50,000 µmol mol^{-1} from CK Isotopes Limited, UK with CO_2-free (< 1 µmol mol^{-1}) air from BOC, UK; used only for $\delta^{13}C$ calibration). Each standard was sampled by flushing it for 4 min through pre-evacuated 12 mL Exetainers® (Labco, Ceredigion, UK) with 10 replicates, and CO_2 concentrations and $\delta^{13}C$ values measured at the James Hutton Institute using infra-red gas analysis (EGM4, PP Systems, Amesbury, USA) and isotope-ratio mass spectrometry (IRMS; Finnigan DeltaPlus Advantage connected to a GasBench II System, Thermo Fisher Scientific, Bremen, Germany).

To account for instrumental drift between the three-point slope and offset calibration points, an additional offset calibration is performed thrice daily. Each 24 h period is divided into three 7.8 h cycles of measurements, during which each lysimeter is sampled once; between each measurement cycle, the CRDS analyser samples a reference cylinder of compressed air (independently-certified CO_2 concentration of 358 µmol mol^{-1} and $\delta^{13}C$ -9.35 ‰) for 12 min 24 s. This gives an 8 min period of stable reference cylinder measurements. The mean CO_2 concentration and $\delta^{13}C$ of this period was compared with the post-calibration values from the same reference cylinder at the proximate three-point slope and offset calibration point. A smoother was generated using a sequence of these reference standard comparisons using a generalised additive model (c.f. Snell *et al*., 2014), and applied to CO_2 and $\delta^{13}C$ measurements following the three-point slope and offset calibration.

2.2.2.3 Flux calculation

For each chamber sampling event, the chamber headspace CO_2 concentration (C) and $\delta^{13}C$ are recorded at approx. 0.5 s intervals (i.e. 1600 measurements per flux chamber closure) and the results are used to calculate the net CO_2 flux and its overall $\delta^{13}C$ using Keeling plots as follows.

As CO_2 respired by plants and soil microbes mixes with the original CO_2 in a chamber, the $\delta^{13}C$ of the chamber air will change as some function of the isotope composition of the respired CO_2. For steady-state conditions, the $\delta^{13}C$ value will vary in inverse proportion to the CO_2 concentration. From mass balance we have

$$C = C_0 + C_R \,, \qquad \textbf{Equation 2-1}$$

and

$$\delta^{13}C \times C = \delta^{13}C_0 \times C_0 + \delta^{13}C_R \times C_R \,, \qquad \textbf{Equation 2-2}$$

where subscripts 0 and R refer to the contributions of the initial background and the CO_2 source, respectively. Rearranging Equation 2-2 and substituting for C_R from Equation 2-1 gives

$$\delta^{13}C = \frac{C_0}{C}\left(\delta^{13}C_0 - \delta^{13}C_R\right) + \delta^{13}C_R \,. \qquad \textbf{Equation 2-3}$$

Hence plots of $\delta^{13}C$ against $1/C$ will have slope $C_0\left(\delta^{13}C_0 - \delta^{13}C_R\right)$ and y-axis intercept $\delta^{13}C_R$, which can be found thereby. Values of $\delta^{13}C_R$ for individual chamber sampling events were obtained by least squares regression using R (R Core Team, 2017).

The proportions of C_R attributable to soil respiration (C_3 origin) and plant respiration (C_4), f_{soil} and f_{plant} respectively, are calculated from

$$f_{\text{soil}} = \frac{\delta^{13}C_R - \delta^{13}C_{\text{plant}}}{\delta^{13}C_{\text{soil}} - \delta^{13}C_{\text{plant}}}, \qquad \textbf{Equation 2-4}$$

and

$$f_{\text{plant}} = 1 - f_{\text{soil}}.$$ **Equation 2-5**

It should be noted that f_{plant} includes all respiration of C substrates of C_4 origin, thus combining microbial breakdown of fresh plant inputs in the soil as well as plant respiration.

The SOM and plant end-member $\delta^{13}C$ values were measured as follows. For $\delta^{13}C_{soil}$, unplanted soil, unexposed to the C_4 grass, was moistened to field capacity and packed to a depth of 3 cm in 15-cm internal diameter plastic pipes with acrylic disks glued to their bases. A pneumatically-operated gas flux chamber (eosAC, Eosense, Nova Scotia, Canada) was fitted on top, and connected to a Picarro G2201-*i* isotope analyser and Picarro A0702 diaphragm pump. Measurements of CO_2 respired and its $\delta^{13}C$ were taken and $\delta^{13}C_{soil}$ obtained using Keeling plots. This gave $\delta^{13}C_{soil}$ for the Temple Balsall soil = -30.9 ± 0.1 ‰ (mean ± standard error of seven repeat measurements in two replicate mesocosms). For $\delta^{13}C_{plant}$, seeds of *B. dactyloides* were germinated and grown for 2 months in moist sand heat-treated to remove any organic matter. Mesocosms of grass were placed in gas flux chambers and measurements of CO_2 respired and its $\delta^{13}C$ were taken as above for $\delta^{13}C_{soil}$. This gave $\delta^{13}C_{plant}$ = -15.3 ± 0.2 ‰ (mean ± standard error of four repeated measurements of three replicate mesocosms).

2.2.3 Tests of the system

2.2.3.1 Sampling loop leakiness

The gas-permeability of the sampling loop was assessed by bridging the inflow and outflow ports of a lysimeter gas flux chamber with a 1.5 m length of 1/8 inch ID Bev-A-line tubing, via a 4.5 L glass mixing chamber containing a flexible 5 V fan (Aerb Portable USB Powered Cooling Fan). Expected low and high extremes of CO_2 concentration were tested: 134 ± 7 µmol mol^{-1} achieved by partially flushing the loop with helium, and 1526 ± 29 µmol mol^{-1} achieved by injecting a pulse of pure CO_2 into the sampling loop. After 10 min to allow mixing, the CO_2 concentration was monitored over 40 min. The mean

concentration was obtained from the values at 1 and 40 min, and the change in concentration was obtained from the difference between these values.

2.2.3.2 Measurement response time

The time lag between a CO_2 increase in a lysimeter and its detection by the CRDS analyser was assessed by bridging the lysimeter inflow and outflow ports as above, and injecting 10 mL of 99.8% pure CO_2 (BOC, UK) into a port downstream of the mixing chamber, taking 10 s. The CO_2 concentration was measured over the subsequent 150 s. This was repeated for six lysimeters, one from each manifold substation.

2.2.3.3 Precision of CRDS measurements

The precision and instrumental drift of the CRDS measurements were measured by sampling a reference gas cylinder of medical-grade compressed air with 352 µmol CO_2 mol^{-1} (BOC, UK) for 48 h and monitoring the absolute CO_2 concentrations and $\delta^{13}C$ values, and their drift over time. This was used to inform the calibration regime detailed previously.

2.2.3.4 Concentration dependence of $\delta^{13}C$ measurements

To assess the effect of CO_2 concentration on $\delta^{13}C$ values over the relevant concentration range, gas from a cylinder of pure CO_2 (BOC, UK) was mixed with CO_2-free air (BOC, UK) in 3 L Tedlar® bags (Merck KGaA, Darmstadt, Germany) to give 11 CO_2 concentrations ranging from 80–2010 µmol mol^{-1}. Gas from each Tedlar® bag was pumped at approx. 25 mL min^{-1} through the CRDS analyser with the exhaust vented to the atmosphere. Starting after 5 min, CO_2 concentrations and $\delta^{13}C$ values were recorded for three periods of 10 min with 3 min between each measurement interval. Each mix was sampled five times into 12 mL Exetainers® (Labco, Ceredigion, UK) and the $\delta^{13}C$ of the CO_2 in these was analysed with an IRMS (Finnigan DeltaPlus Advantage connected to a GasBench II System, Thermo Fisher Scientific, Bremen, Germany) at the James Hutton Institute, with four separate measurements per sample. The CRDS and IRMS results were compared to assess the concentration-dependence of the CRDS $\delta^{13}C$ measurements.

2.2.3.5 Precision of flux measurements

To assess the precision of the CO_2 flux measurements we generated linear models of CO_2 concentration against time, and $\delta^{13}C$ against $1/C$, for all measurements taken with blackout covers on between 4 and 30 July 2018. From these we found the standard errors for the slope of CO_2 concentration against time, and for the intercept of $\delta^{13}C$ against $1/C$ plots. Coefficients of variation were calculated for the flux magnitude and its $\delta^{13}C$ value by finding (a) the standard error of the slope as a percentage of the slope for the CO_2 concentration against time model, and (b) the standard error of the $\delta^{13}C$ against $1/C$ intercept as a percentage of the intercept, respectively. Standard errors were used rather than standard deviations in order to find the coefficients of variance of the slope and intercept specifically, rather than of the individual CO_2 concentration and $\delta^{13}C$ measurements used to construct these models. For comparison, inter-lysimeter coefficients of variation were calculated for the same period from the mean CO_2 flux magnitude and its $\delta^{13}C$ for each of 12 lysimeters by finding the standard deviation of this set of means as a percentage of the mean of the 12 lysimeters means.

2.2.3.6 Data analysis

Data analysis was conducted using R version 3.5.1. Allan deviation was calculated using the allanvar package in R (R Core Team, 2017). This is an estimate of the frequency stability in an oscillator due to noise rather than systematic errors. It indicates the agreement with the expected relationship between the standard deviation of frequency fluctuations and the infinite-time average of the standard deviation.

2.3 Results

2.3.1 Growth of the C_4 grass

The initial germination and growth of *B. dactyloides* were slow but a healthy and uniform sward was established by June 2018. Peak above-ground growth rates (July 2019) were 4.3 ± 1.3 g m^{-2} d^{-1} (mean ± standard error), as measured from dry mass of clippings taken over 3 weeks. The active growing season lasted

from May to October, which is sufficient to observe seasonal dynamics in plant and soil C fluxes and their response to varied environmental conditions.

2.3.2 System performance

2.3.2.1 Sampling loop leakiness

Rates of change in concentration due to gas leaks ranged from an increase of 0.31 ± 0.04 µmol mol^{-1} min^{-1} at CO_2 concentration = 134 ± 3 µmol mol^{-1}, to a decrease of 0.28 ± 0.04 µmol mol^{-1} min^{-1} at CO_2 concentration = 1526 ± 12 µmol mol^{-1} (means ± standard errors). The volume of the mixing chamber and connected sampling loop was 6.5 L, which is < 5 % of the volume of a lysimeter chamber and sampling loop. Extremes of headspace CO_2 accumulations measured over 13 min ranged from 25 µmol mol^{-1} in January to 1000 µmol mol^{-1} in July. As such, during a 13 min sampling event, we expect losses < 1 % of the total CO_2 increase in January, and a much smaller proportion when fluxes are higher. Given that during the active growing season, losses are an order of magnitude smaller as a proportion of total flux, these leak rates are insubstantial and so we conclude the system as a whole is effectively gas tight.

2.3.2.2 Measurement response time

An example time course of CO_2 concentration in a chamber following injection of a CO_2 pulse is shown in Figure 2-2. The time between injection and CO_2 concentration peaking was 63.4 ± 2.5 s (mean ± standard error). The mean peak duration was 109.5 ± 5.2 s, although the majority of the peak is contained within 50 s. It is essential that measurements from subsequent lysimeters do not overlap. This test indicated that the mean time requirement for the sampling loop to clear between measurements is 173 s. This demonstrates that the minimum time required between consecutive flux chamber samplings is small using a system such as this, enabling frequent measurements.

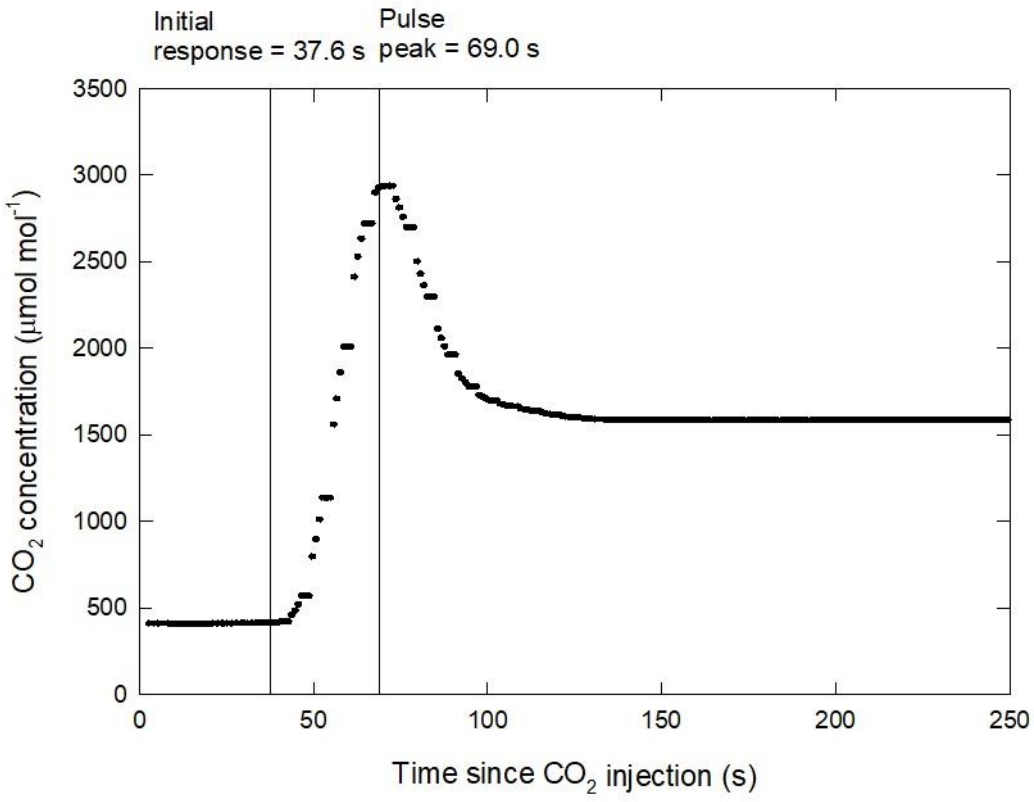

Figure 2-2 Time course of CO_2 concentration in the main sampling loop of the field laboratory following injection of a pulse of pure CO_2 into a mixing chamber downstream from the measurement unit.

2.3.2.3 CRDS precision and drift

Allan deviation plots for CO_2 concentration and $\delta^{13}C$ were used to assess the role of instrumental noise and drift in measurement precision (Figure 2-3). These show the standard deviation of measurements taken over a range of time intervals. For both *C* and $\delta^{13}C$, instrumental noise and drift have antagonistic effects on the precision of measurements. The precision of *C* measurements improves with increasing measurement time up to a duration of 1000 s as increased measurement duration reduced the impact of instrumental noise. At longer durations, however, instrumental drift over the measuring period exceeded the reduction in instrumental noise and the standard deviation of measurements increased with increasing duration. It was therefore necessary to

correct for this. The effect of drift was less pronounced for $\delta^{13}C$ measurements and the critical point for this was between 1000 and 10000 s.

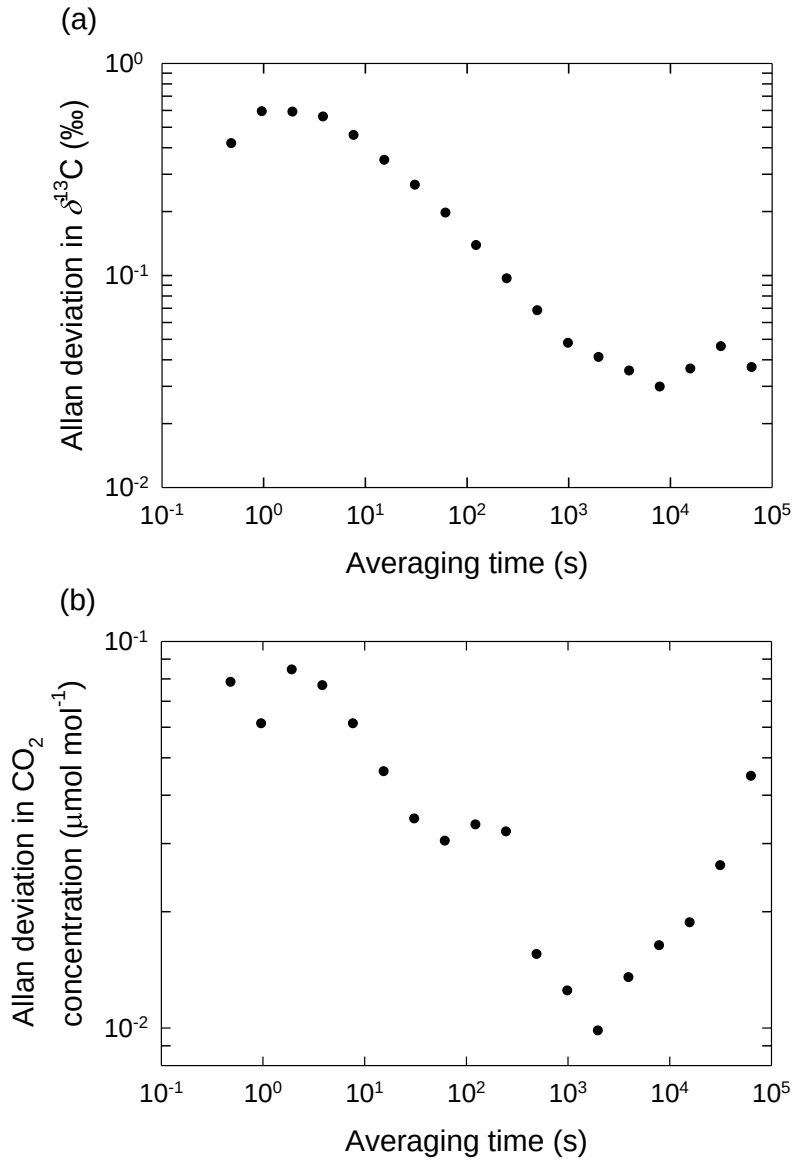

Figure 2-3 Allan deviation plots for (a) $\delta^{13}C$ and (b) CO_2 concentration against averaging time. Allan deviation is a measure of the stability to instrumental noise and drift based on measurement frequency: the full measurement period is divided into consecutive clusters of measurements of consistent duration (the 'averaging time'), and a measure of the mean variation between cluster averages is calculated (Allan, 1966). This is performed over a range of averaging times to show the antagonistic effects of instrumental noise and drift on the precision of averaged measurements.

Using the Allan deviation shown in Figure 2-3 we assessed the duration and frequency of reference gas measurements required to reduce instrumental imprecision to < 0.05 µmol mol^{-1} for CO_2 concentration and < 0.1 ‰ for $\delta^{13}C$. The required measurement time was 200 s with a frequency of once per 17 h. This is not a major issue in terms of duration or frequency.

2.3.2.4 Concentration dependence of $\delta^{13}C$ measurements

Our assessment of the concentration-dependence of $\delta^{13}C$ values, made by diluting a high concentration of CO_2 in air with CO_2-free air, gave less negative $\delta^{13}C$ values by < 0.5 ‰ as the CO_2 concentration decreased from 2000 to 400 µmol mol^{-1} (Fig. 4). Given that this is in the opposite direction to and far smaller than the trend expected for CRDS instrumental bias (Becker *et al*., 2012; Snell *et al*., 2014), and the trend is similar for measurements by IRMS (Fig. 4), we attribute it to small differences in contamination with lab air during the sampling process. From the line fitted to the CRDS data in Figure 2-4, the CO_2 concentration corresponding to the $\delta^{13}C$ value typical of lab air (≈ -8 ‰) is 22 µmol mol^{-1}, which is consistent with small, inevitable contamination of the Tedlar bags in the process of measurements. The scatter in the data is greater for the IRMS measurements, presumably because of differences in the sampling process from that for the CRDS (Section 2.3.4).

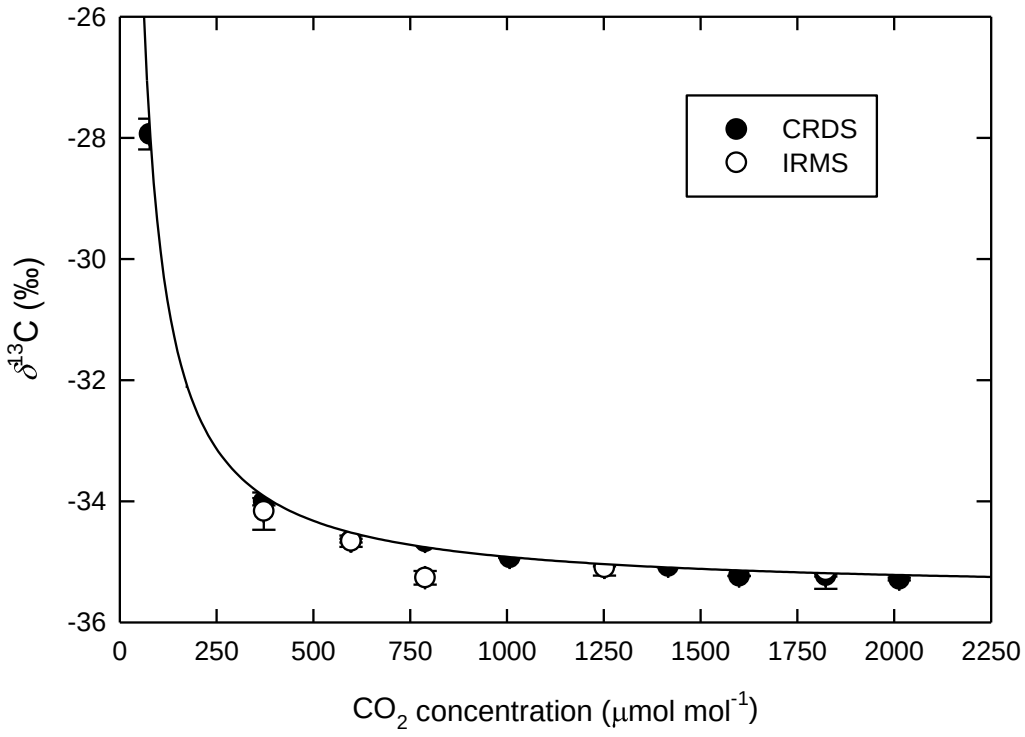

Figure 2-4 The CO_2 concentration-dependence of $\delta^{13}C$ measurements by cavity ring-down spectroscopy (CRDS) compared with isotope-ratio mass spectrometry (IRMS) for gas mixtures made by diluting a high concentration of CO_2 in air with CO_2-free air. Data are means ± standard error (n = 3 for CRDS data, 5 for IRMS data). Line is $\delta^{13}C = -35.5 + 595.0/C$ (r^2 = 0.99) fitted to the CRDS data. The two IRMS data points at CO_2 concentrations < 250 μmol mol^{-1} were outside the certified limits of detection and are not shown. Standard errors of CO_2 concentrations are less than the widths of the data points.

2.3.2.5 Accuracy and precision of net CO_2 flux and $\delta^{13}C$ measurements

Figure 2-5 shows an example plot of CO_2 accumulation in a chamber over time and the corresponding Keeling plot. Some nonlinearity in CO_2 accumulation over time is inevitable because CO_2 accumulation in the chamber will mean the diffusive gradient through the soil to the chamber gradually changes and with it the diffusive flux from the soil will change. To determine the interval over which CO_2 accumulation was effectively linear, we plotted residuals against fitted

values for a linear model of CO_2 concentration against time (Appendix A). We found a strong deviation of residuals from fitted values over the first 3 min after the chamber lids were closed. With this period excluded, there was some deviation from linearity over the following 13 min, but the deviations in residuals were < 1% of the measured CO_2 concentration. This shows CO_2 accumulation was effectively linear over this period and free from perturbations. We plotted residuals against fitted values for a linear model of $\delta^{13}C$ against $1/C$ (Appendix A). While individual residuals were up to 15% of measured $\delta^{13}C$ values, due to instrumental noise, no clear trend was evident to suggest deviation from linearity.

We estimate the precision of the CO_2 flux and flux partitioning measurements from the mean coefficients of variation for respiration measurements in July 2018 to be ± 0.04 % for the flux and ± 0.04 % for the flux partitioning. These are substantially smaller than the corresponding coefficients of variation between lysimeters over the same period (± 6.56 % and ± 3.27 % respectively).

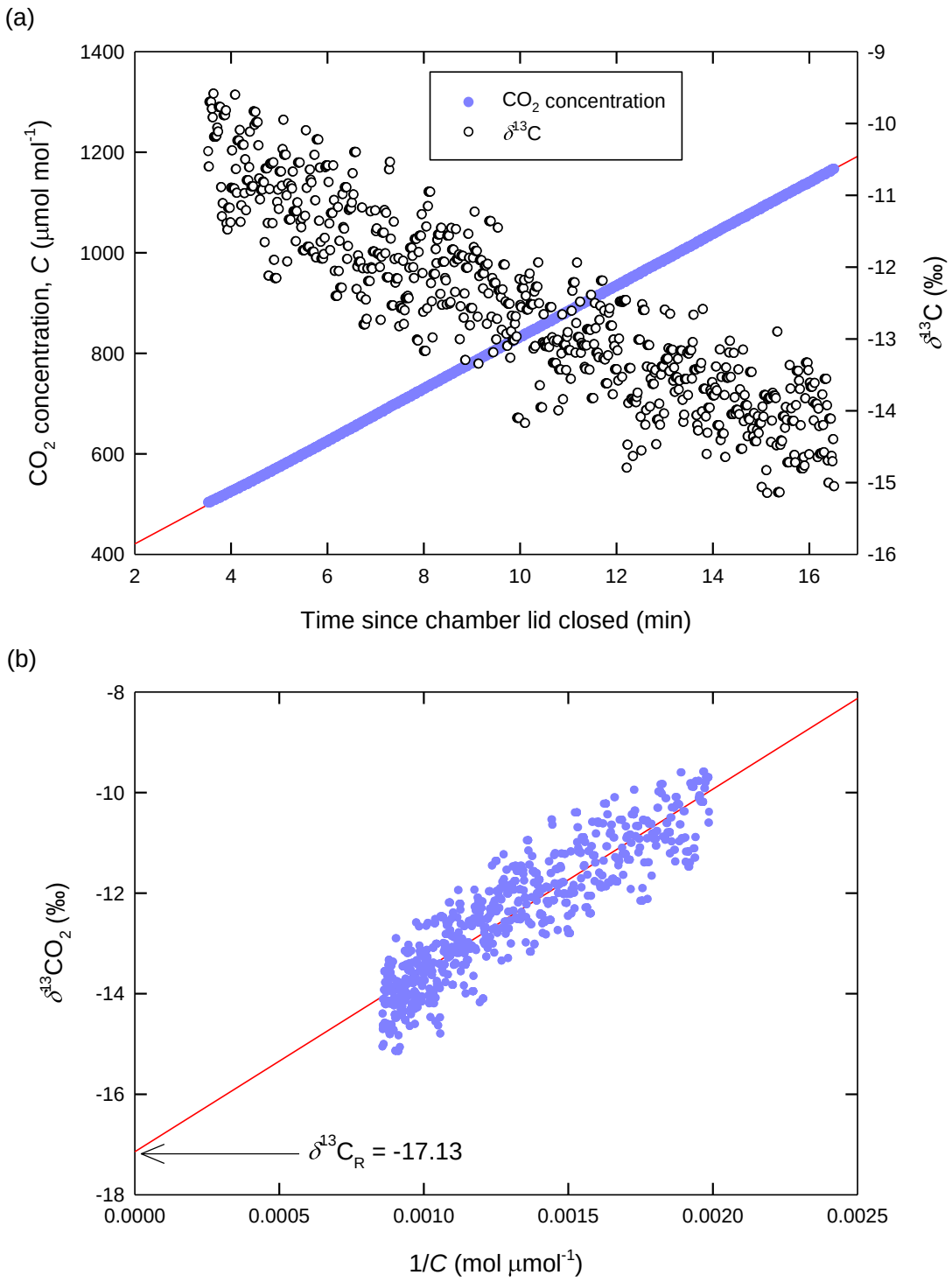

Figure 2-5 Example of (a) CO_2 accumulation and changes in $\delta^{13}C$ in a lysimeter chamber beginning 3.5 min after closing the lid, and (b) the corresponding Keeling plot. Data are individual measurements; lines are linear regressions with fitted parameters (± standard errors): C = (317.9 ± 0.1) + (51.39 ± 0.01)t, r^2 = 1.00; $\delta^{13}C$ = (3606 ± 41)/C - (17.14 ± 0.05), r^2 = 0.81. The $\delta^{13}C$ of plant and soil respiration ($\delta^{13}C_R$ in Equation 2-3) is inferred from the value at 1/C = 0.

2.3.3 Illustrative diurnal and seasonal patterns

Figure 2-6 shows clear diurnal patterns in both plant and soil respiration, and variation over the growing season. Plant and soil C fluxes in October, near the end of the grass's growing season, were approximately a third of those in July, and the diurnal variations were correspondingly reduced.

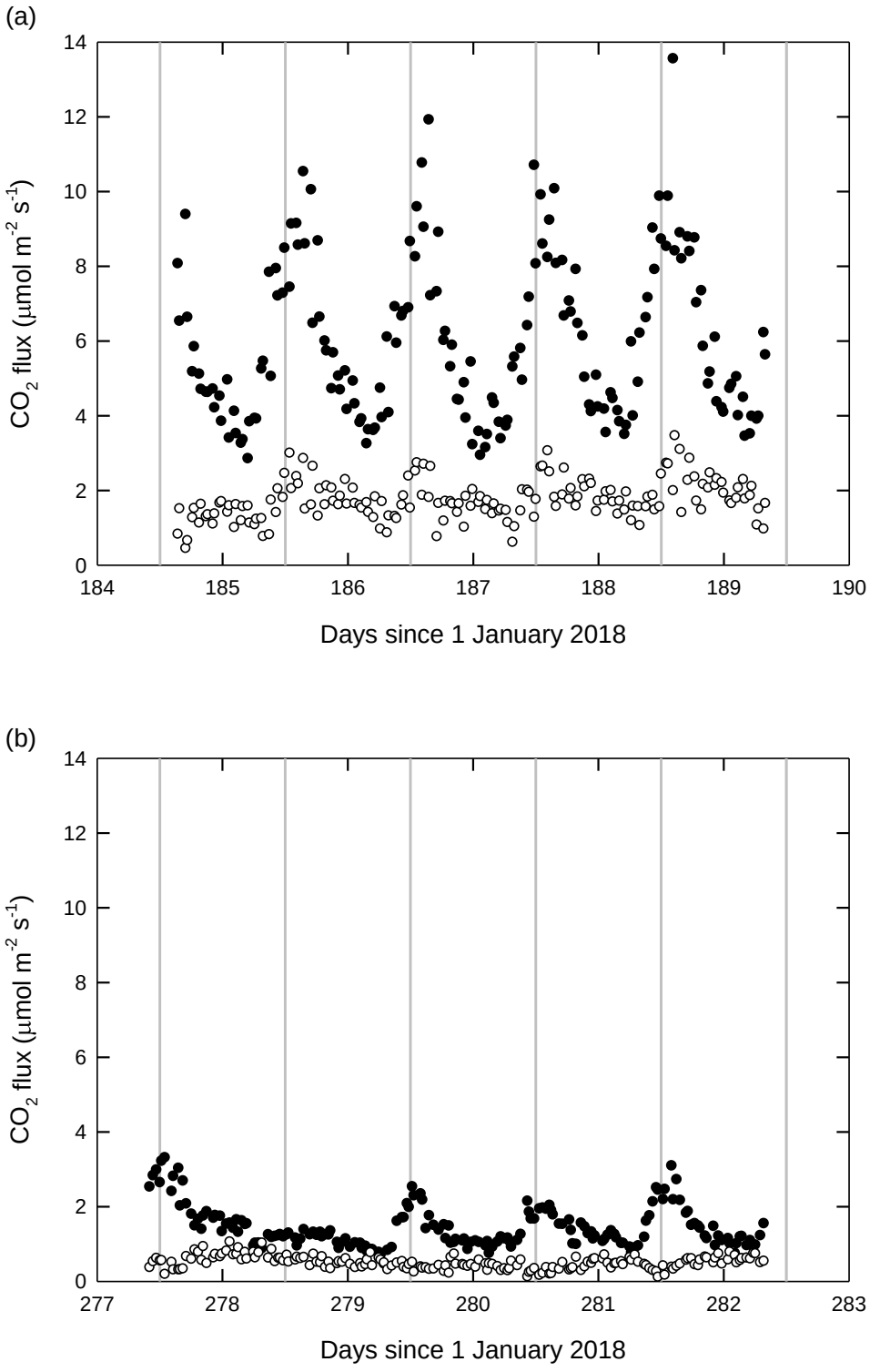

Figure 2-6 Plant (closed symbols) and soil (open symbols) respiration fluxes for (a) 4–9 July and (b) 5–10 October 2018. Data are pooled measurements from 12 lysimeters each measured thrice daily; individual points are for in a single lysimeter. Grey lines indicate midday.

Figure 2-7 shows soil temperature and moisture measurements taken over the same period as in Figure 2-6a. The diurnal variation in soil temperature at 120 mm depth, and at 60 mm depth (data not shown), matched the variation in plant C flux. A diurnal pattern is also evident for soil moisture, with faster drying during the day than at night, with the changes between days punctuated by watering or rainfall events. There were also seasonal trends with an overall increase in soil moisture later in the season (data not shown).

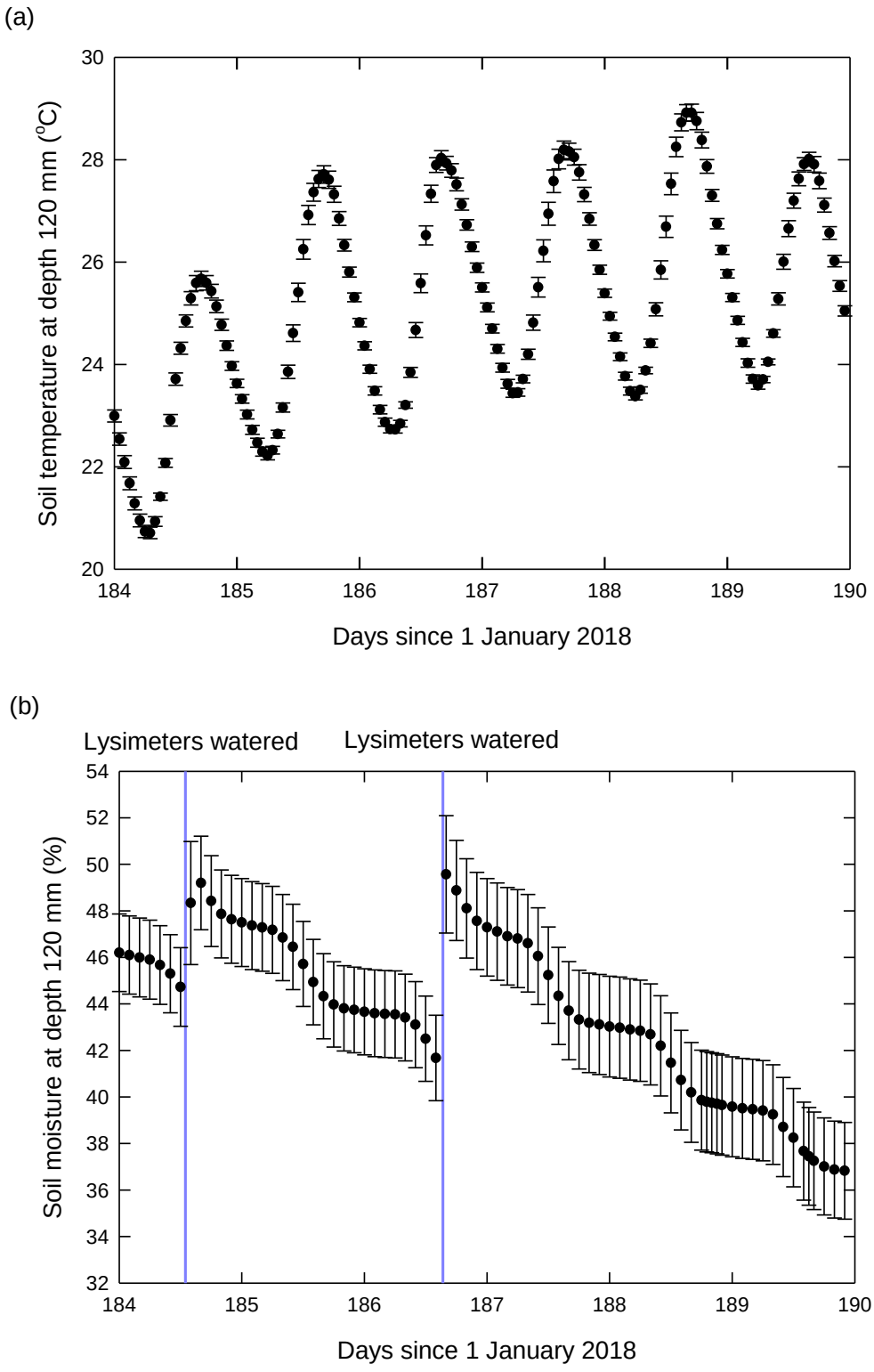

Figure 2-7 Diurnal patterns of (a) soil temperature and (b) volumetric soil moisture content. Data are means ± standard errors of measurements from 12 lysimeters at 120 mm depth. For clarity one measurement per hr is shown in (a) and two in (b).

2.4 Discussion

2.4.1 Performance of the measurement system

We have shown that the five potential sources of error investigated do not significantly affect the measured CO_2 fluxes or their isotope signatures. These sources of error are gas leaks from the sampling loops; the response time of the measurement system; the instrument precision after correcting for drift; the concentration-dependence of isotope measurements; and the linearity of CO_2 accumulation in the chambers. These potential sources of error depend on the engineering quality of the system and instruments, not on the particular plant-soil system tested.

After correcting for noise and drift, the precision of our $\delta^{13}C$ measurements by CRDS was < 0.1 ‰. This is two orders of magnitude smaller than the difference in $\delta^{13}C$ between typical C_4 plant and C_3 soil end members, so is adequate for our purposes. Our $\delta^{13}C$ measurements were effectively independent of CO_2 concentration over the relevant range, given the large $\delta^{13}C$ differences we need to measure. Snell *et al*. (2014) found $\delta^{13}C$ values measured by an earlier Picarro CRDS instrument (G1101-*i*) increased non-linearly with increasing CO_2 concentration, as compared with those measured by an isotope ratio mass spectrometer. Evidently this bias has been satisfactorily corrected in the newer Picarro G2201-*i* instrument used in this study. We note there is the possibility of spectral interferences from matrix gases (H_2O, O_2) in isotope assays by laser spectroscopy, as discussed by Rella *et al*. (2015) for CH_4 and Harris *et al*. (2019) for N_2O. It is therefore important to minimise differences in composition between samples and reference gases.

The Keeling plot method of calculating the flux $\delta^{13}C$ requires a linear relationship between $\delta^{13}C$ and $1/C$. To the extent that CO_2 accumulation in the chamber alters the concentration gradient through the soil, diffusion is no longer at steady state, and so $\delta^{13}C$ values will be biased because of the slower diffusion of $^{13}CO_2$ than $^{12}CO_2$ (Nickerson & Risk, 2009; Moyes *et al*., 2010;

Ohlsson, 2010). We tested for this by plotting residuals against fitted values for a linear model of $\delta^{13}C$ against $1/C$ (Appendix A). Very little nonlinearity was evident, and slopes of lines of best fit for residuals were close to zero. This indicates there was no substantial isotopic bias over the course of a 13 min chamber measurement.

To allow an additional complete set of flux measurements from the 24 lysimeters in a day would require the measurement time to be reduced from 13 to 8 min. This increases the mean coefficients of variance to ± 0.05 % for the flux and ± 0.77 % for the flux partitioning. This remains a low level of imprecision and would be acceptable to allow greater temporal resolution of measurements.

Advantages of a fully automated system over manual systems include the much finer temporal resolution that can be achieved. We are able to measure and partition fluxes from each lysimeter at least four times per day, which is sufficient to resolve diurnal variations in all 24 lysimeters in one 24 h period. Automation also allows semi-continuous measurements over a full season and beyond. That is not practicable with manual methods.

The clear diurnal and seasonal patterns in both plant and soil respiration show that the system is sufficiently sensitive to separate these. The system was also capable of resolving diurnal and seasonal variation in soil temperature and moisture. The diurnal temperature variation was more marked than that in moisture, presumably due to faster heat than moisture transfer through soil. The variation in moisture between lysimeters is much larger than that for temperature, presumably due to greater sensitivity of moisture to plant and soil heterogeneity.

2.4.2 Separation of plant and soil C fluxes

Most previous systems for separating plant and soil C fluxes seek to isolate the below-ground plant and soil fluxes from the above-ground plant fluxes, whereas, by enclosing the above-ground plant parts as well as the soil surface in our flux chambers, we measure whole-plant and soil fluxes. This allows us to

measure both C fixation by the plants in photosynthesis when the chambers are left transparent, and the respiration-only flux when the chambers are blacked out. Hence, coupled with measurements of leaching losses from the base of the lysimeters, we can obtain a complete C balance for the plant-soil system.

Resolution of the measured net flux into plant and soil components requires values of the plant and soil end-member $\delta^{13}C$ values in Equation 2-4. Because we measure whole-plant respiration, the relevant plant end member is that for the whole plant. Also, because we measure the whole flux, the flux is more dominated by plant respiration than in below-ground only systems, and the flux partitioning is correspondingly more sensitive to errors in the plant $\delta^{13}C$ end-member. What potential errors are specific to our system?

We measure the plant $\delta^{13}C$ end-member with plants grown in C-free sand using opaque chambers. It is known that CO_2 respired by darkened, light-adapted leaves is enriched in ^{13}C during the first minutes following darkening due to rapid changes in leaf biochemistry (Barbour *et al*., 2011). Since our plant end-member is measured under similar conditions to the respiration measurements in the lysimeters, with opaque chambers closed for a similar period, this should be a small source of error.

Some proportion of the below-ground respiration may escape from the soil via the roots to the plant shoots and atmosphere, and this additional soil flux will be captured by our system. It is a large part of the net flux in wetland plants with aerenchymatous roots such as rice (Kirk et al., 2019), but also a significant part of the flux in some dryland plants via the xylem stream (Aubrey & Teskey, 2009). Assuming that this CO_2 has the same $\delta^{13}C$ as soil respiration, i.e. it undergoes no isotopic fractionation during its passage through the plant, the flux will be correctly accounted for in the total soil flux. That this additional flux is captured by our system, but not by systems in which only the below-ground flux is measured, is an advantage.

The $\delta^{13}C$ of root respiration may be 2–3 ‰ more negative than that of shoot respiration (Bowling *et al*., 2008). This may introduce error to the extent that root:shoot ratios and plant physiological status differ between the lysimeters

and the end-member measurement system. However, all other approaches using plant end-member measurements are subject to similar constraints.

Other generic sources of error in the plant end member $\delta^{13}C$, shared with other systems, include the effects of varying plant nutrient status, lighting, temperature, moisture and mycorrhizal colonization (Bowling *et al*., 2008; Paterson *et al*., 2009). Generic sources of error in the soil end member $\delta^{13}C$ shared with other systems include that the soil end member is generally measured in disturbed, re-packed soil, but soil disturbance exposes labile ^{13}C-depleted substrates that are more-rapidly decomposed than average SOM (Zakharova *et al*., 2014).

2.4.3 Movement of the C_4 signal through the soil

The switch from C_3 to C_4 vegetation means that the plant C is homogenously labelled – unlike with more-widely used pulse labelling to partition plant and soil C sources – so that the isotopic signature of C entering the soil is constant, allowing a quantitative partitioning of the CO_2 efflux. Over time, the C_4 signal from the decomposing plant residues will move through soil carbon pools with differing turnover rates and alter their $\delta^{13}C$ signatures. In principle, this provides a means of testing soil carbon models and measuring the rates of turnover of model SOM pools. This requires that the pools and their $\delta^{13}C$ signatures are measurable, and that the movement of the C_4 signal through the pools is not too rapid. An indicative calculation of the rate of movement is as follows.

Assuming a simple one-pool model of SOM turnover, the ratio of the ^{13}C content of the soil at time t after switching to C_4 grass, to that at steady state, is $C_t^*/C_\infty^* = 1 - e^{-kt}$ where k is the decomposition rate constant (definitions of variables are given in Appendix B). A typical value of k for grassland soils in England and Wales is 0.04 yr^{-1} (Kirk & Bellamy, 2010). This gives $C_t^*/C_\infty^* = 0.04$ at t = 1 yr. That is, following a switch from C_3 to C_4 grass, the soil ^{13}C content would change by only 4% towards that of the C_4 grass over a year.

This calculation lumps together all the SOM in a single pool with a single rate constant, whereas in reality there is a continuum of SOM forms and

accessibilities turning over at different rates, and in the early stages a larger proportion of the C_4-C will be in more-rapidly turned-over SOM pools. Rate constants for more labile SOM may be an order of magnitude larger than for the more humified material. Nonetheless, the calculation indicates the order of magnitude of the rate of progress of the C_4 signal through the SOM and that the progress through different pools would be detectable over one to many growth seasons.

2.5 Conclusions

1. The automated field system presented measures net ecosystem respiration fluxes and their plant and soil components with sufficient precision to resolve diurnal and seasonal patterns in both.
2. Errors in CO_2 concentration and isotope measurements due to the measurement system and instruments were negligible relative to the required precision.
3. For the loamy grassland soil and US prairie grass tested, we estimate the precision of measurements to be ± 0.04 % for CO_2 fluxes and ± 0.40 % for flux partitioning.
4. By eliminating manual sampling, this system provides a means of gathering long-term near-continuous C flux data under realistic field conditions.

Acknowledgements

We thank the following for their involvement in the design and construction of the field laboratory: Sam Barker formerly of Sercon Ltd for the gas sampling system, and Roger Heron of Heron Engineering Consultancy for the flux chambers and related pneumatics. The field laboratory was built with a Royal Society Wolfson Laboratory Refurbishment Grant (WL080021/Kirk). The CRDS analyser was provided by the Agri-Epi Centre. CM was supported by the Soils Training and Research Studentships (STARS) Centre for Doctoral Training, funded by the Biotechnology and Biological Sciences Research Council and the Natural Environment Research Council (grant number NE- M009106-1). The

James Hutton Institute receives funding from the Rural and Environment Science and Analytical Services Division (RESAS) of the Scottish Government.

Authorship

GK conceived and coordinated the construction of the field laboratory. CM, GK, WO and EP conceived this study. CM carried out the experimental work and data analysis. BI wrote the software for the lysimeter sampling process. CM and GK wrote the initial manuscript and all contributed to the final version.

Funding information

Natural Environment Research Council Grant Number NE/M009106/1; Royal Society Grant Number WL080021/Kirk

Data Sharing and Data Accessibility statement

The data used in this article will be available at CORD c/o the Cranfield University Library.

Conflict of Interest statement

The authors have no conflicts of interest related to the work presented in this manuscript.

2.6 References

Allan, D.W. 1966. Statistics of Atomic Frequency Standards. *Proceedings of the IEEE, 54,* 221–230.

Aubrey, D.P. & Teskey, R.O. 2009. Root-derived CO_2 efflux via xylem stream rivals soil CO_2 efflux. *New Phytologist, 184,* 35–40.

Bader, N.E. & Cheng, W. 2007. Rhizosphere priming effect of *Populus fremontii* obscures the temperature sensitivity of soil organic carbon respiration. *Soil Biology & Biogeochemistry, 39,* 300–306.

Balesdent, J., Mariotti, A., & Guillet, B. 1987. Natural ^{13}C abundance as a tracer for studies of soil organic matter dynamics. *Soil Biology & Biogeochemistry, 19,* 25–30.

Barbour, M.M., Hunt, J.E., Kodama, N., Laubach, J., McSeveny, T.M., Rogers, G.N.D., Tcherkez, G. & Wingate, L. 2011. Rapid changes in $\delta^{13}C$ of ecosystem-respired CO_2 after sunset are consistent with transient ^{13}C enrichment of leaf respired CO_2. *New Phytologist, 190,* 990–1002.

Becker, M., Andersen, N., Fiedler, B., Fietzek, P., Körtzinger, A., Steinhoff, T. & Friedrich, G. 2012. Using cavity ringdown spectroscopy for continuous monitoring of $\delta^{13}C(CO_2)$ and fCO_2 in the surface ocean. *Limnology and Oceanography: Methods, 10,* 752–766.

Bowling, D.R., Pataki, D.E., & Randerson, J.T. 2008. Carbon isotopes in terrestrial ecosystem pools and CO_2 fluxes. *New Phytologist, 178,* 24–40.

Carney, K.M., Hungate B.A., Drake, B.G., & Megonigal, J.P. 2007. Altered soil microbial community at elevated CO_2 leads to loss of soil carbon. *Proceedings of the National Academy of Sciences USA, 104,* 4990–4995.

Dijkstra, F.A., & Cheng, W. 2007. Interactions between soil and tree roots accelerate long-term soil carbon decomposition. *Ecology Letters, 10,* 1046–1053.

Farquhar, G.D., Ehleringer, J.R., & Hubick, K.T. 1989. Carbon isotope discrimination and photosynthesis. *Annual Review of Plant Physiology and Plant Molecular Biology, 40,* 503–537.

Garcia-Pausas, J., & Paterson, E. 2011. Microbial community abundance and structure are determinants of soil organic matter mineralisation in the presence of labile carbon. *Soil Biology & Biogeochemistry, 43,* 1705-1715.

Harris, S.J., Liisberg, J., Xia, L., Wei, J., Zeyer, K., Yu, L., Barthel, M., Wolf, B., Kelly, B.F.J., Cendón, D.I., Blunier, T., Six, J., and Mohn, J. 2019. N_2O isotopocule measurements using laser spectroscopy: analyzer characterization and intercomparison, *Atmospheric Measurement Techniques Discussions*, https://doi.org/10.5194/amt-2019-451.

Iversen, C.M., Keller, J.K., Garten, C.T. Jr, & Norby, R.J. 2012. Soil carbon and nitrogen cycling and storage throughout the soil profile in a sweetgum plantation after 11 years of CO_2-enrichment. *Global Change Biology, 18,* 1684–1697.

Kirk, G.J.D. & Bellamy, P.H. 2010. Analysis of changes in organic carbon in mineral soils across England and Wales using a simple single-pool model. *European Journal of Soil Science, 61,* 406–411.

Kirk, G.J.D., Boghi, A., Affholder, M.C., Keyes, S.D., Heppell, J. & Roose, T. 2019. Soil carbon dioxide venting through rice roots. *Plant Cell & Environment, 42,* 3197–320.

Lu, J., Dijkstra, F.A., Wang, P., & Cheng, W. 2009. Roots of non-woody perennials accelerated long-term soil organic matter decomposition through biological and physical mechanisms. *Soil Biology & Biogeochemistry, 134,* 42–53.

[dataset]McCloskey, C.S., Otten, W., Paterson, E., Ingram, B., and Kirk, G.J.D.; 2020, Data for assessing a field system for measuring plant and soil carbon fluxes using stable isotope methods, CORD c/o the Cranfield University Library; DOI: 10.17862/cranfield.rd.14216069

Millard P, Midwood, A.J., Hunt, J.E., Whitehead, D., & Boutton, T.W. 2008. Partitioning soil surface CO_2 efflux into autotrophic and heterotrophic components, using natural gradients in soil $\delta^{13}C$ in an undisturbed savannah soil. *Soil Biology & Biochemistry, 40,* 1575–1582.

Moinet, G.Y.K., Midwood, A.J., Hunt, J.E., Whitehead, D., Hannam, K.D., Jenkins, M., Brewer, M.J., Adams, M.A., & Millard, P. 2018. Estimates of rhizosphere priming effects are affected by soil disturbance. *Geoderma, 313,* 1–6.

Moyes, A.B., Gaines, S.J., Siegwolf, R.T.W., & Bowling, D.R. 2010 Diffusive fractionation complicates isotopic partitioning of autotrophic and heterotrophic sources of soil respiration. *Plant Cell & Environment, 33,* 1804–1819.

Nickerson, N., & Risk, D. 2009. Keeling plots are non-linear in non-steady state diffusive environments. *Geophysical Research Letters, 36,* L08401.

Ohlsson, K.E.A. 2010. Reduction of bias in static closed chamber measurement of $\delta^{13}C$ in soil CO_2 efflux. *Rapid Communications in Mass Spectrom*etry*, 24,* 180–184.

Paterson, E., Midwood, A.J., & Millard, P. 2009. Through the eye of the needle: a review of isotope approaches to quantify microbial processes mediating soil carbon balance. *New Phytologist, 184,* 19–33.

R Core Team. 2017. *R: A language and environment for statistical computing*. Vienna, Austria: R Foundation for Statistical Computing.

Rella, C.W., Hoffnagle, J., Y. He, Y., & Tajima, S. 2015. Local- and regional-scale measurements of CH_4, $\delta^{13}CH_4$, and C_2H_6 in the Uintah Basin using a mobile stable isotope analyser. *Atmospheric Measurement Techniques, 8,* 4539–4559.

Schnyder, H., Schäufele, R., Lötscher, M., & Gebbing, T. 2003. Disentangling CO_2 fluxes: direct measurements of mesocosm-scale natural abundance $^{13}CO_2/^{12}CO_2$ gas exchange, ^{13}C discrimination, and labelling of CO_2 exchange flux components in controlled environments. *Plant Cell & Environment, 26,* 1863–1874.

Snell, H.S.K., Robinson, D., & Midwood, A.J. 2014. Minimising methodological biases to improve the accuracy of partitioning soil respiration using natural abundance ^{13}C. *Rapid Communications in Mass Spectrometry, 28,* 2341–2351.

Taneva. L., Pippen, J.S., Schlesinger, W.H., & Gonzàlez-Maler, M.A. 2006. The turnover of carbon pools contributing to soil CO_2 and soil respiration in a temperate forest exposed to elevated CO_2 concentration. *Global Change Biology, 12,* 983–994.

USDA. 2019. *Bouteloua dactyloides (Nutt.) J.T. Columbus Buffalograss*. Washington, USA: United States Department of Agriculture. URL

https://plants.usda.gov/core/profile?symbol=BODA2 [accessed on 14 November 2019].

Zakharova, A., Midwood, A.J., Hunt, J.E., Graham, S.L., Artz, R.R.E., Turnbull, M.H., Whitehead, D. & Millard, P. 2014. Loss of labile carbon following soil disturbance determined by measurement of respired $\delta^{13}CO_2$. *Soil Biology & Biochemistry, 68,* 125–132.

Zhu, Z.-C., Di, D.-R., Ma, M.-G., & Shi, W.-Y. 2019. Stable isotopes in greenhouse gases from soil: a review of theory and application. *Atmosphere, 10,* 377.

3 On allowing for transient variation in end member $\delta^{13}C$ values in isotopic partitioning of ecosystem respiration

Christopher S. McCloskey[1,2] | Wilfred Otten[1] | Eric Paterson[2] | Guy J. D. Kirk[1]

[1]School of Water, Energy & Environment, Cranfield University, Cranfield, Bedford MK43 0AL, UK

[2]The James Hutton Institute, Craigiebuckler, Aberdeen, AB15 8QH, Scotland, UK

Correspondence

Guy Kirk, School of Water, Energy & Environment, Cranfield University, Cranfield, Bedford MK43 0AL, UK. E-mail: g.kirk@cranfield.ac.uk

Abstract

The use of stable isotope analysis to resolve ecosystem respiration into its plant and soil components rests on how well the end-member isotope signatures ($\delta^{13}C$) are characterised. But there is necessarily some degree of uncertainty in end member values due to transient changes in environmental conditions. We analyse diurnal and seasonal patterns of ecosystem respiration and its $\delta^{13}C$ in a C_4 grass growing in a C_3 soil using fixed and diurnally-varying plant and soil $\delta^{13}C$ end members. We measure the end members independently, and we assess the effects of expected variation in values. We show that variation in end members within realistic ranges, particularly diurnal changes in the plant end member, can cause partitioning errors exceeding 100%. The effect depends on how close the end member is to the measured net respiration $\delta^{13}C$, i.e. the proportion of the respiration due to that end member. We conclude that, while it is not practicable to independently measure the full temporal variation in end member values over a growing season, with long-term datasets with sufficient temporal resolution, part of the dataset can be used to fine-tune end members to allow for important transient shifts.

Highlights

- End member $\delta^{13}C$ values used to partition ecosystem respiration vary diurnally and seasonally
- We analyse patterns of ecosystem respiration and its $\delta^{13}C$ in a C_4 grass growing in a C_3 soil
- We find that ignoring changes in end member $\delta^{13}C$ values can cause large errors in partitioning
- Long-term datasets with sufficient temporal resolution can be used to correct for this

KEYWORDS

C_3 and C_4 photosynthesis, ecosystem respiration, isotopic flux partitioning, natural abundance, rhizosphere priming effect, soil carbon.

3.1 Introduction

Due to the difficulties in studying below-ground processes, allocation of plant carbon (C) to roots and the rhizosphere and its effects on soil C turnover remain among the most poorly understood aspects of the terrestrial C cycle (Hartmann *et al*., 2020). A key method for studying such processes exploits differences in the C isotope composition of plants and soil to partition ecosystem respiration into its plant and soil components (Paterson *et al*., 2009; Werth & Kuzyakov, 2010; Brüggemann *et al*., 2011). The $\delta^{13}C$ of ecosystem respiration will lie between the plant and soil 'end member' values, and so can be used to partition fluxes with a mass balance mixing model. As a result of isotopic fractionations that occur in most biochemical and biophysical processes, soil organic matter (SOM) is typically enriched in ^{13}C compared to the plants from which it was derived by approximately 2–4 ‰ (Bowling *et al*., 2008). Such small differences are close to detection limits. But larger differences can be created, either by labelling plants with CO_2 enriched or depleted in ^{13}C, which is expensive, or by exploiting the large $\delta^{13}C$ difference between C_3 and C_4 photosynthetic pathways, typically approximately 10–20 ‰ (Balesdent *et al*., 1987; Farquhar *et al*., 1989). This may be done by growing a C_4 plant in a soil that has previously only hosted C_3 plants, or vice-versa (e.g. Rochette & Flanagan, 1997; Wang *et al*., 2016), or with natural $\delta^{13}C$ gradients across transects of C_3–C_4 vegetation (Millard *et al*., 2008). In all cases, however, reliable partitioning depends on how well the plant and SOM $\delta^{13}C$ end members are characterised. This paper is about how best to measure end members, and how to allow for diurnal, seasonal or other transient sources of variation.

Figure 3-1 shows ranges of $\delta^{13}C$ values reported in the literature for C_4 plants and C_3 soils. The largest variation is between photosynthetic pathways, but there is substantial variation within C_4 plants (-16 to -8 ‰) and C_3 soils (-30 to -20 ‰), and between measurements on plant and soil dry matter versus measurements of respiration fluxes, the latter tending to be less negative by approximately 2 ‰ but with a larger spread. Much of this variation may be due to differences in measurement methods, such as with instrument calibration, as

well as inherent differences within plant species and soil types. But a large part is due to environmental factors.

(a)

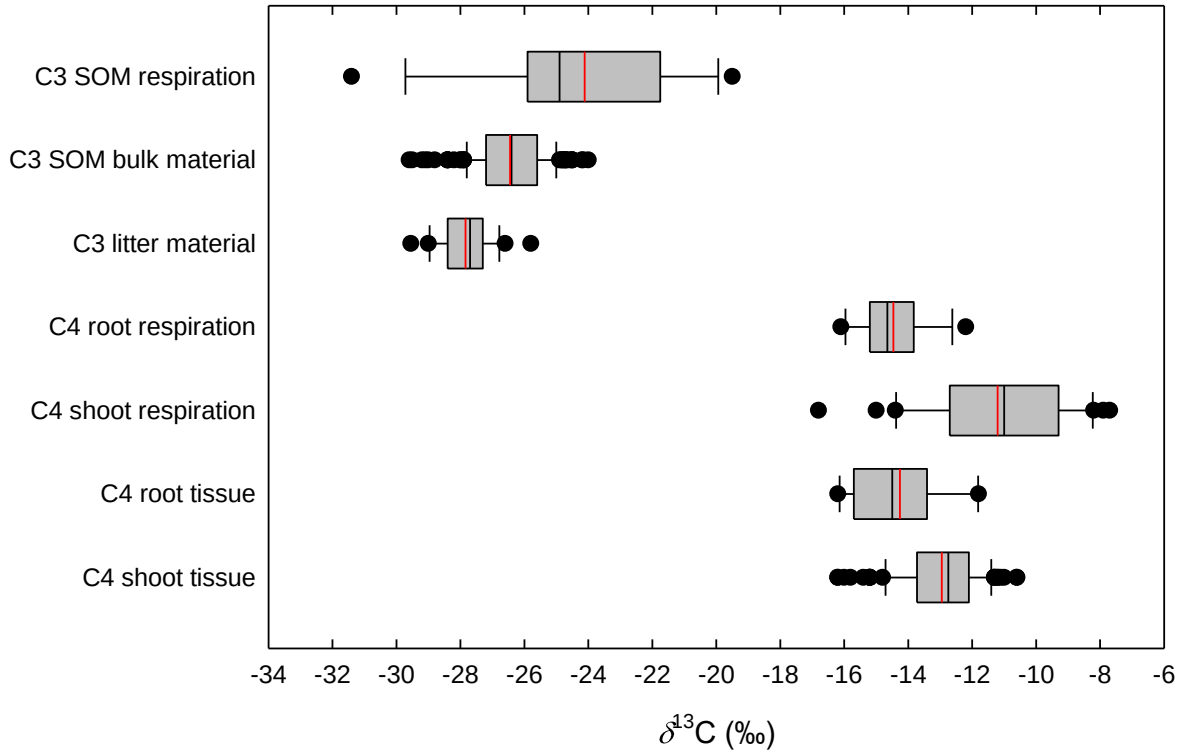

(b)

Pool or flux	*n*	Reference
C_3 SOM respiration	13	Boström *et al*. (2007); Pausch & Kuzyakov (2012); Snell *et al*. (2014); Werth *et al* (2006)
C_3 SOM bulk material	171	Barbour *et al*. (2005); Boström *et al*. (2007); Bowling *et al*. (2002, 2003); Fessenden & Ehleringer (2003); Flanagan *et al*. (1996); Fu & Cheng (2002); Hemming *et al*. (2005); Hobbie *et al*. (1999, 2001); Kohzu *et al*. (1999); Kramer & Gleixner (2006), Pausch and Kuzyakov (2012); Scartazza *et al*. (2004); Trudell *et al*. (2004); Werth & Kuzyakov (2008, 2009)
C_3 litter	28	Barbour *et al*. (2005); Boström *et al*. (2007); Bowling *et al*. (2002); Fessenden and Ehleringer (2003); Hobbie *et al*. (2001); Kohzu *et al*. (1999); Scartazza *et al*. (2004)
C_4 root respiration	16	Lloyd *et al*. (2016); Millard *et al*. (2008); Pausch & Kuzyakov (2012); Werth & Kuzyakov (2006)
C_4 shoot respiration	30	Sun *et al*. (2010); Zhong *et al*. (2017)
C_4 root tissue	15	Rochette & Flanagan (1997); Wedin *et al*. (1995); Werth & Kuzyakov (2006, 2008, 2009); Zhu & Cheng (2011)
C_4 shoot tissue	102	Ghannoum *et al*. (2002); Hattersley (1982); Weiguo *et al*. (2005); Rochette & Flanagan (1997); Sun *et al*. (2010); von Caemmerer *et al*. (2014); Wang *et al*. (2005); Wedin *et al*. (1995); Werth & Kuzyakov (2006, 2008, 2009); Zhu & Cheng (2011)

Figure 3-1 (a) Range of reported $\delta^{13}C$ values for C_3 soil and C_4 plant pools and respiration fluxes. Boxes indicate 25th, 50th and 75th percentiles; whiskers 10th and 90th percentiles; red lines means. (b) Numbers of reported values (*n*; NB in studies with treatment replicates *n* = 1) and references. Studies were excluded where plants were not grown under atmospheric $\delta^{13}C$ conditions, for SOM respiration where roots were not excluded, and where only relative fractionation of ^{13}C (rather than $\delta^{13}C$) was given.

Variation in ^{13}C enrichment between C_4 species grown under the same conditions is relatively small. In a study of 31 C_4 grasses, Hattersley (1982) found a range in leaf $\delta^{13}C$ of just -13.5 to -10.6 ‰, with most species falling between -12.5 and -11.0 ‰. A larger variation is due to the effects of

environmental conditions. Water stress can cause large $\delta^{13}C$ shifts in C_3 species (Cernusak *et al*., 2013; Peters *et al*., 2018). Stomatal closure in response to water stress reduces leaf conductance and lowers the internal ^{12}C:^{13}C ratio, resulting in a lessening of the usual photosynthetic discrimination against ^{13}C. However, this effect is small in C_4 plants, typically < 1 ‰, owing to their greater water use efficiency (Ghannoum *et al*., 2002; Cernusak *et al*., 2013). Seasonal and particularly diurnal variation in light intensity is a greater source of variation, with differences of 2–8 ‰ between light and dark (Cernusak *et al*., 2013). Leaf respiration immediately after a period of illumination is ^{13}C-enriched whereas it is progressively ^{13}C-depleted during darkness. In C_3 grasses, Barbour *et al*. (2011) observed a decrease in leaf respiration $\delta^{13}C$ of approximately 5 ‰ over 6 h of darkness, with the change almost entirely taking place in the first 2 h, and Tcherkez *et al*. (2003) found a decrease of approximately 10 ‰ over 5 d in a C_3 forb. There have been fewer studies in C_4 species. But Sun *et al*. (2010) and Zhong *et al*. (2017) found decreases from 1–4 ‰ (mostly 2–4 ‰) over 6 h of dark in C_4 grasses. The daytime ^{13}C enrichment is linked to differences in C substrate availability and metabolite partitioning during photosynthesis (Sun *et al*., 2010; Zhong *et al*., 2017). Such short-term variation with environmental conditions may show up in measurements of the $\delta^{13}C$ of fluxes, but not in $\delta^{13}C$ of plant dry matter, which integrates over short-term variations.

In comparison, soil isotopic composition is less affected by short-term variation in environmental conditions (e.g. Scartazza *et al*., 2004). There is variation in the $\delta^{13}C$ of SOM pools and respiration with soil depth, in part due to differences between litter and SOM (Figure 3-1), but also due to biophysical processes (Trudell *et al*., 2004; Boström *et al*., 2007; Nickerson & Risk, 2009). Inputs of plant residues and root exudates vary with depth and follow seasonal patterns, and differences in the rates of decomposition of different inputs add to temporal variation in the $\delta^{13}C$ of cycling SOM pools (Werth & Kuzyakov, 2010). Hence the $\delta^{13}C$ of SOM respiration may differ from that of the bulk SOM, and may also vary over a season. Few studies have measured the $\delta^{13}C$ of both bulk root-free soil and its respiration, and those that have report contrasting differences

(Boström *et al*., 2007; Pausch & Kuzyakov, 2012). Fractionation between microbial biomass (itself more ^{13}C enriched than SOM) and microbial respiration is highly variable, ranging from a 4.3 ‰ enrichment to a 3.2 ‰ depletion (Werth & Kuzyakov, 2010). Further, in a C_3 to C_4 vegetation change, the C_4 inputs will gradually become incorporated into the SOM, potentially providing a means of separating SOM pools but also complicating end member evaluations.

What does this mean for partitioning fluxes and whether or not to allow for transient variation in end member $\delta^{13}C$ values? It is not practicable to independently measure the full temporal variation in end member values over a growing season, given the variables discussed above and particularly the sensitivity of diurnal shifts in the plant end member to field conditions. However, with long-term, sufficiently dense and well-resolved datasets showing diurnal and seasonal patterns in ecosystem respiration and its $\delta^{13}C$, an alternative approach is possible in which part of the dataset is used to correct end members for important transient shifts, for use in analysing the rest of the dataset. We explore this approach here with a dataset of diurnal and seasonal patterns of C fluxes and $\delta^{13}C$ in a C_4 plant–C_3 soil field system, using as baseline end-members the $\delta^{13}C$ of plant and soil dry matter sampled from the field. These integrate over short-term variations. We give a sensitivity analysis of C flux partitioning to the plant and soil end members within realistic ranges, and compare partitioning with and without a daytime change in the plant end member.

3.2 Materials and methods

3.2.1 Respiration measurements and partitioning

Measurements were made using the field laboratory system described in McCloskey *et al*. (2020). Briefly, the system contains 24 0.8-m diameter, 1-m deep soil monoliths in lysimeters, connected to automated gas-flux chambers and instruments for gas and stable isotope measurements. The data used in this analysis are for 12 lysimeters of a poorly-drained, seasonally waterlogged loamy soil over clay, formerly under old C_3 pasture at Temple Balsall, Warwickshire, and sampled as undisturbed, naturally-structured monoliths. The

soil was sown with C_4 Buffalo grass (*B. dactyloides*) in January 2018 and then maintained under ambient field conditions, with periodic clipping to maintain an approximately 10-cm high sward.

During a plant and soil respiration measurement, an opaque lysimeter chamber is closed with an opaque lid and air in the headspace is circulated via a sampling loop to a gas analyser (Picarro G2201-*i* cavity ring-down spectroscopy instrument, calibrated against a Thermo Finnigan Delta^{Plus} XP isotope ratio mass spectrometer as described in McCloskey *et al*., 2020) for near continuous measurement of the headspace CO_2 concentration and its $\delta^{13}C$. The total sampling and measurement interval is approximately 20 min, allowing three measurements in each of the 24 lysimeters over 24 h. The combined plant and soil respiration flux (F_R) is found from the rate of change in headspace concentration after a period of equilibration, and its isotope ratio ($\delta^{13}C_R$) is found from plots of $\delta^{13}C$ versus the inverse of the CO_2 concentration according to the Keeling plot method (McCloskey *et al*., 2020). The flux is then partitioned between C_3 SOM and C_4 plant sources as follows. By definition

$$F_R = F_{\text{plant}} + F_{\text{soil}} \qquad \textbf{Equation 3-1}$$

$$F_{\text{plant}} = f_{\text{plant}} F_R \qquad \textbf{Equation 3-2}$$

$$F_{\text{soil}} = f_{\text{soil}} F_R \qquad \textbf{Equation 3-3}$$

and

$$\delta^{13}\text{C}_R F_R = \delta^{13}\text{C}_{\text{plant}} F_{\text{plant}} + \delta^{13}\text{C}_{\text{soil}} F_{\text{soil}} \qquad \textbf{Equation 3-4}$$

where $\delta^{13}\text{C} = \left[\frac{\left(\frac{^{13}\text{C}}{^{12}\text{C}}\right)_{\text{sample}}}{\left(\frac{^{13}\text{C}}{^{12}\text{C}}\right)_{\text{standard}}} - 1 \right] \times 1000$, and $\delta^{13}C_{plant}$ and $\delta^{13}C_{soil}$ are the plant and soil end-member values, respectively. Combining Equations 3-1 to 3-4 and rearranging gives

$$f_{\text{soil}} = \frac{(\delta^{13}\text{C}_R - \delta^{13}\text{C}_{\text{plant}})}{(\delta^{13}\text{C}_{\text{soil}} - \delta^{13}\text{C}_{\text{plant}})}, \qquad \textbf{Equation 3-5}$$

and

$$f_{\text{plant}} = 1 - f_{\text{soil}}$$ **Equation 3-6**

3.2.2 End member measurements

3.2.2.1 From plant and soil dry matter

For $\delta^{13}C_{plant}$, grass shoot clippings were taken on 3–4 October 2019 from six randomly-selected lysimeters. The samples were dried at 65ºC to constant weight, and ground in a planetary ball-mill (Fritsch Pulverisette 6, Gerhardt, Brackley, UK) for 6 min at 300 rpm. The samples were analysed for $\delta^{13}C$ by combustion using a Delta^{Plus} XP IRMS connected via a Conflo III to a Flash EA 1112 Series Elemental Analyser (all Thermo Finnigan, Bremen, Germany). Six replicate sub-samples were analysed.

For $\delta^{13}C_{soil}$, bulk soil was sampled in April 2018 (before seeding with *B. dactyloides*) by taking 2-cm diameter cores to 10-cm depth with a stainless steel auger. Ten samples were taken from each of four randomly-selected lysimeters, air dried and bulked for each lysimeter. Sub-samples of the soil were ground using a pestle and mortar to pass a 2 mm sieve, and analysed by combustion as for the plant material.

3.2.2.2 From respiration

For $\delta^{13}C_{soil}$, air-dry samples of the original field soil, unexposed to the C_4 grass, were moistened to field capacity, packed to a depth of 3 cm in 15-cm internal diameter plastic pipes with acrylic disks glued to their bases, and incubated for 41 days at ambient laboratory temperature. A pneumatically-operated gas flux chamber (eosAC, Eosense, Nova Scotia, Canada) was fitted on top, and connected to a Picarro G2201-*i* analyser via a multiplexer (eosMX, Eosense) and Picarro A0702 diaphragm pump. Measurements of CO_2 respired and its $\delta^{13}C$ were taken over 22 min and $\delta^{13}C_{soil}$ obtained using Keeling plots. Two replicate mesocosms were used, with seven repeated measurements per mesocosm.

For $\delta^{13}C_{plant}$, seeds of *B. dactyloides* were germinated and sown in moist sand that had been heat-treated to remove organic matter, and packed into plastic pipes as for the $\delta^{13}C_{soil}$ measurements. The grass was then grown for 2 months in a glasshouse under ambient summer lighting with watering to constant weight. Respiration measurements were made by bringing the mesocosms into an indoor laboratory and attaching flux chambers over the grass in the dark as for the $\delta^{13}C_{soil}$ measurements, with a 17 min measurement period, and $\delta^{13}C_{plant}$ was obtained using Keeling plots. Three replicate mesocosms were used, with four repeated measurements per mesocosm.

3.2.3 Sensitivity analysis

To assess the effect of variation or uncertainty in end-member values, we conducted a sensitivity analysis using flux data gathered as above over periods when the grass was actively growing (2–7 August 2018). We partitioned the measured fluxes using end-member values spanning the ranges presented in Figure 3-1: $\delta^{13}C_{soil}$ = -21, -24, -27 and -30 ‰ with $\delta^{13}C_{plant}$ = -14.2 ‰ (as measured on dry plant material); and $\delta^{13}C_{plant}$ = -10, -12, -14, and -16 ‰ with $\delta^{13}C_{soil}$ = -28.8 ‰ (as measured on dry soil material). We calculated daily means, maxima and minima of F_{soil} and F_{plant} over the measurement periods for all $\delta^{13}C_{soil}$ and $\delta^{13}C_{plant}$ values. Data analysis was conducted using R version 3.5.1 (R Core Team, 2017).

To assess the effect of a diurnal shift in $\delta^{13}C_{plant}$, we compared a fixed $\delta^{13}C_{plant}$ = -14.2 ‰ (as measured on dry plant material) with a value enriched under light conditions by 3 ‰ (based on the 2–4 ‰ variation discussed in Introduction), both with fixed $\delta^{13}C_{soil}$ = 28.8 ‰ (as measured on dry soil material). We reason that the $\delta^{13}C_{plant}$ of night-time respiration will more-closely track the long-term average value, indicated by the dry plant matter value, and the day-time value will represent the perturbation caused by altered substrate availability and metabolite partitioning during photosynthesis (Introduction). Day-time conditions were defined as when incoming solar radiation ≥ 0.05 W m^{-2} nm^{-1}, as measured by a weather station (Vaisala WXT520) on the site.

Total daily SOM respiration for each day over the growing season was found by fitting a natural cubic spline to the measured data, and calculating the area under the resulting curve. Days for which > 6 measurements (out of the target 36) were missed (because of photosynthesis measurements, system maintenance or other reasons) were excluded. Cumulative SOM respiration over the season was then found by fitting a cubic spline to the daily SOM respiration data so obtained.

3.3 Results

3.3.1 Measured respiration and $\delta^{13}C_R$

Figure 3-2 shows the combined plant and soil respiration fluxes and their $\delta^{13}C$ values for (a) early July 2018 when the grass sward was still becoming established, (b) early August when grass growth was most active, and (c) late December when the grass was dormant. In July and August diurnal patterns in both the total flux magnitude and its $\delta^{13}C$ are clear, with $\delta^{13}C$ values higher in August than July. In December the fluxes are smaller and there are no clear diurnal patterns to either the total flux or its $\delta^{13}C$. In July and August, the respiration flux peaks after midday, matching diurnal variation in solar radiation and air temperature (data not shown). The $\delta^{13}C$ of respiration also peaks after midday with a maximum value 2–4 ‰ less negative than the night-time minimum.

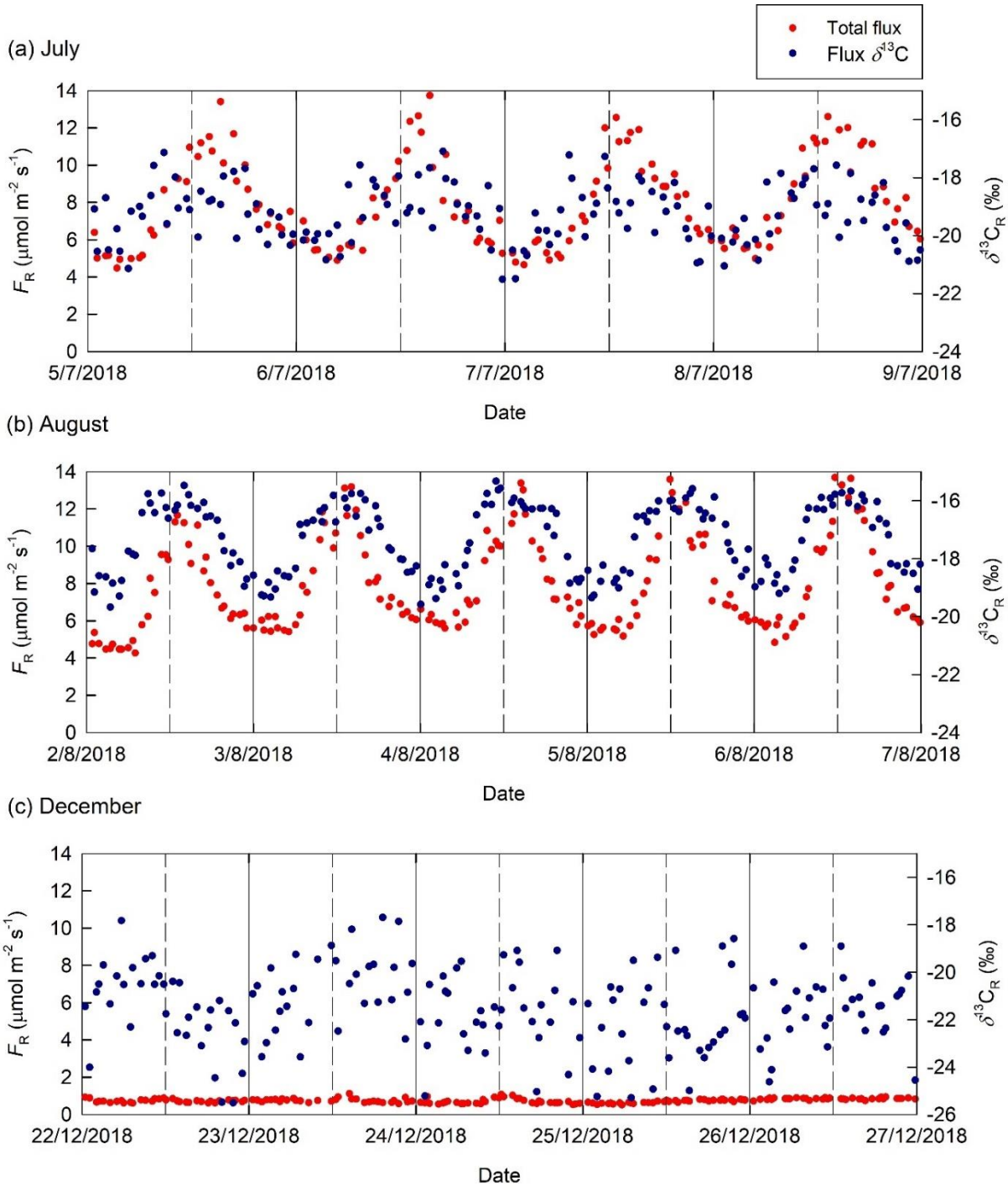

Figure 3-2 Total plant and soil respiration flux and its $\delta^{13}C$ during (a) 5–8 July, (b) 2–6 August and (c) 22–26 December 2018. Data are measurements from 12 lysimeters, each measured thrice daily; individual points represent a measurement from a single lysimeter. Solid lines indicate midnight; dashed lines indicate midday.

3.3.2 End member values

Results are shown in Table 3-1. The $\delta^{13}C_{plant}$ values measured from night-time respiration were < 1 ‰ more negative than those from plant dry matter. The C_4 soil material had $\delta^{13}C$ approximately 16 ‰ more negative (i.e. more ^{13}C depleted) than the plant material. The $\delta^{13}C_{soil}$ values measured from respiration fluxes were approximately 2 ‰ more negative than those from bulk soil material. These differences in $\delta^{13}C_{plant}$ and $\delta^{13}C_{soil}$ between dry matter and respiration methods are within ranges expected for transient processes discussed in the Introduction, as well as artificial biases between the methods. Based on the dry mater values averaging over transient variations, we take these as the standard values for the sensitivity analysis.

Table 3-1 Plant and soil end member $\delta^{13}C$ values from flux measurements and analyses of dry matter. Data are means ± standard errors (details in Materials and methods).

Measurement method	$\delta^{13}C$ (‰)
Plant flux	-15.3 ± 0.2
Plant material	-14.2 ± 0.0
Soil flux	-30.9 ± 0.1
Soil material	-28.8 ± 0.1

3.3.3 Sensitivity analysis

Figure 3-3 shows the sensitivity of the partitioned plant and soil fluxes to $\delta^{13}C_{plant}$ and $\delta^{13}C_{soil}$ over the period in August shown in Figure 3-2, when grass growth was greatest. The daily mean, minimum and maximum fluxes averaged over the measurement period are shown, with $\delta^{13}C_{plant}$ and $\delta^{13}C_{soil}$ values varied over the ranges indicated in Figure 3-1. In this period, the apparent F_{plant} values are up to an order of magnitude greater than F_{soil}, depending on the end

member values. The difference decreases as growth declines and in December mean F_{soil} is greater than mean F_{plant} at most end-member values tested (data not shown). The effects of end member values depend on how far they differ from $\delta^{13}C_R$. Since in most cases $\delta^{13}C_{soil} < \delta^{13}C_R < \delta^{13}C_{plant}$, it follows from Equation 3-5 that increasing $\delta^{13}C_{soil}$ with $\delta^{13}C_{plant}$ constant, and increasing $\delta^{13}C_{plant}$ with $\delta^{13}C_{soil}$ constant, both result in an increase in f_{soil}, i.e. a greater proportion of the flux comes from the soil. However, where $\delta^{13}C_{soil}$ is more enriched than $\delta^{13}C_R$ the calculated F_{plant} is negative, and vice versa. Negative respiration fluxes are impossible, so this can be used to constrain the possible bounds of $\delta^{13}C_{soil}$ and $\delta^{13}C_{plant}$. From Figure 3-3 this limits $\delta^{13}C_{soil}$ in our system to values more depleted than approximately -25 ‰ and $\delta^{13}C_{plant}$ to values more enriched than approximately -15.5 ‰.

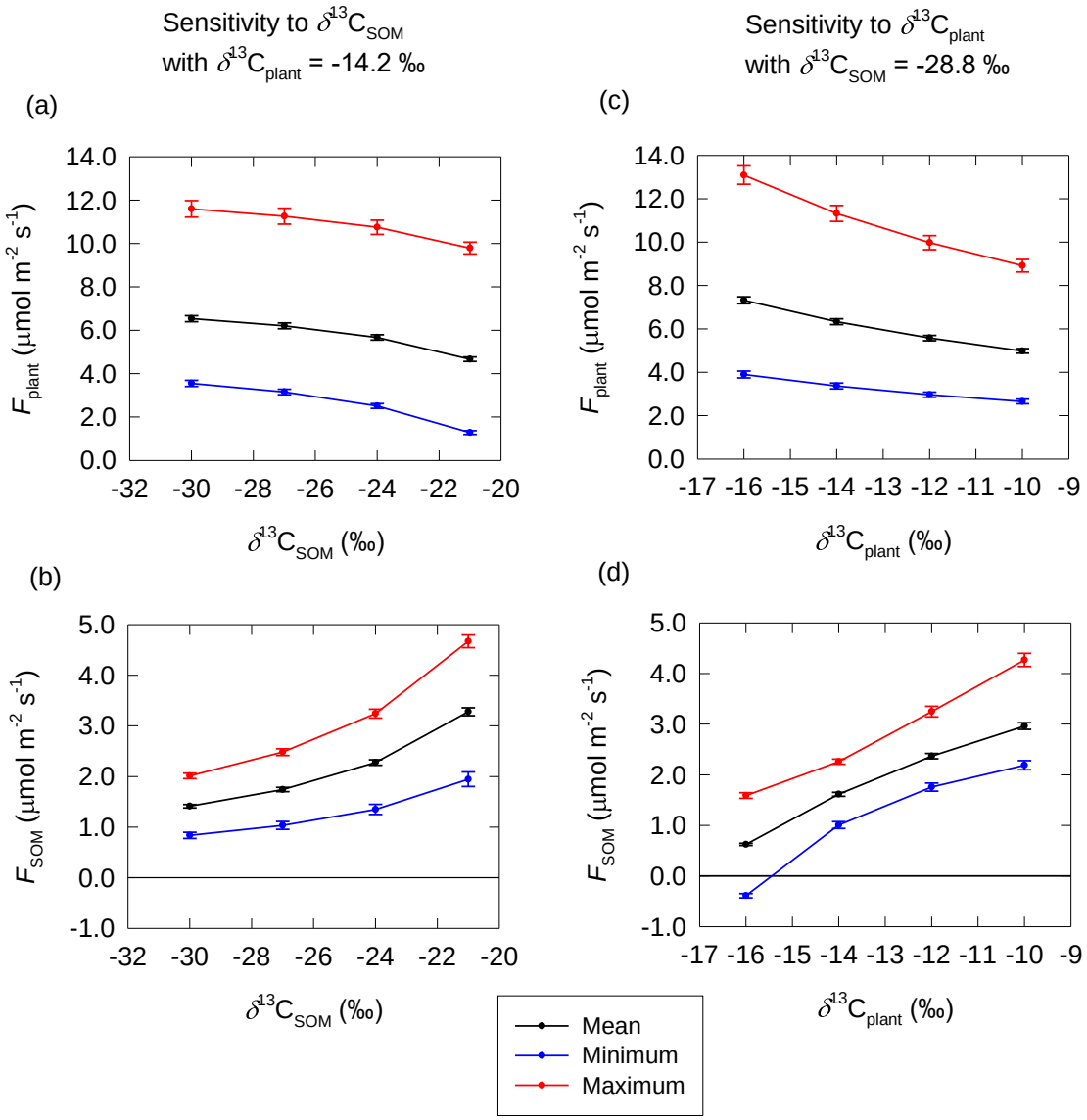

Figure 3-3 Sensitivity of partitioned plant and SOM respiration fluxes over 2–7 August 2018 to end-member values. Daily mean, minimum and maximum values averaged over the measurement period are shown. Left hand panels (a, b) show sensitivity to $\delta^{13}C_{soil}$ at the $\delta^{13}C_{plant}$ measured on plant material; right hand panels (c, d) show sensitivity to $\delta^{13}C_{plant}$ at the $\delta^{13}C_{soil}$ measured on soil material. The mean total flux $\delta^{13}C$ over this period was -17.3 ± 0.1 ‰. Data are means ± standard errors.

The diurnal variation in partitioned plant and SOM fluxes using fixed $\delta^{13}C_{plant}$ and $\delta^{13}C_{soil}$ values equal to the dry matter values (-14.2 and -28.8 ‰,

respectively) are shown in Figure 3-4a-c. Clear diurnal patterns in both plant and SOM fluxes are evident in July, both peaking after midday. However in August, when plant growth and respiration are greater, the apparent diurnal trend in SOM fluxes is inverted, peaking around midnight, though the plant fluxes show the same diurnal pattern as in July peaking after midday. In December, both fluxes are small and without clear diurnal trends.

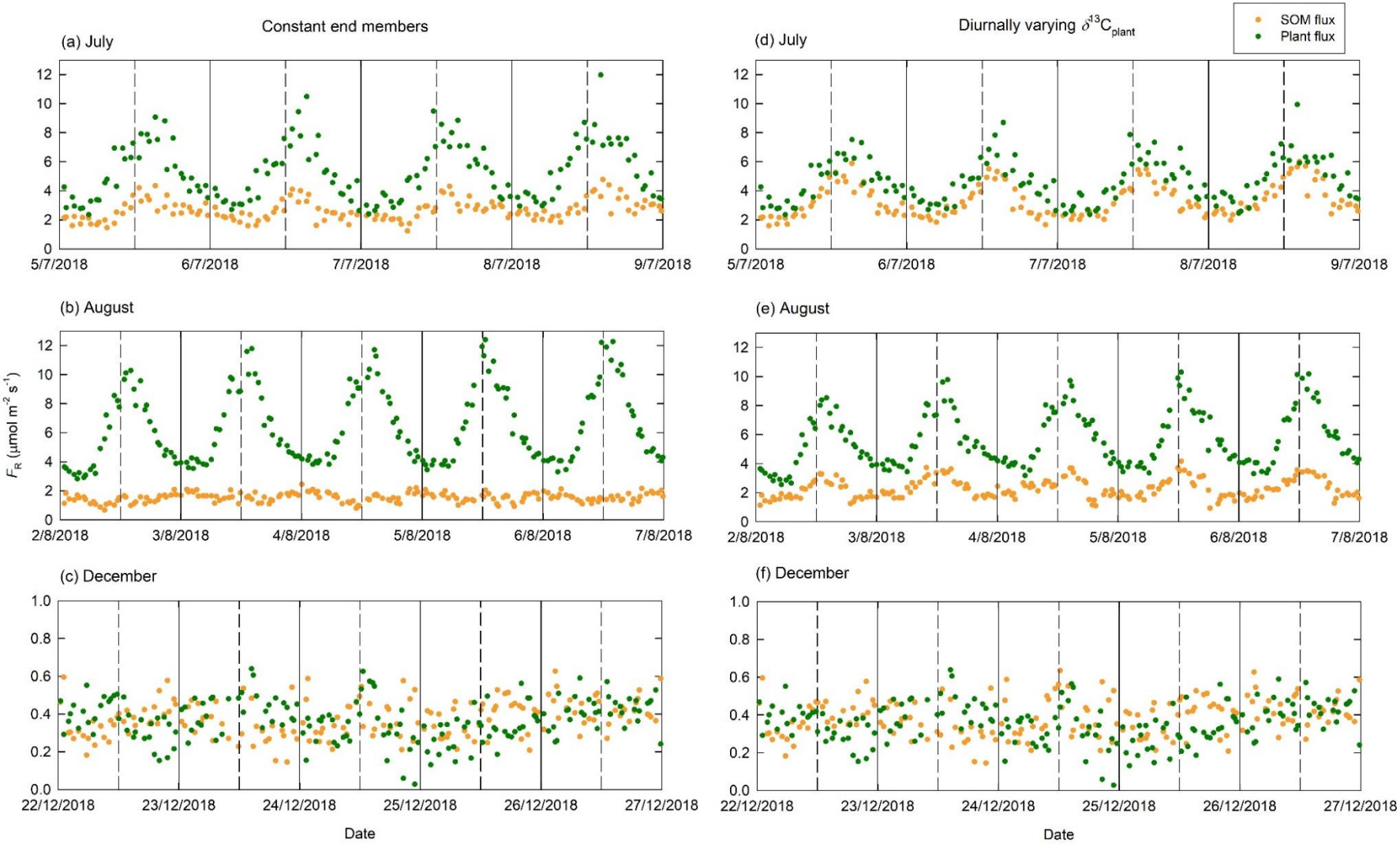
Constant end members
Diurnally varying $\delta^{13}C_{plant}$
SOM flux
Plant flux
(a) July
(b) August
(c) December
(d) July
(e) August
(f) December
F_R (µmol m^{-2} s^{-1})
Date
5/7/2018
6/7/2018
7/7/2018
8/7/2018
9/7/2018
2/8/2018
3/8/2018
4/8/2018
5/8/2018
6/8/2018
7/8/2018
22/12/2018
23/12/2018
24/12/2018
25/12/2018
26/12/2018
27/12/2018

Figure 3-4 Partitioned plant and SOM respiration fluxes with $\delta^{13}C_{soil}$ = -28.8 ‰ and (a)-(c) $\delta^{13}C_{plant}$ = -14.2 ‰ or (d)-(f) a +3 ‰ daytime shift in $\delta^{13}C_{plant}$ (-14.2 ‰ during the day, -11.2 ‰ at night) during 5–8 July, 2–6 August and 22–26 December 2018, respectively. Data are measurements from 12 lysimeters, each measured thrice daily; individual points represent a measurement from a single lysimeter. Solid lines indicate midnight; dashed lines indicate midday.

Figure 3-4d–f shows the fluxes for the same periods, partitioned using $\delta^{13}C_{soil}$ = -28.8 ‰ and a diurnal increase in $\delta^{13}C_{plant}$ of 3 ‰ from -14.2 ‰ in the dark to -11.2 ‰ in the light. The results in Figure 3-4d–e show similar diurnal plant and SOM flux patterns in July and August to those for July in Figure 3-4a, with peaks in both plant and SOM respiration after midday. Increased f_{soil} with the less negative day-time $\delta^{13}C_{plant}$ is as expected from Equation 3-5. We also found, with fixed $\delta^{13}C_{soil}$ = -28.8 ‰ and $\delta^{13}C_{plant}$ = -11.2 ‰, the diurnal plant and SOM respiration patterns in July and August were aligned, both peaking after midday (data not shown). The main changes compared to Figure 3-4a-c were that in July, the night-time SOM and plant fluxes are roughly equal; in August, the diurnal variation in the SOM flux is reduced; and in December, the SOM flux is generally greater than the plant flux, rather than roughly equal.

Figure 3-5 shows the effect of allowing for a diurnal shift in $\delta^{13}C_{plant}$ on the cumulative SOM respiration over the 2018 growing season. Allowing for a diurnal shift increased total SOM respiration by 26 % from August to December. The majority of this difference occurred between mid-July and mid-September, when plant respiration was most dominant.

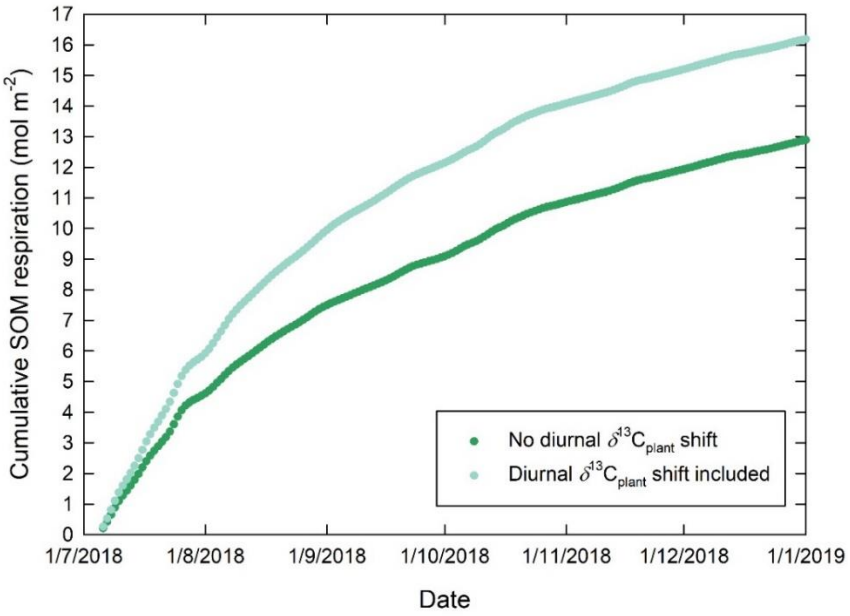

Figure 3-5 Effect of allowing for a +3 ‰ diurnal shift in the plant δ^{13} end member on cumulative SOM respiration over the 2018 growing season.

3.4 Discussion

In early July there was strong diurnal environmental variation – and corresponding variation in total C flux and its δ^{13}C – but with the soil flux comparable to the plant flux. The diurnal pattern in SOM fluxes is clearly evident, with a peak after midday, suggesting that the apparent night-time peak in SOM flux observed when the plant flux was greater was erroneous. Daytime increases in plant and soil respiration and night-time decreases are expected with diurnal changes in temperature. We found this pattern with flux partitioning using the fixed end-member values from dry matter analysis in early July, when the grass sward was still becoming established, but not in August, when the sward was well established and the plant flux was more dominant. Rather, in August, the diurnal changes in SOM respiration were inverted, with a peak around midnight. Potential causes of this inversion include: (1) the real plant end-member, while stable over diurnal timescales, was more ^{13}C enriched than the value we used; (2) the real plant end-member was ^{13}C enriched during the

day due to the influence of light; or (3) soil microbial respiration decreased during the day, perhaps due to preferential use of root exudates rather than SOM, combined with a diurnal pattern to root exudation.

A daytime ^{13}C plant flux enrichment would link the daytime increase in total flux to an exaggerated partitioning shift in favour of the plant flux. With increasing dominance by the plant flux, this would distort flux partitioning to the point that daytime SOM flux peaks would first disappear, and then become inverted. As such ^{13}C enrichment of both C_3 and C_4 respiration during photosynthesis is well-established in the literature (Introduction) we consider this to be the likely cause of the inverted SOM flux peaks we observed in August. When we incorporated a ^{13}C enriched plant end member during daylight, we found a diurnal pattern to SOM respiration similar to that seen in July. We did also reproduce the daytime SOM respiration peak with a fixed plant end member, more ^{13}C-enriched than the measured dry matter value by 3 ‰. However we see no reason why the dry matter should misrepresent the long-term average $\delta^{13}C_{plant}$ to this extent.

Likewise we see no good reason for favouring our third suggested explanation above, that SOM respiration decreased during the day through some mechanism. Rather we expect the opposite: that SOM turnover should be enhanced during the day by priming effects of root exudates. Addition of labile C in exudates to the rhizosphere soil is thought to increase the production of enzymes that degrade SOM to release nutrients; that is, microbes use the extra C available in the rhizosphere to 'mine' nutrients that limit their activity (Paterson *et al*., 2009; Werth & Kuzyakov, 2010). Exudation and rhizosphere microbial activity are typically greater during the day (Hubbard *et al*., 2018).

Diurnal variation in the plant end-member has not previously been used in flux partitioning studies, despite clear evidence for it from short-term physiological studies (Introduction). The field laboratory system we used allows for high temporal resolution, and our results suggest not allowing for a diurnal shift in $\delta^{13}C_{plant}$ may cause substantial errors in flux partitioning. As we have shown, this has the potential to obscure trends in SOM respiration and prevent the correct assessment of factors driving SOM turnover. We therefore suggest that

flux partitioning studies based on ^{13}C abundance need to incorporate light-driven changes in the plant end member, particularly where diurnal trends are of interest.

We applied a daytime ^{13}C enrichment by 3 ‰ based on the 2–4 ‰ variation under light conditions discussed in the Introduction. In principle it would be possible to systematically fit a variable end member value to the dataset using model-data fusion techniques. We have not done so because a full analysis of the dataset is beyond the scope of the paper. Our objective is to illustrate the potential of the approach.

During the main growing season, $f_{plant} >> f_{soil}$ and since we measure shoot as well as root respiration, errors in $\delta^{13}C_{plant}$ will have a disproportionate effect on the calculated SOM flux. In systems that exclude above-ground respiration from flux measurements, with chambers placed on bare soil between the above-ground plant parts so that only root and soil respiration is assayed, it may nonetheless be necessary to allow for diurnal shifts in the plant end member as root respiration varies diurnally with photosynthesis.

Environmental factors affect both plant respiration flux and biomass $\delta^{13}C$, although to different extents. Respiration fluxes are more subject to artefacts of measurement methods. They may better represent environmental factors, such as light levels or water stress. On the other hand the $\delta^{13}C$ of plant tissues provides a long-term average of the effects of varying environmental conditions. As such, in a varying environment it may be more appropriate to use a plant end-member measured through plant tissue analysis as the baseline value.

3.5 Conclusions

There is necessarily transient variation in plant and soil $\delta^{13}C$ end members over the course of a growing season and on diurnal timescales, due to varying environmental conditions. Large day-night variation in the plant end member is well established. If not allowed for, such variation can cause substantial errors in flux partitioning.

Potential errors are greatest when (a) the end member value is far from $\delta^{13}C_R$, or (b) ecosystem respiration is low, so that a small change in flux has a proportionally greater effect.

It is not practicable to independently measure the full temporal variation in end member values over a growing season. However, with long-term datasets with sufficient temporal resolution, part of the dataset can be used to fine-tune end members to allow for important transient shifts, for use in analysing the rest of the dataset.

End-member measurements on plant and soil dry matter integrate across transient variations, and provide a realistic baseline for this approach.

Acknowledgements

The field laboratory was built with a Royal Society Wolfson Laboratory Refurbishment Grant (WL080021/Kirk). The CRDS analyser was provided by the Agri-Epi Centre, Cranfield Hub. CM was supported by the Soils Training and Research Studentships (STARS) Centre for Doctoral Training, funded by the Biotechnology and Biological Sciences Research Council and the Natural Environment Research Council (grant number NE-M009106-1). The James Hutton Institute receives funding from the Rural and Environment Science and Analytical Services Division (RESAS) of the Scottish Government.

Conflict of interest

The authors have no conflicts of interest related to the work presented in this manuscript.

Author contributions

CM, GK, WO and EP conceived this study. CM carried out the experimental work and data analysis. CM and GK wrote the initial manuscript and all contributed to the final version.

Data availability statement

The data used in this article will be available at CORD c/ o the Cranfield University Library.

3.6 References

Balesdent, J., Mariotti, A. & Guillet, B. 1987. Natural ^{13}C abundance as a tracer for studies of soil organic matter dynamics. *Soil Biology and Biogeochemistry, 19*, 25–30.

Barbour, M.M., Hunt, J.E., Dungan, R.J., Turnbull, M.H., Brailsford, G.W., Farquhar, G.D. & Whitehead, D. 2005. Variation in the degree of coupling between $\delta^{13}C$ of phloem sap and ecosystem respiration in two mature Nothofagus forests. *New Phytologist, 166*, 497–512.

Barbour, M.M., Hunt, J.E., Kodama, N., Laubach, J., McSeveny, T.M., Rogers, G.N., Tcherkez, G. & Wingate, L. 2011. Rapid changes in $\delta^{13}C$ of ecosystem-respired CO_2 after sunset are consistent with transient ^{13}C enrichment of leaf respired CO_2. *New Phytologist, 190*, 990–1002.

Boström, B., Comstedt, D. & Ekblad, A. 2007. Isotope fractionation and ^{13}C enrichment in soil profiles during the decomposition of soil organic matter. *Oecologia, 153*, 89–98.

Bowling, D.R., McDowell, N.G., Bond, B.J., Law, B.E. & Ehleringer, J.R. 2002. ^{13}C content of ecosystem respiration is linked to precipitation and vapor pressure deficit. *Oecologia, 131*, 113–124.

Bowling, D.R., Pataki, D.E. & Ehleringer, J.R. 2003. Critical evaluation of micrometeorological methods for measuring ecosystem–atmosphere isotopic exchange of CO_2. *Agricultural and Forest Meteorology, 116,* 159–179.

Bowling, D.R., Pataki, D.E. & Randerson, J.T. 2008. Carbon isotopes in terrestrial ecosystem pools and CO_2 fluxes. *New Phytologist, 178*, 24–40.

Brüggemann, N., Gessler, A., Kayler, Z., Keel, S., Badeck, F., Barthel, M., Boeckx, P., Buchmann, N., Brugnoli, E. & Esperschütz, J. 2011. Carbon

allocation and carbon isotope fluxes in the plant–soil–atmosphere continuum: a review. *Biogeosciences, 8*, 3457–3489.

Cernusak, L.A., Ubierna, N., Winter, K., Holtum, J.A.M., Marshall, J.D. & Farquhar, G.D. 2013. Environmental and physiological determinants of carbon isotope discrimination in terrestrial plants. *New Phytologist, 200*, 950–965.

Farquhar, G.D., Ehleringer, J.R. & Hubick, K.T. 1989. Carbon isotope discrimination and photosynthesis. *Annual Review of Plant Physiology and Plant Molecular Biology, 40*, 503–537.

Fessenden, J.E. & Ehleringer, J.R. 2003. Temporal variation in $\delta^{13}C$ of ecosystem respiration in the Pacific Northwest: links to moisture stress. *Oecologia, 136*, 129–136.

Flanagan, L.B., Brooks, J.R., Varney, G.T., Berry, S.C. & Ehleringer, J.R. 1996. Carbon isotope discrimination during photosynthesis and the isotope ratio of respired CO_2 in boreal forest ecosystems. *Global Biogeochemical Cycles, 10*, 629–640.

Fu, S. & Cheng, W. 2002. Rhizosphere priming effects on the decomposition of soil organic matter in C_4 and C_3 grassland soils. *Plant and Soil, 238*, 289–294.

Ghannoum, O., von Caemmerer, S. & Conroy, J.P. 2002. The effect of drought on plant water use efficiency of nine NAD–ME and nine NADP–ME Australian C_4 grasses. *Functional Plant Biology, 29*, 1337–1348.

Hartmann, H., Bahn, M., Carbone, M. & Richardson, A.D. 2020. Plant carbon allocation in a changing world – challenges and progress: introduction to a Virtual Issue on carbon allocation. *New Phytologist, 227*, 981–988.

Hattersley, P.W. 1982, δ^{13} values of C_4 types in grasses. *Functional Plant Biology, 9*, 139–154.

Hemming, D., Yakir, D., Ambus, P., Aurela, M., Besson, C., Black, K., Buchmann, N., Burlett, R., Cescatti, A., Clement, R. *et al*. 2005. Pan-European

$\delta^{13}C$ values of air and organic matter from forest ecosystems. *Global Change Biology, 11*, 1065–1093.

Hobbie, E., Macko, S. & Shugart, H. 1999. Insights into nitrogen and carbon dynamics of ectomycorrhizal and saprotrophic fungi from isotopic evidence. *Oecologia, 118*, 353–360.

Hobbie, E.A., Weber, N.S. & Trappe, J.M. 2001. Mycorrhizal vs saprotrophic status of fungi: the isotopic evidence. *New Phytologist, 150*, 601–610.

Hubbard, C.J., Brock, M.T., van Diepen, L.T.A., Maignien, L., Ewers, B.E & Weinig, C. 2018. The plant circadian clock influences rhizosphere community structure and function. *The ISME Journal, 12*, 400-410.

Kohzu, A., Yoshioka, T., Ando, T., Takahashi, M., Koba, K. & Wada, E. 1999. Natural ^{13}C and ^{15}N abundance of field-collected fungi and their ecological implications. *New Phytologist, 144*, 323–330.

Kramer, C. & Gleixner, G. 2006. Variable use of plant- and soil-derived carbon by microorganisms in agricultural soils. *Soil Biology and Biochemistry, 28*, 3267–3278.

Lloyd, D., Ritz, K., Paterson, E. & Kirk, G.J.D. 2016. Effects of soil type and composition of rhizodeposits on rhizosphere priming phenomena. *Soil Biology and Biochemistry, 103*, 512–521.

McCloskey, C.S., Otten, W., Paterson, E., Ingram, B. & Kirk, G.J.D. 2020. A field system for measuring plant and soil carbon fluxes using stable isotope methods. *European Journal of Soil Science.* Doi: 10.1111/ejss.13016.

Millard, P., Midwood, A.J., Hunt, J.E., Whitehead, D. & Boutton, T.W. 2008. Partitioning soil surface CO_2 efflux into autotrophic and heterotrophic components, using natural gradients in soil $\delta^{13}C$ in an undisturbed savannah soil. *Soil Biology and Biochemistry, 40*, 1575–1582.

Nickerson, N. & Risk, D. 2009. Keeling plots are non-linear in non-steady state diffusive environments. *Geophysical Research Letters, 36*, L08401.

Paterson, E., Midwood, A.J. & Millard, P. 2009. Through the eye of the needle: a review of isotope approaches to quantify microbial processes mediating soil carbon balance. *New Phytologist, 184*, 19–33.

Pausch, J. & Kuzyakov, Y. 2012. Soil organic carbon decomposition from recently added and older sources estimated by $\delta^{13}C$ values of CO_2 and organic matter. *Soil Biology and Biochemistry, 55*, 40–47.

Peters, W., van der Velde, I.R., van Schaik, E., Miller, J.B., Ciais, P., Duarte, H.F., van der Laan-Luijkx, I.T., van der Molen, M.K., Scholze, M., Schaefer, K. *et al*. 2018. Increased water-use efficiency and reduced CO_2 uptake by plants during droughts at a continental-scale. *Nature Geoscience, 11*, 744–748.

R Core Team. (2017) *R: A language and environment for statistical computing*. Vienna, Austria: R Foundation for Statistical Computing.

Rochette, P. & Flanagan, L.B. 1997. Quantifying rhizosphere respiration in a corn crop under field conditions. *Soil Science Society of America Journal, 61*, 466–474.

Scartazza, A., Mata, C., Matteucci, G., Yakir, D., Moscatello, S. & Brugnoli, E. 2004. Comparisons of $\delta^{13}C$ of photosynthetic products and ecosystem respiratory CO_2 and their responses to seasonal climate variability. *Oecologia, 140*, 340–351.

Snell, H.S.K., Robinson, D. & Midwood, A.J. 2014. Minimising methodological biases to improve the accuracy of partitioning soil respiration using natural abundance ^{13}C. *Rapid Communications in Mass Spectrometry, 28*, 2341–2351.

Sun, W., Resco, V. & Williams, D.G. 2010. Nocturnal and seasonal patterns of carbon isotope composition of leaf dark-respired carbon dioxide differ among dominant species in a semiarid savanna. *Oecologia, 164*, 297–310.

Tcherkez, G., Nogues, S., Bleton, J., Cornic, G., Badeck, F. & Ghashghaie, J. 2003. Metabolic origin of carbon isotope composition of leaf dark-respired CO_2 in French bean. *Plant Physiology, 131*, 237– 244.

Trudell, S.A., Rygiewicz, P.T. & Edmonds, R.L. 2004. Patterns of nitrogen and carbon stable isotope ratios in macrofungi, plants and soils in two old-growth conifer forests. *New Phytologist, 164*, 317–335.

von Caemmerer, S., Ghannoum, O., Pengelly, J.L.L. & Cousins, A.B. 2014. Carbon isotope discrimination as a tool to explore C_4 photosynthesis. *Journal of Experimental Botany, 65*, 3459–3470.

Wang, G., Han, J., Zhou, L., Xiong, X. & Wu, Z. 2005. Carbon isotope ratios of plants and occurrences of C4 species under different soil moisture regimes in arid region of Northwest China. *Physiologia Plantarum, 125*, 74–81.

Wang, X., Tang, C., Severi, J., Butterly, C.R. & Baldock, J.A. 2016. Rhizosphere priming effect on soil organic carbon decomposition under plant species differing in soil acidification and root exudation. *New Phytologist, 211*, 864–873.

Wedin, D.A., Tieszen, L.L., Dewey, B. & Pastor, J. 1995. Carbon isotope dynamics during grass decomposition and soil organic matter formation. *Ecology, 76*, 1383–1392.

Weiguo, L., Xiahong, F., Youfeng, N., Qingle, Z., Yunning, C. & Zhisheng, A.N. 2005. $\delta^{13}C$ variation of C_3 and C_4 plants across an Asian monsoon rainfall gradient in arid northwestern China. *Global Change Biology, 11*, 1094–1100.

Werth, M. & Kuzyakov, Y. 2006. Assimilate partitioning affects ^{13}C fractionation of recently assimilated carbon in maize. *Plant and Soil, 284*, 319–333.

Werth, M. & Kuzyakov, Y. 2008. Root-derived carbon in soil respiration and microbial biomass determined by ^{14}C and ^{13}C. *Soil Biology and Biochemistry, 40*, 625–637.

Werth, M. & Kuzyakov, Y. 2009. Three-source partitioning of CO_2 efflux from maize field soil by ^{13}C natural abundance. *Journal of Plant Nutrition and Soil Science, 172*, 487–499.

Werth, M. & Kuzyakov, Y. 2010. ^{13}C fractionation at the root-microorganisms-soil interface: A review and outlook for partitioning studies. *Soil Biology and Biochemistry, 42*, 1372–1384.

Zhong, S., Chai, H., Xu, Y., Li, Y., Ma, J.-Y. & Sun, W. 2017. Drought sensitivity of the carbon isotope composition of leaf dark-respired CO_2 in C_3 (*Leymus chinensis*) and C_4 (*Chloris virgata* and *Hemarthria altissima*) grasses in northeast China. *Frontiers in Plant Science, 8*, 1996.

Zhu, B., Cheng, W. 2011. ^{13}C isotope fractionation during rhizosphere respiration of C_3 and C_4 plants. *Plant and Soil, 342*, 277–287.

4 Evidence for tight coupling between photosynthesis and soil carbon turnover from diurnal and seasonal patterns in a C_4 grass grown in two C_3 soils under field conditions

Christopher S. McCloskey[1,2] | Wilfred Otten[1] | Eric Paterson[2] | Guy J. D. Kirk[1]

[1]School of Water, Energy & Environment, Cranfield University, Cranfield, Bedford MK43 0AL, UK

[2]The James Hutton Institute, Craigiebuckler, Aberdeen, AB15 8QH, Scotland, UK

Correspondence

Chris McCloskey, School of Water, Energy & Environment, Cranfield University, Cranfield, Bedford MK43 0AL, UK. E-mail: c.mccloskey@cranfield.ac.uk

Abstract

Rhizosphere priming effects are well-documented under laboratory and controlled-environment conditions, but their significance in undisturbed systems under field conditions is less clear. This is in part because it is impracticable to measure rates of rhizodeposition in the field with high resolution over a substantial period. We propose that solar radiation, closely tied via photosynthesis to rhizodeposition, can be used as a proxy for plant root activity. Here we use a field system to measure carbon (C) fluxes at a high temporal resolution, and exploit isotopic differences between two C_3 soils and a C_4 grass to allow partitioning of plant and soil fluxes. We assess the relationship between diurnal patterns in soil respiration and potential drivers, and examine whether model estimates of soil respiration are improved by the inclusion of solar radiation as an explanatory variable alongside soil moisture and temperature. We also test whether higher nitrogen (N) application suppresses soil organic matter turnover, as proposed by the N mining hypothesis. Seasonal and diurnal patterns in plant and soil fluxes were resolved. During summer, soil respiration showed a strong diurnal pattern, varying daily by a factor of two. A significant

positive relationship between solar radiation and soil respiration was found in both soils, consistent with rhizosphere priming enhancing soil C turnover. As rhizodeposition varies on diurnal timescales the detection of this relationship was reliant on high-resolution soil respiration data. Greater N application did not correlate to reduced soil respiration; no evidence for N mining was found in our system.

Highlights

- We propose using solar radiation as a proxy for rhizodeposition as a means to detect rhizosphere priming effects in the field.
- This was coupled with high-frequency soil respiration measurements.
- We detected a significant relationship between solar radiation and greater soil respiration, accounting for soil temperature and moisture. This was dependent on high-resolution flux measurements.
- No evidence was found for N mining as a driver for rhizosphere priming.

Keywords

Rhizosphere priming, soil organic matter, nitrogen mining

4.1 Introduction

Plant root activity and deposition of carbon (C) from roots into the rhizosphere is known to influence the turnover of existing soil organic matter (SOM) in so-called rhizosphere priming effects (RPEs) (Trumbore 2006; Kuzyakov & Gavrichkova 2010). This process may allow soil microbes to access nitrogen (N) and other nutrients held in SOM which are otherwise unavailable to them (Bengtson *et al*., 2012; Cheng *et al*., 2014; Murphy *et al*., 2015). However the magnitudes, drivers and mechanisms of these effects remain poorly understood (Hartmann *et al*., 2020). Laboratory, controlled-environment and a limited number of field studies have demonstrated that priming can occur in a variety of soils and plant types, and measured priming effects range from -50 to +382 % (Cheng *et al*., 2014). Many studies of priming, however, have been at a substantial abstraction from realistic field conditions.

Lab-based studies include applications of labile organic substrates representing rhizodeposits to unplanted soil (e.g. Derrien *et al*., 2014, Lloyd *et al*., 2016, and Zang *et al*., 2016) as well as planted pot experiments (e.g. Shazad *et al*., 2012 and Paterson *et al*., 2016). Such studies, however, may not be representative of undisturbed soils in the field, and may lack important soil-plant feedbacks due to their limited duration. Furthermore, RPEs found through such studies may be artefacts of disturbance facilitating microbial access to protected soil C (Tian *et al*., 2015, Moinet *et al.*, 2018). Further, the majority of studies have been short-term, lasting only weeks or a few months after planting (Huo *et al*., 2017). This may be insufficient to demonstrate whether relationships between soil C fluxes and their drivers persist over longer timescales. Where longer term studies exist, the methods used often do not allow frequent measurements, required to resolve patterns in SOM turnover in response to diel drivers. For example, studies by Bader and Cheng (2007), Dijkstra and Cheng (2007) and Lu *et al*. (2019), running for 247, 395 and 476 days respectively, measured soil C fluxes on just six, seven and three occasions. A recent study has demonstrated long-term SOM priming under frequent glucose addition (Zhou *et al*., 2021) – although as a lab-based experiment this is divorced from the diurnal and seasonal effects of environmental variation. Various studies under field conditions have shown trends in soil respiration on diurnal time scales, apparently linked to rhizosphere priming effects in addition to diurnal temperature fluctuations (Bahn *et al*., 2009; Kuzyakov & Gavrichkova, 2010; Phillips *et al*., 2011; Hopkins *et al*., 2013; Mitra *et al*., 2019).

The relative lack of field studies on rhizosphere priming reflect the experimental difficulties. Directly measuring rhizodeposition and its effects on SOM turnover in the field is impractical, particularly at a high resolution and over a long timeframe. A more practicable approach is to use stable isotope methods to separate measurements of below-ground CO_2 fluxes into their plant and soil sources (McCloskey *et al*., 2020 and references therein). This may be done by exposing the plant leaves to isotopically-labelled CO_2, either as a pulse or more-continuously (Kuzyakov & Gavrichkova, 2010). However, such labelling is cumbersome and expensive, and pulse labelling introduces uncertainties into

time lags between photosynthesis and rhizodeposition. An alternative is to exploit differences in the C-isotope signature of plant and soil organic matter. Such differences are typically of the order of 2–4 ‰ (Bowling *et al*., 2008); this small isotopic range limits the resolution of partitioning, which may be particularly vulnerable to measurement error and background natural abundance variation. A much larger difference can be created by exploiting the 10–20 ‰ difference between C_3 and C_4 photosynthetic pathways (McCloskey *et al*., 2020 and references therein). Growing a C_4 plant in a soil that has only ever had C_3 vegetation, or *vice versa*, creates a readily-measurable difference between plant-derived C fluxes – including microbial respiration fuelled by recent plant inputs – and the turnover of older SOM. This can be used to generate time-courses of partitioned plant respiration and SOM-C fluxes, with which to assess whether diurnal and seasonal patterns of SOM turnover are better explained when a priming effect is accounted for.

A problem is how to obtain a surrogate measure of rhizodeposition with which to assess the effects on the SOM-C flux. Rates of rhizodeposition are closely linked to rates of photosynthesis, particularly in small herbaceous plants (Dilkes *et al*., 2004; Mencuccini & Hölttä, 2009) and trends in both rhizodeposition and rhizosphere community structure have been found over diurnal timescales (Hubbard *et al*., 2018). Rates of photosynthesis, in turn, are tightly linked to solar radiation intensity (Harmer, 2009). Solar radiation may therefore serve as a readily-measured surrogate for root exudation.

The purpose of this study was to explore use of the above methods for measuring rhizosphere priming effects under field conditions. We obtained a dataset of diurnal and seasonal patterns of plant and soil C fluxes in a C_4 plant–C_3 soil field system, with two contrasting, naturally-structured soils over two growing seasons. We test the hypothesis that including solar radiation as an explanatory variable improves model-based estimation of soil respiration, compared to estimates based on soil moisture and temperature alone. Secondly, we investigate whether N mining is a driver for any priming effects detected.

4.2 Methods

4.2.1 Measurements of plant and soil C fluxes

Measurements were made using the field laboratory system described in McCloskey *et al*. (2020) over two growing seasons in 2018 and 2019. The system comprises 24 0.8-m diameter, 1-m deep soil monoliths contained in lysimeters and connected to automated gas flux chambers and instruments. The soil monoliths are of two types: a clay-loam over clay formerly under old pasture at Temple Balsall, Warwickshire, UK, with topsoil (0–15 cm depth) pH (H_2O) 6.1 and organic C content 39.8 g kg^{-1} with C:N ratio 9.9; and a sandy loam formerly under bracken/grass at Shuttleworth College, Bedfordshire, UK, with, following liming, topsoil pH (H_2O) 6.3 and organic C content 36.3 g kg^{-1} with C:N ratio 16.1. The soils were collected as intact monoliths from the respective field sites and brought to Cranfield. After 6 years under a mix of ryegrass species, in the spring of 2017 the grass was removed and in January 2018 the bare soils were sown with C_4 buffalo grass (*B. dactyloides*). The buffalo grass was maintained under ambient field conditions, with periodic clipping to maintain an approximately 15-cm high sward in the first year and 10 cm high in the second year when the grass was better established. In 2019 two levels of nitrogen were applied factorially to the two soils: a high treatment of 3.94 g N m^{-2} and a low treatment of 1.66 g N m^{-2}. The initial portion (0.81 g N applied equally to all) was as an all-purpose plant food (Phostrogen, Bayer CropScience Ltd, Cambridge, UK); the remaining as NH_4NO_3 in five splits from July to October.

To conduct a plant and soil respiration measurement from a lysimeter, the opaque lysimeter chamber was closed with an opaque lid and the chamber headspace connected via a sampling loop to a gas analyser (Picarro G2201-*i* cavity ring-down spectroscopy instrument, calibrated against a Thermo Finnigan Delta^{Plus} XP isotope ratio mass spectrometer as described in McCloskey *et al*., 2020). Flux measurements lasted approximately 20 min, during which headspace CO_2 and its $\delta^{13}C$ were measured near-continuously. Daily flux measurements were separated into three 8-hr periods: 0000–0800, 0800–1600,

1600–2400. Within each period, all lysimeters were tested in a random sequence. Random sequences were generated for 0800–1600 each day, and repeated for the following two 8-hr periods.

The Keeling plot method was used to calculate the $\delta^{13}C$ of the combined plant (F_{plant}) and soil (F_{soil}) respiration fluxes (F_R) (McCloskey *et al*., 2020). Partitioning between plant and soil sources was performed as follows:

$$f_{soil} = \left(\delta^{13}C_R - \delta^{13}C_{plant}\right) \Big/ \left(\delta^{13}C_{soil} - \delta^{13}C_{plant}\right) \quad \textbf{Equation 4-1}$$

$$f_{plant} = 1 - f_{soil} \quad \textbf{Equation 4-2}$$

$$F_R = F_{plant} + F_{soil} \quad \textbf{Equation 4-3}$$

$$F_{plant} = f_{plant} F_R \quad \textbf{Equation 4-4}$$

$$F_{soil} = f_{soil} F_R \quad \textbf{Equation 4-5}$$

where $\delta^{13}C_{plant}$ and $\delta^{13}C_{soil}$ are the plant and soil end member values respectively. A diurnally-varying $\delta^{13}C_{plant}$ value was used to account for the ^{13}C enrichment of plant respiration under light conditions (McCloskey *et al*., 2021). The value was -11.2 ‰ at night and -14.2 ‰ during daylight, defined as when solar radiation was ≥ 0.01 W m^{-2}. The $\delta^{13}C_{soil}$ values were -27.1 and -28.8 ‰ for the Shuttleworth and Temple Balsall soils, respectively (McCloskey *et al*., 2021).

Each lysimeter contains Delta-T SM150T temperature and moisture sensors at 6 and 12 cm depth. Temperature and moisture were recorded with a resolution of 30 min in 2018 and 5 min in 2019. A Vaisala WXT520 weather station at the site measures air temperature and solar radiation, recorded with a resolution of 5 min in both years.

4.2.2 Mass balances

Mass balances between C removed from the lysimeters in clippings and that estimated from the measured fluxes were calculated to validate the methodology. Grass clippings were dried at 65 ^{o}C to constant weight, and then

ground using a ball mill (Fritsch Pulverisette 6, Fritsch, Germany) for 6 min at 300 rpm. Samples were analysed for total C and N content in an elemental analyser (Elementar Vario EL III). Clippings were not taken in the Shuttleworth soil in 2018 due to relatively poor growth. To measure net ecosystem exchange (NEE), flux measurements were made every c. 2 weeks with the chamber covers removed, with a 1.5-min measurement duration to avoid excessive depletion of chamber CO_2 in photosynthesis. Ecosystem respiration (ER) and F_{plant} during these measurements were estimated from relationships between measured ER and F_{plant} and air temperature established during periods when covers were in place using a linear mixed effects (LME) model. For periods in which only ER measurements were made, NEE was estimated using a relationship between NEE and solar radiation. For periods where no measurements were recorded these relationships were used to estimate hourly ER, F_{plant}, and NEE. Daily totals were obtained with a natural cubic spline fitted to the data.

4.2.3 Data analysis

The results were analysed using linear mixed-effects (LME) models to determine if including solar radiation as an explanatory variable improved model-based estimation of SOM turnover compared with soil moisture and temperature alone. Since flux data for a given lysimeter at different times were not independent of one another, we used the restricted maximum likelihood (REML) method to fit the models (Lark & Cullis, 2004). Two random effects were included as follows. Lysimeters were positioned in rows such that soil moisture and temperature sensors either faced northwards or southwards. These rows were used as blocks in the allocation of the two soils, with an equal number allocated to random positions in each block. Row orientation was therefore treated as a random effect, with lysimeter ID as a nested random effect within it. Normality (i.e. randomness) of the effects of lysimeter ID was tested using the Shapiro-Wilk normality test (normality was assumed for row orientation).

We tested whether solar radiation (taken as a proxy for plant productivity) and soil type affected SOM turnover using the 2018 data. Models including only soil moisture (θ) and temperature (T) as fixed variables took the form

$$F_{soil} = a_1\theta + b_1T + c_1 \quad \textbf{Equation 4-6}$$

and those also including solar radiation (G) took the form

$$F_{soil} = a_2\theta + b_2T + c_2G + d_2GT + e_2 \quad \textbf{Equation 4-7}$$

where a_1, b_1, etc. are fitted coefficients. The two soils were assessed separately. Then the effect of soil type (S) was tested by combining the datasets and including S as a further fixed variable. These models were selected using the criteria described below.

Model fit was assessed using the Akaike information criterion (AIC), which estimates the amount of information lost by a model relative to alternative models. The preferred model is the one with the smaller AIC value (Banks & Joyner, 2017). The significance of fixed variables with each model, and the significance of any differences between models, was tested using ANOVA. We began with models including factorial interactions between all the fixed variables, and then removed interactions that did not significantly ($P \leq 0.01$) improve model fit. To ensure comparability we used the same set of variables and variable interactions throughout. Plant growth varied substantially during a growing season, and the grass was dormant during the winter. We focused on short periods to ensure seasonal differences in plant growth did not obscure plant-mediated effects on SOM turnover. These were 1–15 August 2018, at the height of the growing season, and 1–15 November 2018, as the grass was entering winter dormancy.

To assess whether high resolution flux measurements were instrumental for detecting any relationship found between soil respiration and solar radiation, these relationships were also tested using daily means. Only days where no more than six (out of 36) measurements for a given soil had been missed were used. We used linear regression models of daily average soil respiration to

assess whether including daily average *G* alongside daily averages of θ and *T* improved model fit, again assessed by AIC value.

To ensure that any detected effect from solar radiation on F_{soil} was not an artefact of the diurnal shift in $\delta^{13}C_{plant}$ value, we tested this with data from 5–8 July 2018. During this period the grass was still becoming established and F_{plant} was less dominant, so the true diurnal $\delta^{13}C_{plant}$ change did not distort partitioned F_{soil} as substantially as later in the season (McCloskey *et al*., 2021).

We used the 2019 data to test the effect of N treatment (*N*). Three periods were examined: 15-30 July, immediately prior to the first N addition; 15–30 August, between the second and third additions; and 12–27 September, which included the fourth N addition. Models including θ, *T* and *G* with and without *N* were compared for the two soils separately.

Data analysis was conducted using R version 4.0.3 (R core team, 2020). The package 'nlme' (Pinheiro *et al.* 2020) was used to perform mixed effects model analysis.

4.3 Results

4.3.1 Diurnal and seasonal time-courses of plant and soil respiration

Figure 4-1 shows diurnal patterns of plant and soil fluxes in the two soils in early August 2018 with the corresponding patterns of soil moisture (θ), temperature (*T*) and solar radiation (*G*). The same is shown in Figure 4-2 for early July. Clear diurnal trends are visible for both soils. The diurnal trends in November were much weaker, with no diurnal trends in plant respiration (data not shown). From late November through January no diurnal pattern was apparent in either plant or soil fluxes (data not shown). The diurnal variation in plant respiration was approximately twice that of soil respiration in the Temple Balsall soil in August, whereas there was less difference in magnitude and variation in plant and soil C fluxes in the Shuttleworth lysimeters.

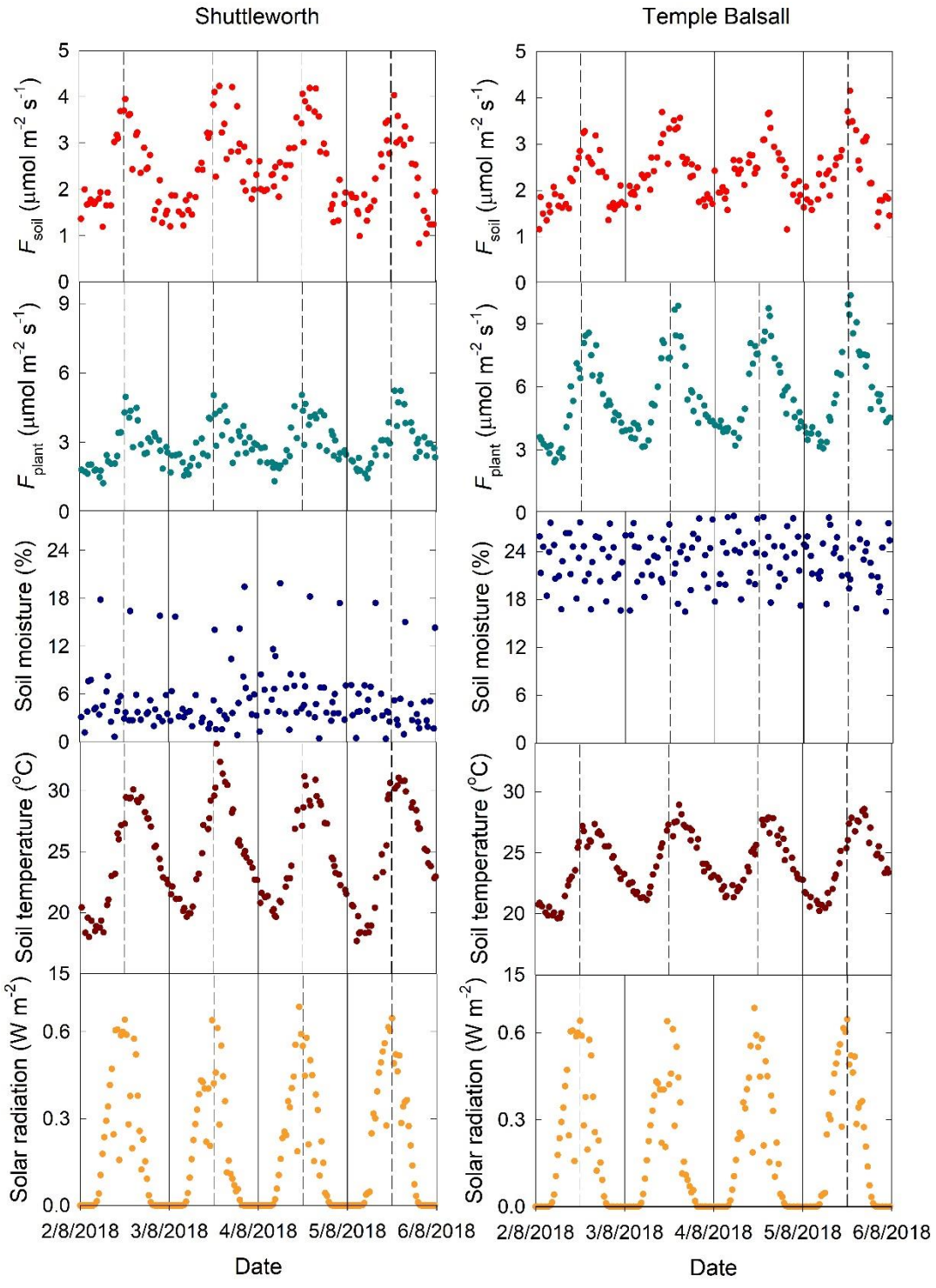

Figure 4-1 Diurnal time-courses for (left) Shuttleworth and (right) Temple Balsall lysimeters, 2–5 August 2018. Upper panels show soil respiration fluxes, followed by plant respiration fluxes, soil moisture, soil temperature, and solar radiation. Solid lines mark midnight, dashed lines midday.

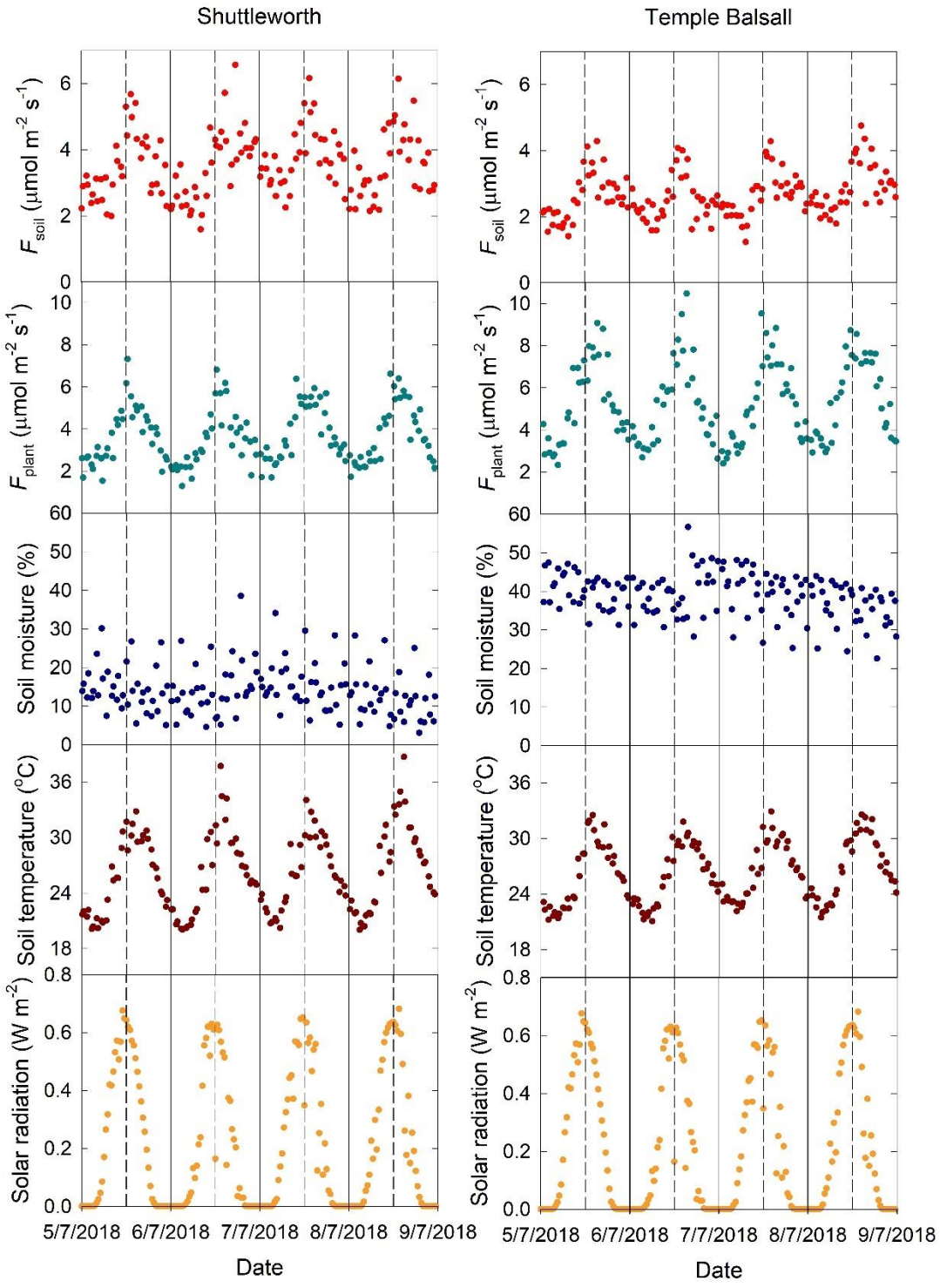

Figure 4-2 Diurnal time-courses for (left) Shuttleworth and (right) Temple Balsall lysimeters, 5-8 July 2018. Upper panels show soil respiration fluxes, followed by plant respiration fluxes, soil moisture, soil temperature, and solar radiation. Solid lines mark midnight, dashed lines midday. Fluxes were partitioned without allowing for a diurnal ^{13}C enrichment of plant respiration.

Figure 4-3 shows the seasonal time-courses of daily plant and soil fluxes from July 2018 to January 2019. The time-courses from May to November 2019 are included in Appendix C. Seasonal trends are clear in both years. In 2018 the grass sward in the Temple Balsall soil established and grew substantially better than that in the Shuttleworth soil (Appendix F). This is reflected in lower plant respiration in 2018 (Fig. 4-3a). In 2019 the trends and magnitudes of plant and soil respiration did not differ substantially between the two soils. Daily plant and soil respiration were largely the same in late autumn and winter, plant respiration was approximately double soil respiration in June and early July 2019. The seasonal peak for plant respiration was also earlier, around the start of July, while soil respiration peaked in late July and August.

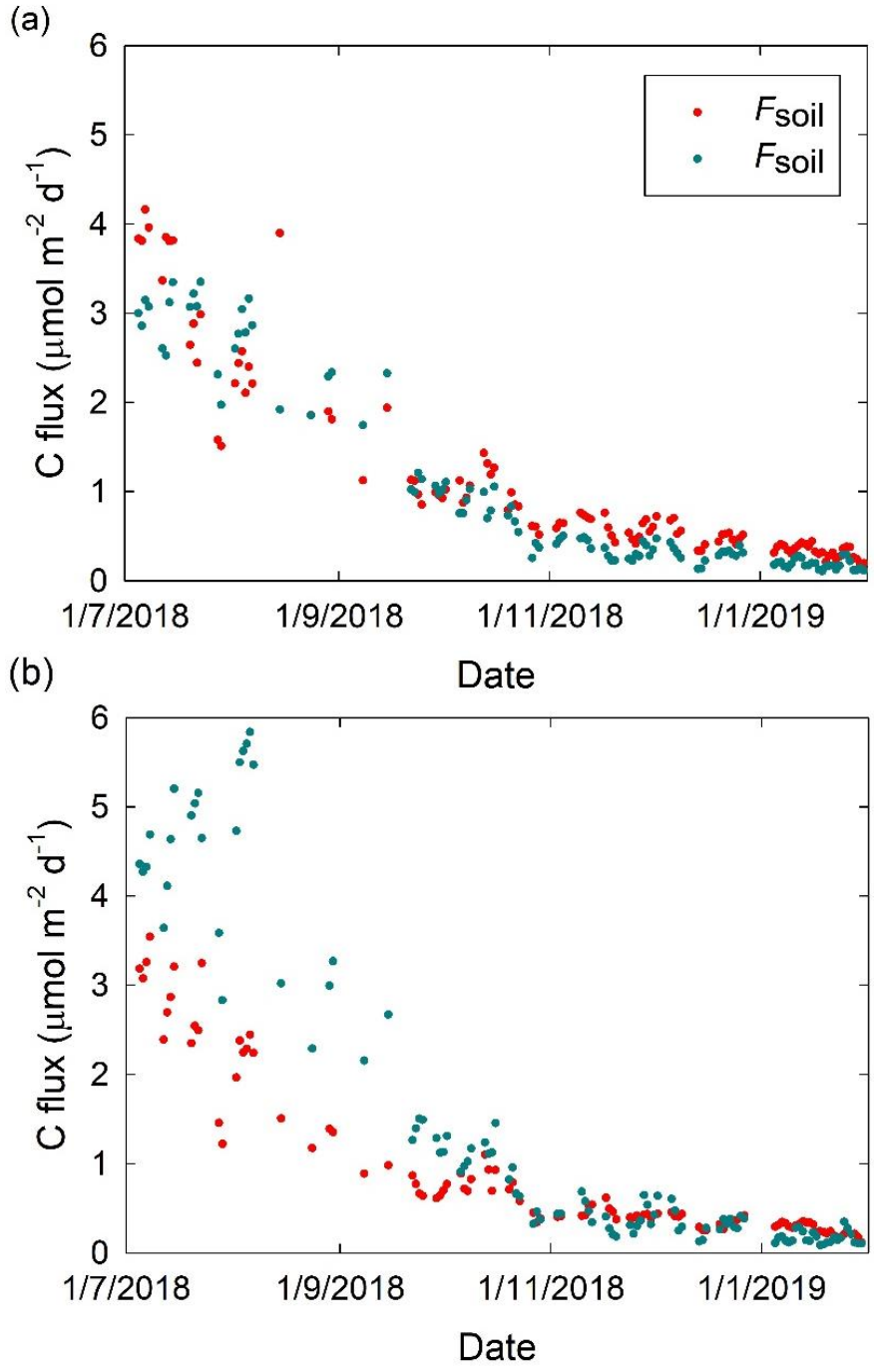

.

Figure 4-3 Daily totals for F_{soil} and F_{plant} for the (a) Shuttleworth and (b) Temple Balsall lysimeters, July 2018 – January 2019. Days with under 30 measurements were excluded.

To test the overall reliability of our flux measurements, we calculated a mass balance for the plant components of the system. We did this for the Temple Balsall soil in 11–31 August 2018 when the grass was well established and growing well, so that estimates of growth from harvested biomass were most reliable. The estimated NPP over this period indicated an input of 124 g C into the system per lysimeter, and this was balanced against an output of 72 g C in plant respiration plus 17 g C of above ground growth estimated from the mass of grass clippings. This amounts to a surplus of 35 g C in NEE, or 28% of the estimated NEE. However the actual surplus is somewhat smaller as below ground C allocation is not accounted for. Total ecosystem respiration (including soil) was an output of 103 g C; when the system is considered as a whole it is close to balanced with a net gain of 4 g C. Given the errors in these estimates, the agreement is satisfactory.

4.3.2 Assessment of rhizosphere priming effects

A positive relationship between soil respiration and solar radiation was found in both soils, as tested in August and November 2018 ($P \leq 0.05$). Models with and without solar radiation were significantly different from each other, and, except in the Shuttleworth soil in July, accounting for solar radiation improved model fit as shown by smaller AIC values (Table 4-1).

Table 4-1 Effect of including solar radiation in models of the variation in soil respiration with soil moisture and temperature (Eqns 6 and 7). AIC = Akaike information criterion, θ = soil moisture, T = soil temperature, G = solar radiation, SW = Shuttleworth soil, TB = Temple Balsall soil. Values of the coefficients in Eqns 4-6 and 4-7 are in Appendix D.

Time interval in 2018	Soil	AIC (θ, T)	AIC (θ, T, G)
5–8 July	SW	253.53	260.75
5-8 July	TB	167.92	149.63
1–15 August	SW	576.42	542.80
1–15 August	TB	414.104	303.08
1–15 November	SW	-477.75	-505.99
1–15 November	TB	-475.60	-530.82

To illustrate this, Figure 4-4 shows the fitted time courses of soil respiration with and without allowing for solar radiation. In the latter case, fitted values were out of step with measured values, with predicted soil respiration peaking later in the day, and reaching its minimum later after midnight (Fig. 4-4a). The peaks in measured soil respiration fluxes aligned more closely with peaks in solar radiation, which occurred earlier in the day than soil temperature peaks (Fig. 4-1). The fitted and measured values agreed better when solar radiation was allowed for, with the diurnal pattern in residuals less apparent (Fig. 4-4b). Significant differences ($P \leq 0.01$) between the Shuttleworth and Temple Balsall lysimeters were found when both soils were included in LME models. Adding soil type as a categorical fixed variable improved model fit (Table 4-2).

Table 4-2 Effect of soil type (*S*) as a fixed variable in the models fitted in Table 4-1 with the data for the two soils pooled.

Time interval in 2018	AIC (θ, T, G)	AIC (θ, T, G, S)
1–15 August	1205.91	892.71
1–15 November	-1030.32	-1058.34

We assessed whether the significant relationship between solar radiation and soil respiration was present in the absence of a diurnal $\delta^{13}C_{plant}$ change using data from July 2018 (Fig. 4-2) which had been partitioned without imposing a daytime plant end-member. A significant relationship was found in the Temple Balsall soil, and including solar radiation in a LME model improved fit. This was, however, not the case for the Shuttleworth soil. The Temple Balsall data was examined to ascertain whether a mismatch between measured and fitted values existed when solar radiation was excluded in July (Appendix E). Although a repeating pattern in residuals was apparent, this did not align exclusively with peaks in measured F_{soil}.

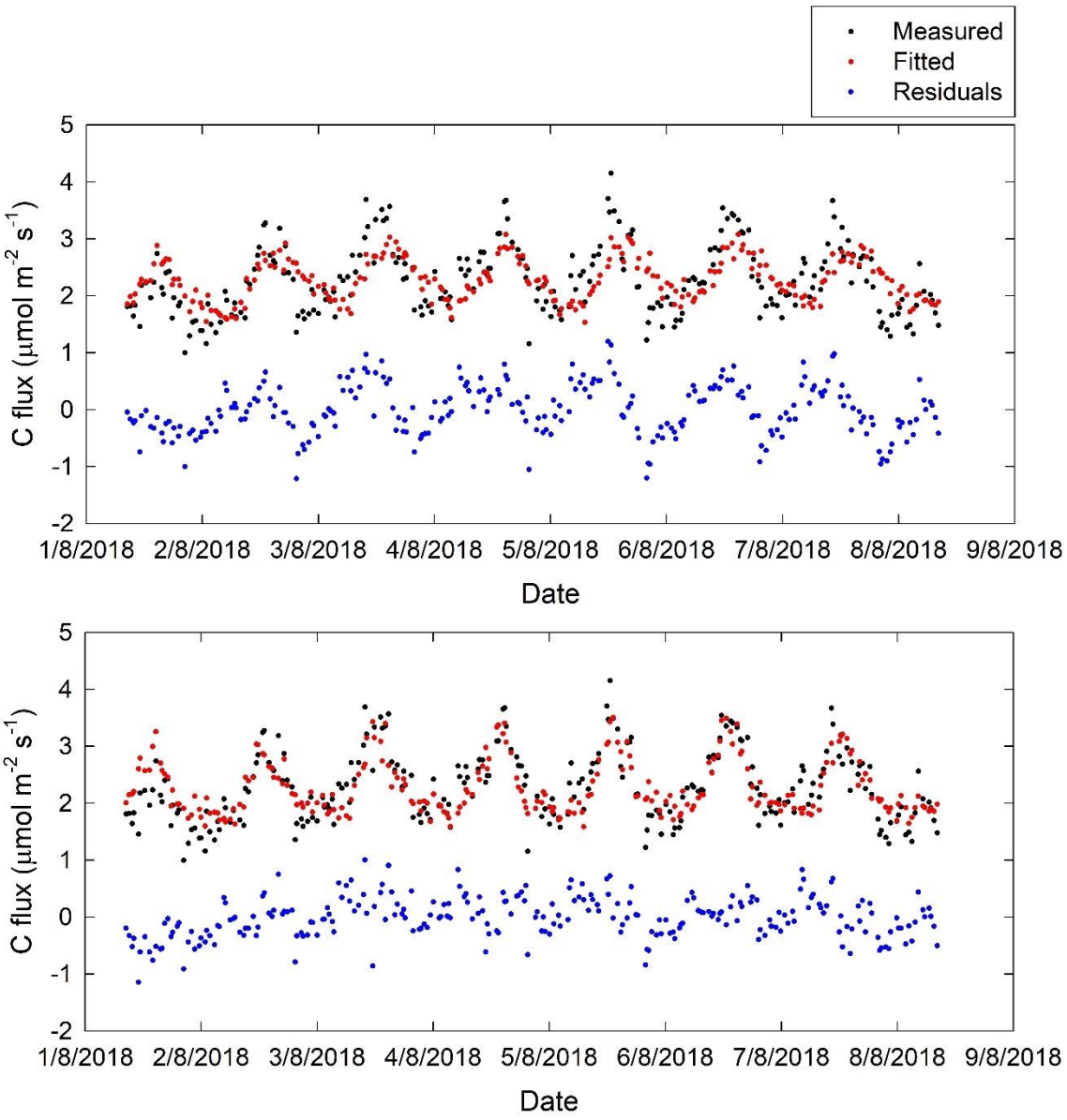

Figure 4-4 Measured values for soil respiration, Temple Balsall soil, 1-8 August 2018 alongside fitted values and residuals from a linear mixed model incorporating (a) soil temperature and moisture, and (b) soil temperature, soil moisture, and solar radiation.

No significant relationship between daily average soil respiration and daily average solar radiation was found in August or November in linear models also including daily average soil temperature and moisture. Adding daily average *G* as a variable did not improve model fit, and models with and without daily average *G* were not significantly different. The relationship between soil

respiration and solar radiation detected using full time-course data was therefore dependent on resolution of diurnal patterns in soil respiration and its drivers.

4.3.3 Effects of nitrogen application

In both soils, allowing for N fertilizer treatment by including *N* as a categorical variable in 2019 did not affect model fits to the soil respiration data over any of the tested time periods (Table 4-3). Models including *N* were not significantly different from equivalent models based on θ, *T* and *G* only.

Table 4-3 Effect of allowing for N fertilizer treatments in the models fitted in Table 4-2 for the 2019 results. Fertilizer was applied in five splits between July and October.

Time interval in 2019	Soil	AIC (θ, *T*, *G*)	AIC (θ, *T*, *G*, *N*)
15–30 July	SW	704.44	713.79
15–30 July	TB	670.58	679.67
15–30 August	SW	396.23	406.20
15–30 August	TB	507.75	507.94
15–30 September	SW	-15.12	-10.12
15–30 September	TB	16.54	14.59

Table 4-4 gives the effects of N addition on the grass growth and tissue N concentration. The grass grew better in the Temple Balsall soil, with and without N, producing 463 ± 12 g of clippings over the 2019 season versus 285 ± 11 g in the Shuttleworth soil (Appendix F). The grass N concentration increased with N fertilization in both soils, and to a greater extent in the Temple Balsall soil (Table 4-4). However, there were no differences ($P \leq 0.05$) in the dry mass of clippings between N treatments in either soil. In both soils, there were small differences ($P \leq 0.05$) between the lysimeters in mean tissue N concentration before the N treatments were applied in July (Table 4-4). Nonetheless the increase in tissue

N concentration at the higher N addition in the Temple Balsall soil was significant.

Table 4-4 Mean N concentration of grass clippings before (July 2019) and after (August 2019) N fertilizer applications, and dry mass of grass clippings taken during August and September 2019. Data are means ± standard errors (*n* = 6).

Soil	N treatment	N concentration in July (%)	N concentration in October (%)	Mass of clippings (g)
Shuttleworth	High	1.74 ± 0.04	2.15 ± 0.02	76.4 ± 5.0
Shuttleworth	Low	1.89 ± 0.04	2.11 ± 0.05	73.4 ± 2.1
Temple Balsall	High	2.08 ± 0.09	2.45 ± 0.03	106.8 ± 4.3
Temple Balsall	Low	1.80 ± 0.05	2.14 ± 0.07	96.5 ± 8.1

4.4 Discussion

4.4.1 Seasonal and diurnal dynamics

A strong seasonal pattern to soil respiration was apparent in both soils. Although there were significant differences in models of soil respiration between the two soils, soil respiration followed similar seasonal patterns. On a diurnal timescale peaks in soil and plant respiration coincided, but on a seasonal timescale plant respiration increased to its peak earlier in the year than soil respiration. Seasonal trends in diurnal respiration patterns are clear: in August soil respiration approximately doubled from the night-time minima to the daytime peaks, while in November this amplitude had declined substantially, and inter-day variation became greater than within-day variation.

4.4.2 Evidence for rhizosphere priming

This study presents the first seasonally- and diurnally-resolved investigation of partitioned SOM and plant C fluxes and potential drivers under field conditions. Previous measurements from undisturbed soil under field conditions have found evidence of priming (Kumar *et al*., 2016), and indicated links between diurnal

trends in photosynthesis and rhizosphere processes which may be linked to RPEs (Kuzyaknov & Gavrichkova 2010; Phillips *et al*., 2011; Hopkins *et al*., 2013; Mitra *et al*., 2019). Our findings are consistent with rhizosphere priming in the field, and provide evidence for a tight link between plant productivity and increased SOM turnover over diurnal timescales.

Our results show that in both August and November solar radiation was a significant predictor of soil respiration in the two soils we investigated. Improvements in model fit when solar radiation was incorporated were found at all timepoints tested in 2018 with the exception of early July for the Shuttleworth soil. The latter may be due to slow establishment of the grass in the Shuttleworth soil. When models of soil respiration at the height of the growing season (in August) do not include solar respiration as an effect, the predicted diurnal soil respiration peaks align with daily soil temperature peaks. However, measured soil respiration peaks aligned more closely with the earlier diurnal solar radiation peaks. This indicates that soil temperature and moisture are not the only controls on soil respiration, and solar radiation has an effect separate from its link to soil temperature. As by August 2018 both soils were covered by a grass sward, any effect of solar radiation, separate from soil temperature, is likely plant-mediated. These findings are consistent with the presence of rhizosphere priming, assuming a close temporal match between rate of photosynthesis and rate of exudation from roots as found by Dilkes *et al*. (2004).

There is a mounting body of evidence for a tight coupling between photosynthesis and microbial access to root exudates. This may not necessitate transport of new assimilate to plant roots as pressure concentration waves through the phloem may stimulate rhizodeposition in response to photosynthesis (Mitra *et al*., 2019). This coupling is sufficiently tight to give increases in soil respiration after only 30 min of illumination (Kaylera *et al*., 2017). Assimilate may be transported rapidly from the root through arbuscular mycorrhizae without diffusion from root to soil (Kaiser *et al*., 2015), and hyphal transport may increase availability to soil bacteria (Gorka *et al*., 2019). This

pathway could allow a rapid microbial response to changing rates of photosynthesis, and our results are consistent with such stimulation of microbial activity and associated RPEs.

Seasonal variation in the drivers of soil respiration was evidenced by improved fits of models over shorter periods. This may be at least partially explained by the presence of rhizosphere priming in this system. There was a strong seasonal pattern to the C_4 grass growth, with complete above-ground dormancy in winter. The strength of the priming effect would thus depend on light intensity as well as plant photosynthetic capacity, varying due to changes in standing plant biomass. In the winter we would expect soil respiration to be decoupled from solar radiation as the diurnal variation in root exudation intensity would be absent. Our data is consistent with this, and inclusion of solar radiation in models of soil respiration in December did not substantially affect model fit (data not shown). The use of mixed models which incorporate date as a non-linear affect may be able to account for variation in plant activity over longer periods. This has the potential to show whether interaction between time of year and solar radiation improves prediction of soil respiration, which would suggest seasonal dynamics in rhizosphere priming.

The strengths of an automated system designed to perform high frequency flux measurements over a full growing season are highlighted here. Measurements spanning the majority of observed seasonal grass phenology allows us to observe how soil respiration is affected by potential rhizosphere priming during contrasting periods of grass growth. Critically, high temporal resolution of flux measurements from this system allowed us to detect probable photosynthesis-driven rhizosphere priming, which was obscured in daily average data. This is as we would expect from plant-driven rhizosphere priming given diurnal patterns of rhizodeposition (Hubbard *et al*., 2018). We found two-fold variation in soil respiration over 24 hr periods during a period of high plant growth, closely coupled to solar radiation patterns. The ability to examine soil respiration patterns over diurnal timescales is thus vital if we are to fully understand drivers of soil C turnover.

The approach taken here estimates the effects of plant root activity on soil respiration solely based on solar radiation. Mass balances performed using NEE estimates based on solar radiation compared with harvested biomass and calculated respiration losses produced reasonable results, albeit with a small underestimation of NPP. Underestimation of the rate of photosynthesis through using solar radiation as a proxy in models of soil respiration would not act to create a spurious appearance of the rhizosphere priming effect in our analysis. As solar radiation provides relatively close estimates of NPP it is a reasonable proxy for plant productivity, and our findings indicate that it is likely to be a viable method of detecting priming effects in the field. Nonetheless, this does simplify potential variation in plant inputs, ignoring variables such as temperature, soil moisture, and nutrient availability which can affect rhizodeposition. Furthermore, under this approach any photosynthesis-driven increase in root exudation is assumed to cease after nightfall. Analysis of diurnal root exudation patterns would allow a more nuanced assessment of priming dynamics.

4.4.2.1 Potential methodological artefacts

While it is clear from McCloskey *et al*. (2021) that a diurnal change in $\delta^{13}C_{plant}$ was required to correctly partition plant and soil C fluxes in our system, this could not fully correct for diurnal variation in $\delta^{13}C_{plant}$. The binary $\delta^{13}C_{plant}$ shift we imposed was a simplification of the real diurnal end-member shift. It has been shown that plant end-members increase under daylight conditions over several hours, and after the cessation of light decrease over a similar timeframe (Sun *et al.*, 2010; Zhong *et al*., 2017). Although we estimated the maximum extent of diurnal variation in the plant end-member, we did not characterise the temporal dynamics of this variation. Furthermore, rates of end-member change are likely to vary based on environmental conditions. To accurately model this would require constant monitoring of $\delta^{13}C_{plant}$, which would be impracticable and beyond the scope of this study.

Where the daytime $\delta^{13}C_{plant}$ value we used was more ^{13}C enriched than the real value, we will have erroneously apportioned part of F_{plant} to F_{soil}. As such,

increased F_{plant} around the times the grass was most photosynthetically active would partially be conflated with the soil flux. This could cause the disjoint we see between soil respiration and soil temperature peaks, rather than rhizosphere priming. We did, however, see improved model fit for the Temple Balsall soil in July when no diurnal $\delta^{13}C_{plant}$ change was used. This indicates that even if misappropriation of part of the plant flux peak to the soil flux did occur, that was not the sole cause of the relationship between soil respiration and solar radiation. Furthermore, time-courses of soil respiration partitioned during a period of lower plant respiration (Fig. 4-2) show similar diurnal trends in F_{soil}. As such, our results remain consistent with plant-driven increases in SOM turnover.

A further potential problem with our approach is that, over time, C_4-origin plant material will become incorporated into SOM pools, changing their isotopic composition. This introduces error into the two end-member model used to partition the fluxes, causing part of the SOM flux to be incorrectly attributed to the plants. However, this will tend to dampen rather than exacerbate measured priming effects.

4.4.3 Lack of evidence for the nitrogen mining hypothesis

Following four differential nitrogen additions, no significant effect of N application level on soil respiration was detected in either soil. While the effect of N treatment can be seen in shoot N content from both soils in October, with significant differences between the treatments in the Temple Balsall soil, and the disappearance of pre-existing differences in the Shuttleworth soil, we found no evidence for nitrogen mining.

There is strong evidence for reduced soil respiration under higher N availability from incubation studies (Craine *et al.*, 2007; Chen *et al.*, 2014; Ramirez *et al*., 2012) and in planted mesocosms (Murphy *et al*., 2017). This does not, however, appear to be universal, and some incubation studies have shown no change or an increase in SOM turnover following N fertilisation (Dijkstra *et al*., 2013, Vargas *et al*., 2020). It is possible that while increased N availability to soil microbes did drive a reduction in the need to obtain N from SOM, this effect was

nullified by a stronger priming effect driven by an increase in rhizodeposition, as increased N availability tends to result in increased C inputs to the soil via rhizodeposition (Bowsher *et al*., 2018). While no evidence for N mining was found in this system the difficulties inherent in investigating this in a planted system prevent us drawing firm conclusions here.

4.5 Conclusions

1. Clear diurnal and seasonal trends in soil respiration were found. While patterns of soil respiration were similar to patterns of plant respiration on a diurnal timescale, seasonal patterns differed.
2. Seasonal and diurnal patterns of soil respiration were similar between the two soils tested, despite contrasting soil characteristics.
3. Solar radiation, taken as a proxy for the rate of photosynthesis, was found to significantly correlate with increased soil respiration during periods of active grass growth. This is consistent with, and best explained by, rhizosphere priming.
4. High-resolution flux measurements were necessary to detect the relationship between solar radiation and increased SOM turnover.
5. We found no evidence for nitrogen mining as the mechanism behind the potential priming effects observed. Increased nitrogen application was not found to correlate with changes in soil respiration in either soil.

Acknowledgements

The field laboratory was built with a Royal Society Wolfson Laboratory Refurbishment Grant (WL080021/Kirk). The CRDS analyser was provided by the Agri-Epi Centre, Cranfield Hub. CM was supported by the Soils Training and Research Studentships (STARS) Centre for Doctoral Training, funded by the Biotechnology and Biological Sciences Research Council and the Natural Environment Research Council (grant number NE- M009106-1). The James Hutton Institute receives funding from the Rural and Environment Science and Analytical Services Division (RESAS) of the Scottish Government. The authors

declare no conflict of interest. All data are will be available following publication at CORD c/o the Cranfield University Library.

Authorship

CM, GK, WO and EP conceived this study. CM carried out the experimental work and data analysis. CM wrote the initial manuscript, and all contributed to the final version.

Funding information

Natural Environment Research Council Grant Number NE/M009106/1; Royal Society Grant Number WL080021/Kirk

Data Sharing and Data Accessibility statement

The data used in this article will be available at CORD c/o the Cranfield University Library.

Conflict of Interest statement

The authors have no conflicts of interest related to the work presented in this manuscript.

4.6 References

Bader, N.E. & Cheng, W. 2007. Rhizosphere priming effect of *Populus fremontii* obscures the temperature sensitivity of soil organic carbon respiration. *Soil Biology & Biogeochemistry, 39*, 300–306.

Bahn, M., Schmitt, M., Siegwolf, R., Richter, A. & Brüggemann, N. 2009. Does photosynthesis affect grassland soil-respired CO_2 and its carbon isotope composition on a diurnal timescale? *New Phytologist*, *182*, 451–460.

Balesdent, J., Mariotti, A. & Guillet, B. 1987. Natural ^{13}C abundance as a tracer for studies of soil organic matter dynamics. *Soil Biology and Biogeochemistry 19*, 25–30.

Banks, H.T. & Joyner, M.L. 2017. AIC under the framework of least squares estimation. *Applied Mathematics Letters*, *74*, 33-45.

Bengtson, P., Barker, J., & Grayston, S. J. 2012. Evidence of a strong coupling between root exudation, C and N availability, and stimulated SOM decomposition caused by rhizosphere priming effects. *Ecology and Evolution*, *2*, 1843–1852.

Bowling, D.R., Pataki, D.E., & Randerson, J.T. 2008. Carbon isotopes in terrestrial ecosystem pools and CO_2 fluxes. *New Phytologist, 178,* 24–40.

Bowsher, A.W., Evans, S., Tiemann, L.K., & Friesen, M.L. 2018. Effects of soil nitrogen availability on rhizodeposition in plants: a review. *Plant Soil*, *423*, 59–85.

Chen, R., Senbayram, M., Blagodatsky, S., Myachina, O., Dittert, K., Lin, X., Blagodatskaya, E., & Kuzyakov. Y. 2014. Soil C and N availability determine the priming effect: microbial N mining and stoichiometric decomposition theories. *Global Change Biology*, *20*, 2356–67.

Cheng, W., Parton, W.J., Gonzalez-Meler, M.A., Phillips, R., Asao, S., Mcnickle, G.G., Brzostek, E. & Jastrow, J.D. 2014. Synthesis and modelling perspectives of rhizosphere priming, *New Phytologist*, *201*, 31–44.

Craine, J.M., Morrow, C. & Fierer, N. 2007. Microbial nitrogen limitation increases decomposition. *Ecology*, *88*, 2105–2113.

Derrien, D., Plain, C., Courty, P.-C., Gelhaye, L., Moerdijk- Poortvliet, T.C.W., Thomas, F., Versini, A., Zeller, B., Koutika, L.-S., Boschker, H.T.S. & Epron, D. 2014. Does the addition of labile substrate destabilise old soil organic matter? *Soil Biology & Biogeochemistry*, *76*, 149–160.

Dijkstra, F.A. & Cheng, W. 2007. Interactions between soil and tree roots accelerate long-term soil carbon decomposition. *Ecology Letters*, *10*, 1046–1053.

Dijkstra, F.A., Carrillo, Y., Pendall, E. & Morgan, J.A. 2013. Rhizosphere priming: a nutrient perspective. *Frontiers in Microbiology*, *4*, 183–190.

Dilkes, N.B., Jones, D.L. & Farrar, J. 2004. Temporal Dynamics of Carbon Partitioning and Rhizodeposition in Wheat. *Plant Physiology*, *134*, 706–715.

Farquhar, G.D., Ehleringer, J.R., & Hubick, K.T. 1989. Carbon isotope discrimination and photosynthesis. *Annual Review of Plant Physiology and Plant Molecular Biology*, *40*, 503–537.

Gorka, S., Dietrich, M., Mayerhofer, W., Gabriel, R., Wiesenbauer, J., Martin, V., Zheng, Q., Imai, B., Prommer, J., Weidinger, M. *et al*. 2019. Rapid transfer of plant photosynthates to soil bacteria via ectomycorrhizal hyphae and its interaction with nitrogen availability. *Frontiers in Microbiology*, *26*, https://doi.org/10.3389/fmicb.2019.00168.

Harmer, S.L. 2009. The circadian system in higher plants. *Annual review of plant biology*, *60*, 357–377.

Hartmann, H., Bahn, M., Carbone, M., Richardson, A.D. 2020. Plant carbon allocation in a changing world – challenges and progress: introduction to a Virtual Issue on carbon allocation. *New Phytologist*, *227*, 981–988

Hopkins, F., Gonzalez-Meler, M.A., Flower, C.E., Lynch, D.L., Czimczik, C., Tang, J. & Subke, J.-A. 2013. Ecosystem-level controls on root-rhizosphere respiration. *New Phytologist*, *199*, 339–351.

Hubbard, C.J., Brock, M.T., van Diepen, L.T.A., Maignien, L., Ewers, B.E., & Weinig, C. 2018. The plant circadian clock influences rhizosphere community structure and function. *The ISME Journal*, *12*, 400–410.

Huo, C., Luo, Y., & Cheng, W. 2017. Rhizosphere priming effect: A meta-analysis. *Soil Biology & Biochemistry*, *111*, 78–84.

Kaiser, C., Kilburn, M.R., Clode, P.L., Fuchslueger, L., Koranda, M., Cliff, J.B., Solaiman Z.M. & Murphy, D.V. 2015. Exploring the transfer of recent plant photosynthates to soil microbes: mycorrhizal pathway vs direct root exudation. *New Phytologist*, *205*, 1537–1551.

Kaylera, Z., Keitel, C., Jansen, K. & Gessler, A. 2017. Experimental evidence of two mechanisms coupling leaf-level C assimilation to rhizosphere CO_2 release. *Environmental and Experimental Botany*, *135*, 21–26.

Kumar, A., Kuzyakov, Y. & Pausch, J. 2016. Maize rhizosphere priming: field estimates using ^{13}C natural abundance. *Plant and Soil*, 409, 87–97.

Kuzyakov, Y. & Gavrichkova, O. 2010. Time lag between photosynthesis and carbon dioxide efflux from soil: A review of mechanisms and controls. *Global Change Biology*, *16*, 3386–3406.

Lark, R.M. & Cullis, B.R. 2004. Model-based analysis using REML for inference from systematically sampled data on soil. *European Journal of Soil Science*, *55*, 799-813.

Lloyd, D., Ritz, K., Paterson, E. & Kirk G.J.D. 2016. Effects of soil type and composition of rhizodeposits on rhizosphere priming phenomena. *Soil Biology and Biochemistry 103*, 512–521.

Lu, J., Dijkstra, F.A., Wang, P. & Cheng, W. 2019. Roots of non-woody perennials accelerated long-term soil organic matter decomposition through biological and physical mechanisms. *Soil Biology & Biogeochemistry*, *134*, 42–53.

McCloskey, C.S., Otten, W., Paterson, E., Ingram, B. & Kirk, G.J.D. 2020. A field system for measuring plant and soil carbon fluxes using stable isotope methods. *European Journal of Soil Science*, DOI: 10.1111/ejss.13016.

McCloskey C., Otten W., Paterson E. & Kirk G.J.D. 2021. On allowing for transient variation in end member $\delta^{13}C$ values in isotopic partitioning of ecosystem respiration. *European Journal of Soil Science*, in review.

Mencuccini, M. & Hölttä, T. 2010. The significance of phloem transport for the speed with which canopy photosynthesis and belowground respiration are linked. *New Phytologist*, *185*, 189–203.

Mitra, B., Miao, G., Minick, K., McNulty, S.G., Sun, G., Gavazzi, M., King, J.S. & Noormets, A. 2019. Disentangling the effects of temperature, moisture, and substrate availability on soil CO_2 efflux. *Journal of Geophysical Research: Biogeosciences*, *124*, 2060–2075.

Moinet, G.Y.K., Midwood, A.J., Hunt, J.E., Whitehead, D., Hannam, K.D., Jenkins, M., Brewer, M.J., Adams, M.A. & Millard, P. 2018. Estimates of rhizosphere priming effects are affected by soil disturbance. *Geoderma*, *313*, 1–6.

Murphy, C.J., Baggs, E.M., Morley, N., Wall, D.P. & Paterson, E. 2017. Nitrogen availability alters rhizosphere processes mediating soil organic matter mineralisation. *Plant and Soil*, *417*, 499–510.

Paterson, E., Sim., A., Davidson, J. & Daniell., T.J. 2016. Arbuscular mycorrhizal hyphae promote priming of native soil organic matter mineralisation. *Plant and Soil*, *408*, 243–254.

Phillips, C.L., Nickerson, N., Risk, D., Bond, B.J. 2011. Interpreting diel hysteresis between soil respiration and temperature. *Global Change Biology*, *17*, 515–527

Pinheiro, J., Bates, D., DebRoy, S., Sarkar, D., & R Core Team. 2020. *_nlme: Linear and Nonlinear Mixed Effects Models_*. R package version 3.1-150, <URL: https://CRAN.R-project.org/package=nlme>.

R Core Team. 2020. *R: A language and environment for statistical computing*. R Foundation for Statistical Computing, Vienna, Austria.

Ramirez, K.S., Craine, J.M. & Fierer, N. (2012), Consistent effects of nitrogen amendments on soil microbial communities and processes across biomes. *Global Change Biology*, *18*, 1918–1927.

Shazad, T., Chenu, C., Repinçay, C., Mougin, C., Ollier, J.-L. & Fontaine, S. 2012. Plant clipping decelerates the mineralization of recalcitrant soil organic matter under multiple grassland species. *Soil Biology & Biogeochemistry*, *51*, 73–80.

Sun, W., Resco, V. & Williams, D.G. 2010. Nocturnal and seasonal patterns of carbon isotope composition of leaf dark-respired carbon dioxide differ among dominant species in a semiarid savanna. *Oecologia*, *164*, 297–310.

Tian, J., Pausch, J., Yu, G., Blagodatskaya, E., Gao, Y. & Kuzyakov, Y. 2015. Aggregate size and their disruption affect 14C-labeled glucose mineralization and priming effect. Applied Soil Ecology, *90*, 1–10.

Trumbore, S.E. 2006. Carbon respired by terrestrial ecosystems – Recent progress and challenges. *Global Change Biology*, *12*, 141–153.

Vargas, T.D, Concilio, A., Woyann, L.G., Silva Santos, R.H. & Cheng, W. 2020. Rhizosphere priming effect on N mineralization in vegetable and grain crop systems. *Plant Soil*, *452*, 281–293.

Zang, H., Wang, J. & Kuzyakov, Y. 2016. N fertilization decreases soil organic matter decomposition in the rhizosphere. *Applied Soil Ecology*, *108*, 47-53.

Zhong, S., Chai, H., Xu, Y., Li, Y., Ma, J.-Y. & Sun, W. 2017. Drought sensitivity of the carbon isotope composition of leaf dark-respired CO_2 in C_3 (*Leymus chinensis*) and C_4 (*Chloris virgata* and *Hemarthria altissima*) grasses in northeast China, *Frontiers in Plant Science*, *8*, 1996.

Zhou, J., Wen, Y., Shi, L., Marshall, M.R., Kuzyakov, Y., Blagodatskaya, E. & Zang, H. 2021. Strong priming of soil organic matter induced by frequent input of labile carbon. *Soil Biology and Biochemistry*, *152*, 108069.

5 Discussion, conclusions and future work

5.1 Introduction

The purpose of this study has been to develop the capacity to measure soil respiration fluxes with diurnal and seasonal resolution in field conditions, and to use this to investigate the extent and mechanisms of rhizosphere priming effects (RPEs) in grass growing in contrasting soils. As discussed in Chapter 1, plants may exert a major control on soil carbon (C) turnover through RPEs, driven by labile C inputs into the soil through rhizodeposition. While positive and negative priming effects have been observed positive effects appear most common, and may amount to almost a fourfold increase in SOM turnover. RPEs may play a significant role in determining soil C balances under changing environmental conditions. Elevated CO_2 is predicted to increase rooting depth and overall C allocation to root growth, and in turn increase rhizodeposition. This may lead to more rapid SOM turnover, potentially coupled with higher soil temperatures also driving faster decomposition. However, studies have also shown that under elevated CO_2 plant productivity will increase. Hence the balance between increased C sequestration due to the incorporation of more plant residues, and enhanced SOM turnover through priming, will influence whether soils remain a net C sink or become a C source. Despite the importance of rhizosphere priming in this, however, RPEs are not well understood. To accurately predict future trends in soil C stocks, and to develop management options to enhance C storage, a better understanding of the mechanisms driving RPEs, and their significance in the field, is required.

RPEs are affected by a wide range of soil and plant variables, including soil nitrogen (N) availability. Priming effects have been shown to vary temporally, with evidence pointing towards this being driven by diurnal patterns of rhizodeposition, closely coupled to photosynthesis. This pattern may also show seasonal variation due to the effect of plant phenology on rhizodeposition. To fully understand this effect, either under current conditions or predicted future climate and CO_2 scenarios, we must be able to model RPEs on diel and seasonal timescales. To test and validate models of SOM turnover allowing for

rhizosphere priming we need datasets of soil and plant C fluxes, alongside their drivers, with sufficient resolution to observe diurnal patterns over a seasonal timescale. While priming effects have previously been investigated under field conditions, few studies have involved frequent sampling maintained over a moderate timespan, much less a growing season.

Gathering this data requires a system which can measure the net ecosystem C flux and partition it into soil and plant components. Potential methods for doing so are discussed in Chapter 1. Two principal techniques stand out for this: isotopic labelling (with air enriched or depleted in ^{13}C or ^{14}C compared to the atmospheric concentration of these isotopologues) or natural abundance isotope methods. Labelling methods either apply a continuous or a pulsed label. While the latter may be easier to apply in the field, it is not appropriate for a long-term study, which requires a steady difference between plant and soil end-members. Continuous methods of isotopic labelling, however, require either free air CO_2 enhancement (FACE), resulting in the elevation of CO_2 relative to the atmosphere, or the use of a sealed chamber, and so not practicable under field conditions. In comparison, a natural abundance method makes use of naturally-occurring differences between plant and SOM C fluxes. While these differences are usually small (c. 1 – 2 ‰), exploiting the differences in ^{13}C fractionation between the C_3 and C_4 photosynthetic pathways can create a larger isotopic distance (c. 10 – 20 ‰). Growing a C_4 plant in a C_3 soil, or *vice versa*, can allow clear partitioning of soil and plant C fluxes.

While such stable isotope methods can enable plant and soil respiration flux partitioning in the field, a paucity of studies investigating RPEs under field conditions remains. There are several reasons for this research gap. One is simply that such a system is difficult and costly to construct; this is particularly true for the automation of sampling essential for long-term high-frequency flux measurements. Another difficulty is the potential for error in flux partitioning when exploiting natural plant–SOM stable isotope differences. Although the distance between plant and soil $\delta^{13}C$ values when using a C_3 to C_4 vegetation shift is substantially greater than the magnitude of diurnal variation in $\delta^{13}C$, such

a system is still at risk of major inaccuracies. Through this study I have established and validated a methodology for measuring and partitioning C fluxes while minimising sources of error. I have then used this to explore the effects and mechanisms of RPES under real field conditions with diurnal and seasonal resolution. Below I assess how this study has met the three objectives involved in developing and using this method, as set out in Chapter 1.

5.2 Objective 1: establishment of an experimental field system

The first challenges of this study were to (1) establish an experimental field system capable of near-continuous measurement of C fluxes and their isotopic signatures under field conditions, and (2) assess its accuracy and precision. The establishment and assessment of this system is described in Chapter 2. The first element accomplished was the selection of a C_4 grass species, *Bouteloua dactyloides*, suited to the Bedfordshire climate, and its establishment in all lysimeters. Alongside this the sampling and measurement control system was redesigned to integrate a cavity ring-down spectroscopy (CRDS) instrument into the sampling loop. Although grass establishment in one of the two experimental soils (Shuttleworth) was initially slow, this was successfully accomplished in 2018.

The field system was thoroughly assessed in terms of reliability, precision and accuracy. This included assessments of sampling loop leakiness, response time to CO_2 concentration changes, the linearity of CO_2 accumulation during flux monitoring, the CO_2 concentration dependence of CRDS isotopic measurements, and the precision of CRDS measurements. The precision of the system was shown to be high, with uncertainty in CO_2 concentration and $\delta^{13}C$ over a 13.5 min measurement period two orders of magnitude smaller than inter-lysimeter variation, and substantially smaller than the diurnal range in variation. While previous work found the CO_2 concentration-dependence of ^{13}C measurements taken using an older CRDS model to introduce a significant bias into measurements this was found to be negligible in our system. Overall, no sources of error were identified which were large enough to introduce substantial inaccuracy or bias into flux measurements.

Flux partitioning was successfully demonstrated, and revealed clear diurnal patterns in plant and soil respiration. A key feature of this system is the ability to make automated flux measurements at a relatively high frequency over a long period, giving a near-continuous resolution more than sufficient to detect diurnal patterns in fluxes. This contrasts with other studies of soil C fluxes or priming in the field, which have involved infrequent sampling or limited windows of high-resolution sampling. As discussed under Objective 3, this allowed the assessment of potential rhizosphere priming as driven by diurnal patterns of rhizodeposition (Chapter 4), which would have been missed from daily flux averages or small numbers of low-frequency measurements.

The use of a C_3 to C_4 vegetation shift was successful in creating a clear distinction between plant and SOM fluxes. While, as discussed in Chapter 2, the incorporation of C_4-origin plant residues into SOM limits the useful lifespan of such a system, this did not appear to cause a problem over two growing seasons. As C_4 material becomes increasingly present in the SOM the partitioned SOM flux will appear lower than the true value, while plant respiration will be overestimated due to conflation with turnover of C_4-derived soil C. As shown in Chapter 4, however, diurnal plant and SOM fluxes could still be clearly distinguished in the second growing season (2019), with similar ratios between plant and soil respiration as seen in 2018. This indicates that new plant inputs were not swamping the signal from older SOM turnover. Furthermore, a degree of underestimation in SOM fluxes due to this is not a critical problem for the system for this study as it would not create the illusion of a priming effect. While the incorporation of C_4 material into the soil may complicate the partitioning of fluxes, particularly over longer experimental timescales, it may also create opportunities to explore SOM pool turnover rates and residence times as the C_4 signal moves through SOM pools.

This objective was therefore successfully met, and the Wolfson Field Laboratory is demonstrably capable of long-term field measurements of plant and soil C fluxes and associated soil and weather data with a high degree of temporal resolution. This system possesses substantial advantages over other systems

designed to allow ecosystem flux partitioning in the field. Unlike FACE, this study could be performed at ambient atmospheric CO_2 levels, thus exploring C fluxes and priming under current environmental conditions. In comparison to studies using eddy covariance, flux measurements are taken from discrete mesocosms; this can enable experimental treatments to be tested as in Objective 3. While many other studies have used flux chambers, these have generally been removable chambers mounted atop a small number of soil collars over shorter timespans. The use of lysimeters in this system avoids error emerging from lateral CO_2 diffusion under soil collars, and it has been set up to allow automatic flux measurement over long timescales from a reasonably-sized set of replicates (n = 12 for each of two soils). It is therefore well positioned to allow investigation of flux dynamics in undisturbed soils and field conditions by generating long-term high-resolution datasets much needed to test and improve models of soil C turnover.

5.3 Objective 2: development of methods to analyse measured C fluxes

While the accuracy and precision of net flux measurements were demonstrated within Objective 1, this did not remove all hurdles in the way of reliable flux partitioning. My second objective was therefore to investigate potential sources of error in partitioning, and to develop methods to overcome these. Stable isotope methods based upon differences in ^{13}C fixation in the C_3 and C_4 photosynthetic pathways have been used in many studies, which have assumed a single, temporally unchanging $\delta^{13}C_{plant}$ value. There is, however, clear evidence of environmental factors, such as light levels or drought, impacting plant end-members (Chapter 1). This objective was addressed in Chapter 3, through assessment of a prominent source of partitioning error and sensitivity analysis to gauge the impact of such sources of error on partitioning. Through analysis of the sensitivity of flux partitioning to error or variation in plant and soil end-members, I found that even small variation in an end-member could cause substantial error in partitioned fluxes. This was particularly true when the flux with an erroneous end-member was dominant in the system.

Transient variations in end-member may therefore introduce large inaccuracies in flux partitioning. Indeed, I found substantial inaccuracies caused by this in my data. Soil temperature is a major and well-established factor influencing rates of soil respiration, with higher temperatures driving faster rates of SOM turnover. This gives an expected daily pattern of SOM turnover, peaking during the warmest part of the day. Indeed, during grass sward establishment diurnal peaks in soil respiration were observed. For much of the growing season, however, soil respiration fluxes showed the inverse of the expected diurnal pattern: soil respiration peaked after midnight, and reached its minimum around midday. The work presented in Chapter 3 shows that this is explained by diurnal shifts in ^{13}C enrichment of plant respiration, which is well-evidenced from studies of both measured flux isotopic patterns and plant physiology.

This was corrected for by imposing a diurnal shift in the plant end-member. The $\delta^{13}C$ of dry plant matter was taken as most reliable baseline end-member (i.e. in the absence of diurnal ^{13}C enrichment from respiration of fresh photosynthate) as the grass tissue would integrate the transient effects of environmental variation over time. A diurnal enrichment of 3 ‰ was applied; this was consistent with the literature (diurnal enrichment mostly ranges from +2 ‰ to + 4% although higher values have been measured – see Chapter 1), and gave a diel pattern of SOM flux similar to that observed when the plant flux was not so dominant in the system. This correction therefore allowed me to resolve patterns of soil respiration over diurnal timescales, necessary for exploration of the drivers of RPEs in Objective 3.

This takes on an increased importance considering the close temporal coupling of photosynthesis and rhizodeposition shown in Chapter 4. ^{13}C enrichment of plant respiration was concurrent with the peak period of photosynthesis, thereby acting to obscure any priming effect if not accounted for. My findings indicate that, when trying to detect priming in the field or using similar stable isotope techniques in controlled environments with a day-night cycle, researchers need to consider the potential presence of diurnal shifts in the ^{13}C enrichment of plant respiration. The impact of the diurnal shift in $\delta^{13}C$ plant also suggests that false

positive priming results may be detected when using a C_4 to C_3 vegetation shift. In such a system diurnal enrichment of the plant end-member would cause an apparent increase in soil respiration, rather than the decrease seen in a C_4 plant C_3 soil system, and a dampening of the true diurnal variation in plant respiration. If this was not correctly accounted for the diurnal trend in soil respiration could be perceived as a rhizosphere priming effect, or it could exaggerate of any effects truly present.

It should be noted that the correction we applied was a binary shift from “daytime” to “night-time” end-members. In reality we would expect the plant end-member to start to increase following sunrise, plateau later in the day, and decrease after sunset. Accuracy of flux partitioning could therefore be improved by finer-grained modelling of $\delta^{13}C_{plant}$ changes, although that was beyond the scope of this study. The exact rates of change and maximally enriched $\delta^{13}C_{plant}$ value reached, however, are likely dependent on environmental factors. While improvements in $\delta^{13}C_{plant}$ estimation would be possible a completely accurate plant end-member may require constant monitoring, and would likely be impracticable.

The identification of this problem was possible due to comparison with an earlier period, during which the grass was still becoming established and did not dominate the net flux to the same extent. This served as a useful sense check for unexpected results, and allowed the identification of systematic error within the system, and reflects a significant advantage of a dataset such as ours, spanning growing seasons: the ability to use sections of the data to test and validate other time periods. Assessment of error could be done more formally using model-data fusion techniques to account for uncertainties in flux models and data by testing variation in model properties. This may reveal discrepancies between flux data and model predictions, allowing sources of error within a large dataset to be identified and corrected for.

As detailed in Chapter 1, many factors can cause plant and soil end-members to vary. Only light-driven changes in the plant end-member, however, proved to be a major source of error in our dataset, although small effects on end-

members from other environmental factors (e.g. water availability) may be impossible to disentangle from changes in soil and plant flux rates. Overall, completion of the second stage of this study provided an improvement to our methodology for analysing our flux dataset. These findings go beyond our research, however, and indicate that other studies relying on stable isotope differences between plant and soil C fluxes need to consider whether they need to account for the effects of environmental variation on end-members, e.g. via a plant end-member shift is required under changing light conditions.

5.4 Objective 3: Dataset collection and assessment of potential rhizosphere priming and its causes

The purpose of the third stage of this study was to use the experimental system and analysis methods developed and tested through Objectives 1 and 2 to test for the effects of RPEs in two contrasting soils, and to explore mechanisms behind them. It is not, however, practicable to measure rhizodeposition in the field over the diel timespans over which it may drive RPEs. Based on evidence for close temporal coupling between photosynthesis and rhizodeposition, and building upon previous studies showing diurnal patterns to soil respiration, I therefore assessed whether solar radiation could be used as a proxy for rhizodeposition.

I detected a significant positive relationship between soil respiration and solar radiation in the summer and autumn, additional to the relationship between soil respiration and soil temperature and moisture. Solar radiation hence appeared to act as a driver for SOM turnover. This relationship varied seasonally, present during periods of active grass growth or photosynthesis but absent during winter when the grass was dormant above-ground. This was consistent with the rhizosphere priming effect. Poor model fit over longer periods was also consistent with the RPE, as longer timescales would include greater variations in grass phenology, and thus rates of rhizodeposition at a given level of insolation.

Solar radiation was only a good predictor of SOM turnover on the diurnal timescale, and this effect was not detected when daily averages were

considered. The tight coupling of solar radiation and soil respiration is striking, and closer than that reported in other studies. Rapid transport of assimilate from the grass roots to mycorrhizae, rather than slower diffusion from the root through the soil has been demonstrated, and may be the reason for the lack of substantial lag between variation in photosynthesis and SOM turnover. Stimulation of rhizodeposition by pressure concentration waves through the phloem may also contribute to close coupling of changes in rates of photosynthesis and microbial access to exudates.

As a secondary objective I also assessed whether N mining, as a mechanism driving rhizosphere priming, could be detected in our two soils (Chapter 4). While this has been observed in many studies, others have found no evidence for suppression of soil respiration under higher levels of N availability, or even the reverse (Chapter 1). No evidence was found for N mining in our system. As discussed in Chapter 4 it is not possible to conclude that this effect was not present, as any suppression in N availability due to N mining may have simply been balanced by an increase in priming resulting from greater rhizodeposition. Given the variety of effects on soil respiration following N application documented in the literature (Chapter 4), it is likely that natural differences between soils affect responses, which may explain this. There is evidence for N mining occurring in the field, so this effect is not likely to be due to disturbance alone; however, there are many reasons why different field systems might respond differently to N application, such as prior nutrient deficiency, differences in plant communities, or differences in microbial community structure. More research is needed to explore the causes of such differential effects.

5.5 Conclusions

I successfully established and validated a system to allow the partitioning of plant and soil carbon fluxes with a high temporal resolution, and over multiple growing seasons. The system is sufficiently sensitive to resolve diurnal patterns in these fluxes. Potential sources of inaccuracy in partitioning have been assessed, and the need to account for diurnal shifts in ^{13}C enrichment of the

plant end-member has been demonstrated. More broadly, substantial sensitivity of plant-soil C flux partitioning to transient variation in end-members has been shown. Within this study I have used this system to produce a dataset of soil and plant respiration fluxes, alongside measures of soil temperature and moisture and weather data which is, to my knowledge, unique in its combination of timespan and frequency of measurements. Such data are much needed to investigate soil carbon dynamics, including rhizosphere priming, over seasonal and longer periods. Rhizosphere priming must be accounted for if models of SOM turnover are to accurately represent the interactions between labile carbon, microbial C pools, and SOM pools; such models are starting to be developed, and data of this kind is essential for testing and validating them.

Solar radiation, used as a proxy for rhizodeposition, was found to be a driver of soil respiration. The inclusion of solar radiation in models improved prediction of SOM turnover compared to models including soil moisture and temperature only. These findings are consistent with the rhizosphere priming effect, and are best explained by it. Diurnal patterns of soil respiration were closely linked to solar radiation, suggesting a rapid response of soil microbial communities. This is further evidence that priming effects are not simply artefacts emerging from disturbance within the laboratory, but exist as real, significant processes in the field.

Evidence for nitrogen mining as a mechanism behind rhizosphere priming was not found, with increased nitrogen addition not resulting in a significant effect on SOM turnover. It is not possible to unpick the reasons why this response differed from other findings which have shown positive and negative effects on SOM turnover due to the wide range of effects N fertilisation may have on a planted system.

5.6 Future work

The work presented in this thesis takes us from the development and testing of a system for making high-resolution flux measurements in the field, through the generation of a two-year dataset and consideration of partitioning methods, and to the assessment of whether priming can be detected within that data. A

dataset of this size, however, has substantial untapped potential, and a full analysis of it was beyond the scope of this study. I focused my analysis on short snapshots from contrasting periods of the growing season to avoid differences in grass productivity or cover confounding assessment of the relationship between solar radiation and SOM turnover. Applying models to a full growing season's data, however, would allow us to assess how plant growth and phenology interacts with the effect of solar radiation on soil respiration. In this a measure of plant growth status – perhaps NPP, plant respiration, or simply timepoint in the year, may be taken as a nonlinear variable and used crosswise with solar radiation data.

Most dynamic models of SOM turnover do not account for RPE-driven changes in SOM turnover rates. Furthermore, there is more generally a lack of long-term high-resolution datasets of plant and soil C fluxes measured under field conditions. This dataset offers opportunities for improving dynamic models, and assessment of the circumstances in which including rhizosphere priming effects improves model predictions.

Moving away from the potential of the data generated by this study, many questions relating to rhizosphere priming in the field remain unanswered. This study has provided further evidence for priming effects under field conditions, and indicated a tighter temporal link between photosynthesis and rhizosphere priming. Further work is, however, necessary to demonstrate that this link is indeed mediated by rhizodeposition. Controlled-environment studies may be of great use here to allow measurements of rhizodeposition alongside soil respiration.

An open question remains over why some soils respond to N application by decreasing SOM turnover, while others have no, or the opposite, result. This study adds two further instances where no significant difference was observed, but has not shed new light on why such differences exist. Research is needed, both in the lab and the field, to explore why microbial communities respond in starkly different ways.

APPENDICES

Appendix A Accuracy of fits to Keeling plots

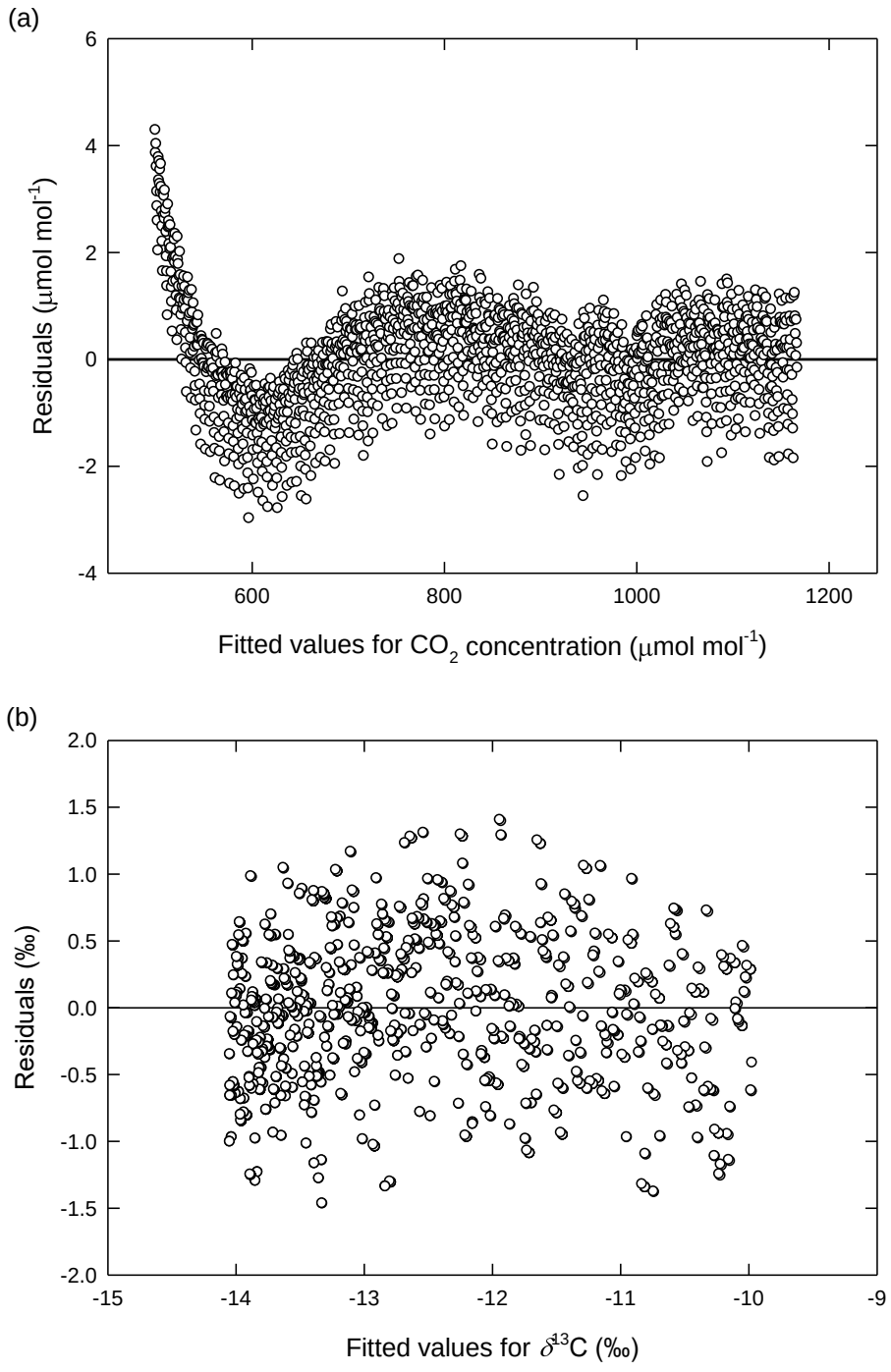

Figure A-1 Plot of residuals against fitted values for a linear model of (a) CO_2 concentration against time since lysimeter closure and (b) $\delta^{13}C$ against $1/CO_2$ concentration.

Appendix B Progress of the plant C_4 isotope signature through the C_3 soil

A simple one-pool model for the mass balance of soil carbon is

$$dC/dt = I - kC \qquad \textbf{Equation B-1}$$

where *C* is the concentration of carbon in the soil, *I* is the rate of input from the plants and *k* is a rate constant for decomposition. Likewise for the mass balance of ^{13}C:

$$dC^*/dt = I^* - kC^* \qquad \textbf{Equation B-2}$$

where C^* is the concentration of ^{13}C in the soil and I^* is the ^{13}C input from the plants. Note, assuming no isotopic fractionation in decomposition, the same rate constant applies as in Equation B-1. The solution of Equation B-2 for constant I^* and *k* and $C_0^* << C_\infty^*$ is:

$$C_t^*/C_\infty^* = 1 - e^{-kt} \qquad \textbf{Equation B-3}$$

where C_t^* is C^* at time *t* and C_∞^* is C^* at steady state, when $dC^*/dt = 0$ and the soil ^{13}C content approaches that of the C_4 plant inputs.

Appendix C Seasonal time-courses, 2019

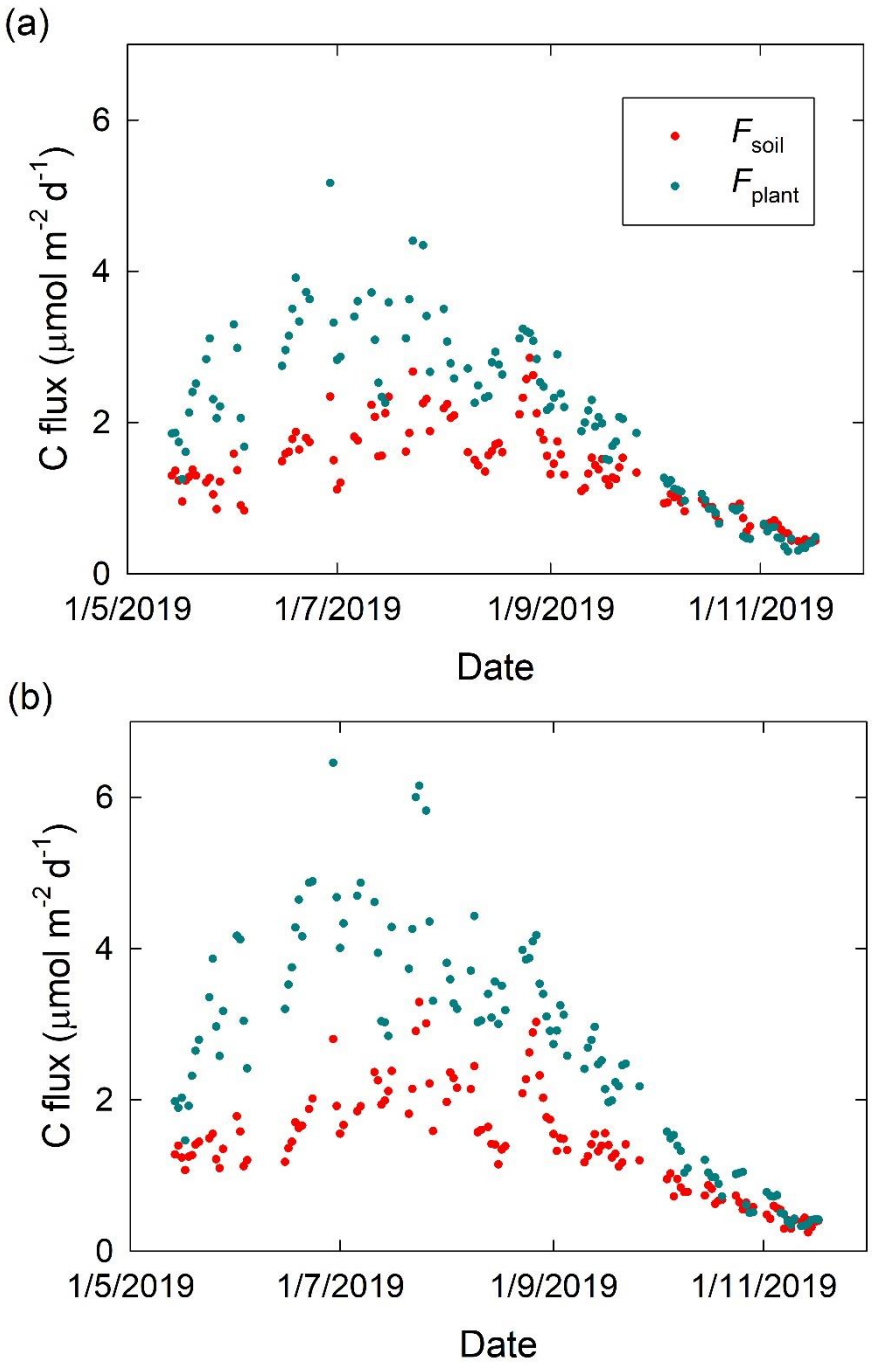

Figure C-1 Daily totals for F_{soil} and F_{plant} for the (a) Shuttleworth and (b) Temple Balsall lysimeters, May 2019 – November 2019. Days with under 30 measurements were excluded.

Appendix D Linear mixed-effects model coefficients

Table D-1 Linear mixed model fixed variable coefficients and goodness of fit metrics for 2018 flux measurements including soil moisture (θ) and soil temperature (T) as fixed variables, separated between the two soils. SW = Shuttleworth soil, TB = Temple Balsall soil.

Time period	Soil	Intercept	θ	T	AIC	R^2 (conditional)	R^2 (marginal)
5-8.7.2018	SW	-1.79	0.06	0.17	253.53	0.82	0.51
5-8.7.2018	TB	0.22	-0.04	0.15	167.92	0.81	0.53
1-15.8.2018	SW	-3.29	0.17	0.19	576.42	0.86	0.60
1-15.8.2018	TB	-1.08	-0.01	0.15	414.104	0.46	0.42
1-15.11.2018	SW	0.02	0.00	0.05	-477.75	0.66	0.30
1-15.11.2018	TB	0.77	-0.02	0.04	-475.60	0.71	0.32

Table D-2 Linear mixed model fixed variable coefficients and goodness of fit metrics for 2018 measurements including soil moisture (θ), soil temperature (T), and solar radiation (G) as fixed variables, separated between the two soils. SW = Shuttleworth soil, TB = Temple Balsall soil.

Time period	Soil	Intercept	θ	T	G	$T*G$	AIC	R^2 (conditional)	R^2 (marginal)
5-8.7.2018	SW	-1.63	0.07	0.16	-1.79	-0.06	260.75	0.83	0.51
5-8.7.2018	TB	1.65	-0.04	0.10	-6.62	0.24	149.63	0.84	0.57
1-15.8.2018	SW	-2.06	0.17	0.13	-2.01	0.12	542.80	0.87	0.62
1-15.8.2018	TB	1.11	-0.02	0.05	-6.41	0.31	303.08	0.64	0.60
1-15.11.2018	SW	-0.01	0.01	0.05	0.42	-0.00	-505.99	0.71	0.34
1-15.11.2018	TB	0.74	-0.02	0.04	0.41	0.01	-530.82	0.76	0.38

Table D-3 Linear mixed model fixed variable coefficients and goodness of fit metrics for 2018 measurements from both soils combined, including soil moisture (θ), soil temperature (T), and solar radiation (G) as fixed variables, with and without soil type (S) as a categorical fixed variable.

Time period	*S* included?	*Intercept*	θ	*T*	*G*	*S*	*T*G*	θ *S	AIC	R^2 (conditional)	R^2 (marginal)
1-15.8.2018	No	-1.74	0.07	0.12	-1.77		0.11		1205.91	0.80	0.42
1-15.8.2018	Yes	-1.47	0.16	0.11	-3.19	1.16	0,17	-0.17	892.71	0.84	0.62
1-15.11.2018	No	0.42	-0.01	0.05	0.56		-0.01		-1030.32	0.74	0.55
1-15.11.2018	Yes	0.02	0.01	0.05	0.48	0.70	0.00	-0.02	-1058.34	0.80	0.55

Table D-4 Linear mixed model fixed variable coefficients and goodness of fit metrics for 2019 measurements from both soils combined, including soil moisture (θ), soil temperature (T), and solar radiation (G) as fixed variables, with and without nitrogen addition treatment (N) as a categorical fixed variable., separated between the two soils. SW = Shuttleworth soil, TB = Temple Balsall soil.

Time period	Soil	*N* included?	Intercept	θ	T	G	$T*G$	N	$\theta*N$	AIC	R^2 (conditional)	R^2 (marginal)
15-30.7.2018	SW	No	-1.71	0.05	0.14	-3.49	0.19			704.44	0.64	0.55
15-30.7.2018	*SW*	*Yes*	*-1.93*	*0.06*	*0.14*	*-3.44*	*0.19*	*0.42*	*-0.01*	*713.79*	*0.64*	*0.56*
15-30.7.2018	TB	No	-1.84	-0.01	0.20	-3.36	0.20			670.58	0.65	0.58
15-30.7.2018	*TB*	*Yes*	*-1.54*	*-0.02*	*0.20*	*-3.37*	*0.21*	*-0.78*	*0.02*	*679.67*	*0.65*	*0.60*
15-30.8.2018	SW	No	-0.63	0.01	0.11	-4.32	0.26			396.23	0.75	0.64
15-30.8.2018	*SW*	*Yes*	*-0.82*	*0.01*	*0.11*	*-4.30*	*0.25*	*0.40*	*-0.01*	*406.20*	*0.75*	*0.67*
15-30.8.2018	TB	No	-0.92	-0.02	0.17	-5.62	0.34			507.75	0.80	0.74
15-30.8.2018	*TB*	*Yes*	-0.45	-0.03	0.17	-5.58	*0.34*	*-1.07*	*0.02*	*507.94*	*0.80*	*0.76*
15-30.9.2018	SW	No	-0.02	0.02	0.05	-0.63	0.08			-15.12	0.70	0.35
15-30.9.2018	*SW*	*Yes*	*-0.30*	*0.02*	*0.05*	*-0.69*	*0.08*	*0.52*	*-0.01*	*-10.12*	*0.71*	*0.46*
15-30.9.2018	TB	No	0.54	-0.02	0.07	-0.60	0.09			-16.54	0.70	0.53
15-30.9.2018	*TB*	*Yes*	*0.79*	*-0.02*	*0.08*	*-0.43*	*0.08*	*-0.75*	*0.02*	*-14.59*	*0.69*	*0.57*

Appendix E July 2018 measured and fitted fluxes without allowing for diurnal plant end-member change

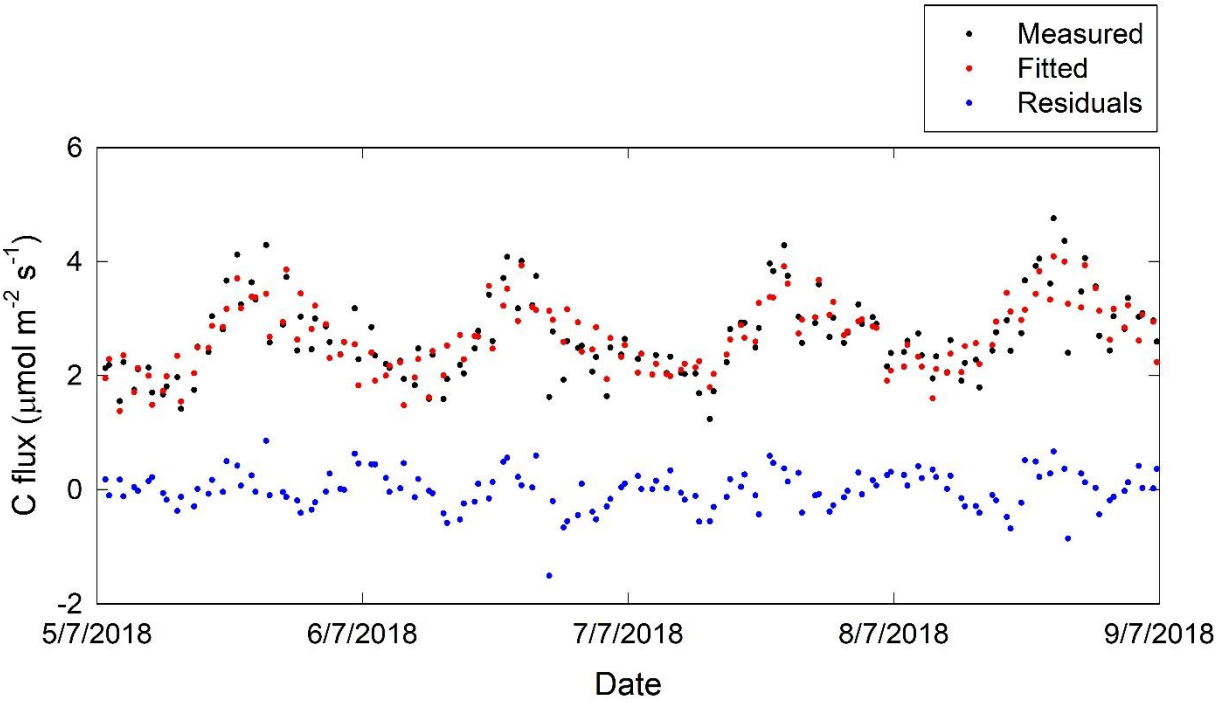

Figure E-1 Measured values for SOM mineralisation, Temple Balsall soil, 5-8 July 2018 alongside fitted values and residuals from a linear mixed model incorporating soil temperature and moisture. A diurnal plant end-member change was not applied.

Appendix F Grass clipping masses

Table F-1 Masses of clippings taken during and after the 2018 growing season, Shuttleworth lysimeters. Grass swards were clipped to a height of 15 cm, with the exception of 24 April to 2 May 2019 where grass was clipped to 5cm.

	Dry mass clipped (g)				
Lysimeter ID	11.8.18	31.8.18	1.10.18	24.4-2.5.19	Total
1	n/a	n/a	n/a	75.01	75.01
2	n/a	n/a	n/a	34.87	34.87
3	n/a	n/a	n/a	58.86	58.86
8	n/a	n/a	n/a	67.51	67.51
10	n/a	n/a	n/a	57.36	57.36
12	n/a	n/a	n/a	65.99	65.99
13	n/a	n/a	n/a	59.19	59.19
14	n/a	n/a	n/a	44.99	44.99
15	n/a	n/a	n/a	63.26	63.26
19	n/a	n/a	n/a	65.41	65.41
21	n/a	n/a	n/a	50.33	50.33
24	n/a	n/a	n/a	45.19	45.19
Mean ± SE				**57.3 ± 3.2**	**57.3 ± 3.2**

Table F-2 Masses of clippings taken during and after the 2018 growing season, Temple Balsall lysimeters. Grass swards were clipped to a height of 15 cm, with the exception of 24 April to 2 May 2019 where grass was clipped to 5cm.

	Dry mass clipped (g)				
Lysimeter ID	11.8.18	31.8.18	1.10.18	24.4-2.5.19	Total
4	21.61	22.16	11.92	87.43	143.12
5	22.28	16.4	11.44	90.52	140.64
6	44.74	29.56	9.22	114.1	197.62
7	69.56	24.3	9.94	96.67	200.47
9	17.47	18.55	6.58	110.14	152.74
11	31.84	20.44	8.68	111.34	172.3
16	49.56	18.73	13.32	101.79	183.4
17	58.85	23.04	14.27	116.04	212.2
18	17.77	10.82	3.73	113.72	146.04
20	35.87	18.2	8.08	124.24	186.39
22	12.11	12.51	7.83	111.13	143.58
23	65.74	24.48	8.06	139.04	237.32
Mean ± SE	**37.3 ± 5.5**	**19.9 ± 1.5**	**9.4 ± 0.8**	**109.7 ± 4.0**	**176.3 ± 8.8**

Table F-3 Masses of clippings taken during and after the 2019 growing season, Shuttleworth lysimeters. Grass swards were clipped to a height of 10 cm, with the exception of 6 May 2020 where grass was clipped to 5cm.

Lysimeter ID	N treatment	Dry mass clipped (g)						
		10-12.7.19	1-2.8.19	22-23.8.19	12-13.9.19	3-4.10.19	6.5.20	Total
2	High	43.6	40.1	29.3	12.3	3.2	68.9	197.2
8	High	79.8	33.8	24.0	18.8	8.7	135.3	300.3
10	High	79.3	27.9	19.8	11.1	3.2	82.9	224.2
12	High	35.9	34.0	22.9	20.9	4.6	53.5	171.8
19	High	65.1	40.4	21.5	21.5	3.6	95.3	247.5
21	High	49.9	28.2	15.5	11.0	1.9	128.8	235.2
Mean ± SE	High	**58.9 ± 6.9**	**34.1 ± 2.0**	**22.2 ± 1.7**	**15.9 + 1.9**	**4.2 + 0.9**	**94.1 + 12.1**	**229.4 ± 16.5**
1	Low	55.6	33.7	18.6	12.8	2.9	67.5	191.1
3	Low	62.2	35.7	21.3	9.2	3.4	58.9	190.6
13	Low	62.1	33.9	15.5	16.2	2.3	58.3	188.2
14	Low	59.0	35.3	20.4	24.4	1.3	114.6	255.0
15	Low	89.2	45.2	13.7	17.2	2.2	104.3	271.8
24	Low	66.6	28.9	27.5	14.7	4.2	118.7	260.6
Mean ± SE	Low	**65.8 ± 4.5**	**35.4 ± 2.0**	**19.5 ± 1.8**	**15.8 ± 1.9**	**2.7 ± 0.4**	**87.1 ± 10.6**	**226.2 ± 14.9**

Table F-4 Masses of clippings taken during and after the 2019 growing season, Temple Balsall lysimeters. Grass swards were clipped to a height of 10 cm, with the exception of 6 May 2020 where grass was clipped to 5cm.

Lysimeter ID	N treatment	Dry mass clipped (g)						
		10-12.7.19	1-2.8.19	22-23.8.19	12-13.9.19	3-4.10.19	6.5.20	Total
2	High	139.6	55.8	34.6	22.5	12.1	100.3	365.0
8	High	105.3	49.6	19.6	22.7	8.5	78.7	284.4
10	High	109.9	52.7	23.8	23.5	8.0	162.7	380.6
12	High	92.3	38.4	30.0	18.8	4.7	68.6	252.8
19	High	102.9	39.9	35.8	35.1	2.6	107.1	323.4
21	High	107.9	50.4	26.4	20.5	4.6	140.8	350.6
Mean ± SE	High	**109.6 ± 5.9**	**47.8 ± 2.6**	**28.4 ± 2.4**	**23.9 ± 2.2**	**6.7 ± 1.3**	**109.7 ± 13.5**	**326.1 ± 18.4**
1	Low	148.4	47.1	28.3	13.0	11.2	128.4	376.4
3	Low	117.1	31.5	22.0	12.4	5.3	79.7	268.0
13	Low	121.1	41.3	41.2	35.9	4.8	153.0	397.3
14	Low	94.0	42.3	20.6	20.9	1.7	132.8	312.2
15	Low	92.1	41.0	21.1	14.7	2.6	130.6	302.0
24	Low	96.9	60.2	37.2	20.1	2.8	83.4	300.5
Mean ± SE	Low	**111.6 ± 8.1**	**43.9 ± 3.5**	**28.4 ± 3.3**	**19.5 ± 3.3**	**4.8 ± 1.3**	**118.0 ± 11.0**	**326.1 ± 18.6**